JPRS L/10110

10 November 1981

Translation

MAN AND SPACE ASTRONAVIGATION

By

Valeriy Fedorovich Bykovskiy, et al.

FBIS FOREIGN BROADCAST INFORMATION SERVICE

FOR OFFICIAL USE ONLY

APPROVED FOR RELEASE: 2007/02/09: CIA-RDP82-00850R000400070025-3

NOTE

JPRS publications contain information primarily from foreign newspapers, periodicals and books, but also from news agency transmissions and broadcasts. Materials from foreign-language sources are translated; those from English-language sources are transcribed or reprinted, with the original phrasing and other characteristics retained.

Headlines, editorial reports, and material enclosed in brackets [] are supplied by JPRS. Processing indicators such as [Text] or [Excerpt] in the first line of each item, or following the last line of a brief, indicate how the original information was processed. Where no processing indicator is given, the information was summarized or extracted.

Unfamiliar names rendered phonetically or transliterated are enclosed in parentheses. Words or names preceded by a question mark and enclosed in parentheses were not clear in the original but have been supplied as appropriate in context. Other unattributed parenthetical notes within the body of an item originate with the source. Times within items are as given by source.

The contents of this publication in no way represent the policies, views or attitudes of the U.S. Government.

APPROVED FOR RELEASE: 2007/02/09: CIA-RDP82-00850R000400070025-3

JPRS L/10110

10 November 1981

MAN AND SPACE ASTRONAVIGATION

Moscow CHELOVEK I KOSMICHESKAYA ASTRONAVIGATSIYA in Russian 1979 (signed to press 26 Jan 79) pp 2-6, 31-71, 103-207, 220-222

[Annotation, introduction, Chapters 2, 3, 5, 6, 7 and table of contents from book "Man and Space Astronavigation", by Valeriy Fedorovich Bykovskiy, Leonid Pavlovich Grimak, Yevgeniy Aleksandrovich Ivanov et al., edited by V. F. Bykovskiy, candidate of engineering sciences, pilot-cosmonaut of the USSR, V. P. Merkulov, doctor of engineering sciences and L. S. Khachatur'yants, doctor of medical sciences, Izdatel'stvo "Mashinostroyeniye", 1700 copies, 224 pages, illustrated]

CONTENTS

UDC: 629.78.05.001.24

ANNOTATION

[Text] This book deals with the inception of astronavigation; it demonstrates the link between aviation and space astronavigation. There is discussion of the equipment for space astronavigation, methods of assessing the accuracy of various astronavigation techniques. Analysis is made of cosmonaut work during space flights.

This book is intended for engineering and technical workers involved in development and use of systems of navigation and control of manned space flights.

INTRODUCTION

Celestial navigation is an ancient science that mankind used to solve numerous practical problems for many centuries. The famous seafarer, Christopher Columbus, who discovered America, realized even then, in 1492, the great importance of astronomy in determining the location of a ship at sea. He said: "There is only one error-free seafaring calculation--astronomic; fortunate is the one who is familiar with it" [47]. Without the help of celestial navigation it would be extremely difficult for man to orient himself, not only in the open sea but, in many cases, on land as well.

For a long time, celestial navigation was an area of applied astronomy. With the development of all types of transportation and, in particular, aviation, astronavigation gradually developed into an independent branch of science dealing with the patterns and methods of spatial orientation with the help of heavenly bodies.

Aviation astronomy is a relatively young discipline, which took over many methods from maritime astronomy. However, because of the differences in aviation, as compared to ships (for example, higher speeds), these methods underwent substantial refinement and changes.

For example, it is considerably more complicated to measure the altitude of heavenly bodies above the planet's horizon in aviation. The reasons for this are, in the first place, the great distance from the horizon, which makes it difficult to superimpose precisely the image of such a body on the horizon due to atmospheric haze; in the second place, inaccurate knowledge about the aircraft's altitude above the surface of the earth and irregularity of earth's topography at the horizon, as well as bumpiness of aircraft in some cases, which makes it difficult to take precise readings. These differences are so significant that they led to the use in aviation of sextants with an artificial horizon, which is formed on the basis of diverse pendulums, often of the liquid type. In order to reduce reading errors due to bumpy flight, special integral averaging devices are also used. In addition, by now some high-precision automatic and automated (i.e., those operating with the participation of an aircraft navigator) navigation systems have been developed and constructed, which permit continuous determination of the geographic coordinates of an aircraft in flight; automatic astronomic course instruments, astrocorrectors for inertial navigation systems and many others were also developed.

Launching in the Soviet Union of the Vostok spacecraft manned by Yuriy Gagarin inaugurated the era of manned space flights. As time passes, the duration of space flights is increasing and their programs are growing more complex. The

knowhow gained in flying aboard modern aircraft and manned spacecraft showed the great importance of operational and accurate navigation support. The increasing complexity of space flight programs makes it necessary to develop and use autonomic [self-contained] ways and means of space navigation involving the use of modern on-board computer equipment.

It is a pressing task to pursue studies for development and improvement of the effectiveness of ways and means of astronomic navigation of manned spacecraft. In this regard, cosmonautics must define the duties of a spacecraft navigator, his role and place when performing the main operations for autonomous navigation.

There are a number of distinctions to solving problems of celestial guidance of spacecraft, and they affect the professional performance of cosmonauts.

The navigation methods that are guided by the sun, stars and planets, which are very accurate and unrelated to distance or duration of flight are quite promising. Astronavigation systems are autonomous in nature, and they require no additional information from ground-based equipment. They can operate at infinitely long distances from earth. These systems, which use heavenly bodies as reference points, are quite resistant to possible artificial interference.

Development of celestial guidance systems is a complex technical task, and it requires work on a wide range of interrelated problems referable to optics, light engineering, precision mechanics and a number of other branches of modern science and technology. The difficulty of navigation support of spacecraft flights lies in the fact that each flight must provide for laying out the optimum trajectories for efficient performance of the specified assignment with specified energy resources. This means that there is a rigid flight schedule which is planned on earth for each mission. However, because of errors in guidance [into orbit?], use of corrective maneuvers and possibility of "overshooting" in flight, it becomes necessary to have autonomous calculation of many navigational data aboard the spacecraft. In this regard, the efficiency of performing the set assignment aboard a manned spacecraft will depend significantly on the characteristics of its navigational equipment and the crew's ability to solve navigation problems at different stages of a flight.

In recent times, development of navigation equipment resulted in the use of inertial navigation systems (INS) with and without platform. Those without platform have several advantages over those with them. Development of such systems involving the use of inertial elements based on new physical principles will make it possible to create inertial systems that will provide for a high degree of precision in determining the piloting-navigational and orbital parameters of flight.

Pressing problems of theory of inertial systems have been studied comprehensively by Soviet and foreign authors [2, 36, 42, 66].

The requirement that accuracy of inertial navigation systems had to be improved first led to an effort to make use of classical statistical methods, such as the least squares or maximum plausibility method. Subsequently, to improve the accuracy of inertial navigation, recurrent methods of statistical evaluation became popular. Analysis of the margin of error of inertial elements (accelerometers, gyroscopes) revealed that it is impossible at the present time to assure the necessary precision of solving navigation problems by inertial systems with or without platforms without using additional external information.

The following sensors of external information can be used to correct inertial navigation systems aboard manned spacecraft: automatic astronavigational devices (astrotelescopes); Doppler flight speed and altitude indicator; unit for determining the direction of the local vertical (IK [infrared?] vertical, radio vertical); visual optic device for determining directions on celestial reference points (optical sight); optical visual devices for determining the altitude of heavenly bodies.

Space flights will continue to be unique events for a long time, and the capabilities of spacecraft will remain limited. For this reason, developers of space equipment will be faced for a long time with the requirements of low weight, small size and low energy consumption. In this respect, the use of optical visual means of correction (sights and sextants) is the most acceptable variant. The expediency of such devices is also due to the fact that the operator-cosmonaut can determine with their help, independently and without communication with earth, not only the coordinates of the position of his spacecraft, but check [monitor, control] such navigational parameters as the direction of the local vertical and altitude of flight.

For a long time, man aboard a spacecraft will remain the principal link in a semiautomated system of self-contained astronavigation.

As we know, the psychophysiological functions of a cosmonaut change during flight, and this is manifested the most obviously by the change in sensorimotor fine coordination functions, which constitute the foundation of professional skill in astronavigational orientation [38, 73, 75].

A designer who plans and designs any system that operates with the participation of a human operator must take into consideration the psychophysiological capabilities of man, not only under conditions of normal function, but with exposure to different space flight factors which alter the level of his work capacity.

Thus, space astronavigation of today is based on many branches of knowledge, which at first glance often appear to be very far removed from one another. For this reason, this monograph is the collective work of various specialists--engineers and psychophysiologists, cosmonauts and physicians, psychologists, mathematicians and methodologists.

The authors concentrated primarily on shedding light on questions of improving the efficiency of operation of a semiautomated system of self-contained astronavigation and formation of recommendations on optimizing its operation.

CHAPTER 2. MAN IN THE SYSTEM OF SPACE ASTRONAVIGATION

2.1. Structure of Cosmonaut's Work in Astronavigation System

At the present time, the opinion has been established that complete automation of solving space astronavigation problems is not efficient. It is imperative to include an element that integrates all other elements to assure the operation of a complex navigation system as a whole. In modern navigation systems, man is such an element, since his mental properties enable him to best solve problems of integration. Expressly man organizes and coordinates the operation of all elements in the system, uniting them into a single whole [53, 74].

While automatic calculations are used in a navigation system, the main observations must still be made and finalized by man. Man is the principal element in all possible approaches with respect to performing reserve functions in solving navigation problems (of both observation and calculation). Moreover, the human operator has definite advantages in solving a number of special problems of space astronavigation.

Thus, it has now become apparent that it is impossible to develop either the main or ancillary navigation system without taking into consideration the capabilities of the human operator.

Development of equipment, with which the operator works, must be preceded by analysis of the structure of his activities in solving a specific problem. In space astronavigation, one of the main operations performed by man is taking astronomical measurements. The entire operation required for this can be illustrated with an abstract algorithm scheme (Figure 20). After receiving an order for an astronavigational operation, the cosmonaut displays "instrument zero." Then he identifies the specified reference points (Θ_1). If the reference point is not identified (n) he works with the next reference points (Θ_2); if it is identified (logic condition (n) not met), he performs the next operation (aiming at reference point) to which the corresponding needle comes. After sighting [aiming], superposition of both reference points and taking readings (P, S, C), the cosmonaut must provide for performance of arithmetic operations (K).

A second operation can be performed to increase the reliability of the results of solving the astronavigation problem, starting with action "0," to which goes a needle with the number 7. Consequently, man's visual and motor analyzers are the psychophysiological basis of this work, as well as his operative memory which is instrumental in identification, guidance, reading instruments and calculations.

Operator	Actions	Predicate	Logical conditions
Ж	issuing order	y	"0" data are normal
0	removal of instrument "0"	n	reference point not identified
Θ_1	identification of reference point	q	reference point in cross-hairs
Θ_2	identification of reserve reference point	m	reference points superimposed
P	sighting measurement device on reference point	a	parameters do not exceed range of mean static series
S	convergence of both reference points	-	--
C	reading instrument	b	correct performance of actions
K	mathematical operations	ω	always false logical condition
J	finding coordinates	-	--

Figure 20. Abstract algorithmic scheme for solving astronavigation problem (variant): actions and logical conditions

2.2. The Cosmonaut's Visual Analyzer During Flight

The cosmonaut's sight is the decisive factor in a number of cases in solving problems of autonomous astronavigation. This applies, first of all, to operations such as measuring angular distances between celestial bodies, between them and the planet's horizon, between objects on the planet's surface and its horizon, etc. In all cases, regardless of the design and parameters of astronomic measuring instruments, the cosmonaut uses the main physiological functions of sight: acuity, discrimination, sensitivity to light and time parameters of visual perception. Of course, proper manufacture of measurement instruments increases the accuracy and reliability of the cosmonaut's work, but none of the listed visual functions is ever excluded from his work.

It should be noted that before publication of the first results of studying visual functions during space flights, the designers and developers of astromeasurement instruments for manned spacecraft used data from ground-based experiments. However, before there were flights into space it was not known what changes could occur in vision in space. Assumptions were expounded that absence of gravity could cause deformation of the eyeball and alter the functional capabilities of the visual analyzer. It was expected that the motor system of the eye would lose, to some extent, coordination of movements that developed in the course of life, as a result of which there would be disturbances of visual functions, deterioration

of depth vision, change in processes of accommodation and convergence, etc. All this had to be checked before man would fly into space.

The first experiments were conducted with aircraft with the use of brief weightlessness. American specialists reported a decrease in acuity of vision by an average of 6% during such flights [18]. Some interesting data were also obtained by Soviet medical men. Thus, L. A. Kitayev-Smyk [46], observed enlargement, vagueness and distortion of visible objects during brief weightlessness. In his study of color perception he found that there was heightened sensitivity to brightness of colors, particularly yellow. Some of his operators observed a purple halo around luminous objects.

Studies revealed that visual acuity diminished with onset of weightlessness, but with further exposure to this state it was restored in some subjects or even exceeded the initial level. These studies were started with the Voskhod spacecraft, then continued aboard Voskhod-2, Soyuz-3, -4, -5, -6, -7, -8 and -9. They consisted of testing visual acuity, visual discrimination or contrast capacity, color vision and a certain general characteristic of sight, which included both the above-mentioned functions and some of the time characteristics of vision. We named the latter general function of vision the operational efficiency of vision [work capacity]. The studies were conducted by means of specially developed tabular tests with the use of lined patterns and objects of different colors and contrast [75].

According to our data, the duration of flights aboard Soyuz spacecraft was adequate for analysis of the dynamics of visual functions. We found that noticeable changes occurred in these functions within the first 2-3 days of space flight. The studies revealed that, while visual functions K diminished by 5-30% during the first days of flight, as compared to the preflight level, there was subsequent restoration as a function of flight duration (n orbital passes), which was indicative of development by the cosmonauts of certain adaptive or compensatory mechanisms (Figure 21). Starting with the 40th-50th passes, this process starts to be affected by other factors, which again lead to some decline of visual functions though not as significant as at the start of the flight. The maximum decline occurred in the 70th-80th orbital passes.

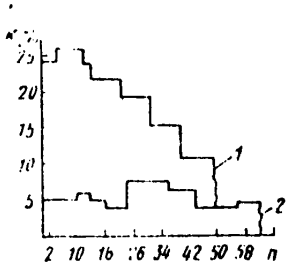

Figure 21.
Changes in visual functions K as related to duration of flight (n--passes)
1) operational visual efficiency
2) visual acuity

Subsequently, visual functions improved again, and it is expected that they would remain more stable than in the period between the 30th and 60th passes. After a considerable period of time, there could be another monotonous decline of all of the body's functional capacities, including sight. We cannot state definitely how long this would last until a sufficient number of appropriate studies is conducted during long-term space flights.

The nature of visual problems, which are solved most often with the use of stars or other luminous point sources, is important to working with

astromeasuring instruments. It is also known that the operator's visual acuity, contrast sensitivity and photosensitivity play a substantial role in solving such problems. Only experiments could show how these parameters of vision would change during space flights. A special technique was developed for this purpose, which involved the use of point light sources of graded intensity located on earth's surface.

We conducted an experiment with the use of such a ground-based visual test during the flight of the Voskhod spacecraft in October 1965. A special lighting situation was created on the ground in a desert region, i.e., far from city and village lights that would hinder the work of the cosmonaut. It consisted of three strips of lights, each of which consisted of six point sources of light and one reference light, which was very bright, for certain detection of the strip.

Floodlights with up to 60° angle of beam divergence, powered by a mobile projector power plant were used as lights. Such projectors can provide a light with intensity of the order of $J_0 = 0.2$ Mcd. Illumination E created in the observer's pupil at a distance L from the floodlight at orbital altitude H, with atmospheric transmittance τ_a and craft's port transmittance [transparency] τ_p, can be calculated with the following formula:

$$E = J_0 H \tau_a \tau_p L^3$$

For the expected flight conditions, the following values of these parameters could be expected: H = 200 km, L = 400 km, $\tau_a = 0.8$ and $\tau_p = 0.75$. In this case, E = 0.4 μlux. With such illumination of the pupil from a point source and with adequate light adaptation, the eye sees this light source in the form of a star of about the first magnitude. If we consider, however, that six such lights will be concentrated in each strip, we can be sure that the distance of L = 400 km is not the maximum when atmospheric conditions are good and there is a good level of dark adaptation.

Types A and B flares were discussed as another light source. They provide light intensity J_0 in the range of 5 to 15 Mcd. Measurement of illumination generated at an altitude of 1000 m by burning flares revealed that the intensity of light from these types of flares constituted 4-5 and 10 Mcd, respectively.

By making calculations analogous to those described above, we will find that intensity of light on the cosmonaut's pupil at a distance of L = 400 km is E = 5 μlux and E = 10 μlux, respectively. We used lights created by flares for the experiment conducted during the flight of the Voskhod spacecraft.

The angular distances between lights diminished because of the distortions of perspective when the cosmonauts observed the light strips. If we use l to designate the horizontal distance to the lights, H for altitude of flight and Δ for the linear distance between the lights on the ground, the angular distance Δα (in angular minutes) between the lights, as observed by the cosmonauts, can be obtained with the following equation:

$$\Delta\alpha = \frac{\Delta \sin \operatorname{arctg} H/l}{\sqrt{l^2 + H^2}} 3438.$$

If the minimum angular distance between lights observed by the cosmonaut constitutes $\Delta\alpha_{min}$, his visual acuity will be $V = 1/\Delta\alpha_{min}$ (for point sources).

During the experiment, the flares were lit 2 min before the spacecraft flew over the lights. At this time, the distance between the manned spacecraft and lights was about 1000 km and Voskhod was so oriented that the axis of the porthole through which spacecraft commander V. M. Komarov looked out was directed forward and tilted by an angle of the order of 60° in relation to earth's surface. The cosmonaut saw earth's horizon in the very top part of the porthole and the rushing surface of the earth in the middle and at the bottom. V. M. Komarov adapted to the dark for 8-10 min before approaching the region of the lights.

V. M. Komarov observed all three light strips at a distance of 400 km and recognized their location from the familiar configuration, which he immediately reported over radio. For 1 min, he observed the lights continuously until they left his field of vision. At the last stage of the overflight, the cosmonaut counted them and reported that he saw 12 separate lights.

At the time Voskhod flew over the area of the lights, these lights were photographed continuously from an aircraft flying on the same course and staying constantly on the line that connected the spacecraft and light strip. Concurrently, measurements were taken of the light intensity from an aircraft flying at an altitude of 1000 m. All this made it possible to check visibility of the lights to the cosmonaut, since cloud conditions constituted 2-3 points (at an altitude of 6-7 km) and visibility was 20 km in the area where the lights were used at the time the spacecraft flew over it. Moreover, the measurements gave us an idea about the intensity of the lights.

In analyzing the results of this experiment, let us consider two aspects of the cosmonaut's visual activities. The first is the visual search for the point sources of light on the dark side of earth. The cosmonaut performed this task quite well. He not only saw the lighting situation, but identified it. As we indicated above, the glare of the lights at the time they were detected constituted 5 μlux for type A flares and 10 μlux for type B. They appeared like stars of 1 and 1.58 stellar magnitude, i.e., about the same as the brightest stars in the sky--Canopus and Sirius.

In the absence of interfering light sources, the detection problem was not difficult. However, there is usually a difference in time of visual detection of photic stimuli. In the process of the search, the operator either does not look where the stimulus is situated, and then detection time increases, or else he looks by chance expressly at the spot where the stimulus is located and then the search time is significantly reduced. For this reason, the fact that the cosmonaut saw the lights at a distance of 400 km is primarily of evaluational value, showing the order of magnitude determining conditions that are sufficient for this visual problem.

The second aspect is determination of the cosmonaut's visual acuity from ground-based lights. It was based on his counting the total number of lights he saw separately. V. M. Komarov made such a count at the last phase of the flight, when the direction of the beam of vision of the lights constituted an angle of about 60° in relation to the plane of the horizon. He counted 12 separate lights in all 3 strips. From this, calculation was made of maximum angles--1.5 to 2.0', which corresponds to visual acuity of 0.7 to 0.5 units.

In evaluating the results, it should be noted that visual acuity determined from point sources situated against a black background is always lower by an average of 2-4 times than when measured by the conventional method (Landolt rings) [13]. If we consider that the visual acuity of V. M. Komarov measured by the lined patterns constituted 1.4-1.5 on the ground and underwent virtually no change during the flight, the obtained decline of visual acuity when measured by point sources of light conforms well with the above-mentioned range, constituting about 2.5-fold.

The studies revealed that there were relatively minor changes in the main physiological functions of sight during the space flight. The levels thereof, which ranged from 5 to 30-40%, depending on the physiological function, were not high enough to be detected by the cosmonauts. This gives us some idea about the distinctions of psychology of visual perception, which is based on comparison of photic stimuli (simultaneously or after short intervals), rather than perception of their absolute parameters. For this reason, the work capacity of the visual analyzer diminishes during a space flight by a magnitude of second order smallness, as compared to the work capacity of different physiological functions of sight given in this chapter, since the ratio of increment of photic stimulus ΔS to its value S, to which the visual analyzer reacts, will remain virtually unchanged if visual sensitivity to this stimulus is diminished, for example, by a%. In this case, the following ratio applies:

$$\frac{\Delta S - a\Delta S/100}{S - aS/100}$$

and after conversion:

$$\frac{\Delta S(1 - a/100)}{S(1 - a/100)} \approx \frac{\Delta S}{S}$$

i.e., again the same initial ratio, distorted only due to nonlinearity of visual perception as a function of magnitude of stimulus.

2.3. Photometric conditions Under Which Cosmonauts Solve Astronavigation Problems

The photometric conditions under which a cosmonaut has to take angle measurements for astronavigation differ substantially from the conditions under which the same tasks are performed in shipping and aviation astronomy.

Knowledge and comprehensive consideration of these conditions constitute a mandatory prerequisite for the cosmonaut's proper performance.

The sun is the chief source of light during orbital and interplanetary flights. However, the composition of its radiation differs appreciably from that present near earth's surface because of the protective effect of the atmosphere. The radiant energy of the sun, which fills the space near the sun, includes the entire range of the electromagnetic spectrum, from long radiowaves and including short radiowaves, infrared, visible and ultraviolet rays, extending to the region of x-rays and gamma rays, bordering on cosmic rays. The earth's atmosphere is "transparent" only for a narrow segment of this spectrum. Man is well-adapted to radiations of this segment. The result of the radiation, including radiowaves, has some deleterious effect on man, which is determined by its intensity, in addition to frequency. As shown by the experimental studies of the last 2 decades, which

were conducted with rockets and artificial earth satellites, the short-wave part of the solar radiation spectrum contains rather intensive ultraviolet (at altitudes of 300 to 100 km) and x- (at less than 100 km) rays. The energy of the visible spectrum does not differ in space in overall intensity and spectrum from the one on earth, so that no special protection against it is required. Radiation in the infrared (IR) part of the spectrum is hazardous in some cases, in view of absence of absorption in the atmosphere essentially due to water vapor, since it can be absorbed markedly by bodies and heat them. In particular, IR radiation has the unpleasant property of having a harmful effect on the cornea and other transparent media of the eye. It has been demonstrated that prolonged exposure to IR rays could cause cataracts, i.e., opacity of the lens. In this respect, short IR rays are of particular significance, since they can penetrate through the cornea and aqueous humor of the anterior chamber of the eye.

X- and ultraviolet (UV) rays are even more dangerous to sight. It is known that UV radiation causes inflammatory processes in the conjunctiva and cornea. The distinction of such lesions is that the morbid symptoms of inflammatory processes (sharp pain, burning of the eyes) do not appear right away, but 6-7 h or more after exposure to UV.

The foregoing must convince one that the first prerequisite for a navigator-cosmonaut to work well when taking astronomic measurements is to protect his vision from the deleterious effects of x-, UV and IR rays from the sun, including reflected radiation.

In addition, determination must be made of levels of brightness, contrast, linear, time and other illumination conditions that provide for optimum measurement quality. Because of the wide diversity of elements that could be used as bases for astro-measurements, it is not expedient to solve this problem in its general form. The elements involved may be as follows: objects of small angular size and brightness against the background of the stellar sky (stars, planets, artificial earth satellites); objects against the background of the dark side of earth (cities, light signals from earth, reference lights, artificial earth satellites); objects on earth's surface illuminated by the sun (cities, seas, rivers, artificial installations, etc.); objects on the sunlit surface of the moon (craters, "seas," mountains); horizons of earth, the moon and planets in the solar system, and other objects.

Let us consider the photometric characteristics of some of the above-listed objects. Of course, stars and planets are and will continue to be the most frequently used objects for space astronavigation. In view of the fact that the angular dimensions of these objects are much smaller than the angular resolution of the eye, they appear as point sources and are characterized by the magnitude of brightness [or glare] E. Stellar brightness is estimated as the illumination it produces on the observer's pupil near the boundary of earth's atmosphere. In addition, stellar magnitude m is a gauge that determines the brightness of a star or other light source. The scale of stellar magnitudes is determined by the equation $m = -13.89 - 2.5 \log E_m$, where E_m is illumination from the star's brightness m produced on the pupil of the observer (in lux).

Minimal illumination on the observer's pupil, which enables him to see the star, is called threshold. This threshold glare [brightness] is a variable that depends on viewing conditions. These conditions should include, first of all, brightness of

the background against which the star is viewed, degree of dark adaptation of vision, fullness of accommodation of the eye to infinity, approximate knowledge by the observer of the location of the star, presence of other stars in the field of vision, light sensitivity of the eyes, experience of the observer in finding a dim star and, in particular, ability to detect it with lateral vision, ability to provide optimum motor activity of the eye during the search and many other factors. This is why reports about visibility during orbital flights are sometimes so contradictory, particularly when flying over the daytime side of earth. One of the most important of the above conditions is background brightness B_b. We know that, while threshold brightness is about E_{thr} = 1 µlux with an absolutely black background, with a background of B_b = 0.01 µcd/m^2, threshold brightness already constitutes 10 µlux, i.e., it increases by 10 times. Thus, the faintest star that the eye sees against the background of a moonless night sky is a star of the sixth magnitude. These are average data, and they could change substantially for different observers in either the direction of increase or decrease of threshold brightness. For example, the results of our studies revealed that the number of stars viewed in the triangle of α, β and δ stars in the Dolphin constellation ranges from 4 to 13 for different observers, which corresponds to a change in brightness of more than one stellar magnitude.

The dependence of threshold brightness on brightness of adaptation background has been the subject of numerous comprehensive studies. There were sometimes rather wide discrepancies between data of different authors. Apparently this is attributable to differences in setting up experiments and, in particular, differences in level of dark adaptation of operators, which does not end entirely even after 50-60 min or more, as well as substantial differences in light sensitivity of different individuals. Nevertheless, we shall submit as tentative data the results obtained by Luizov [54] on determination of threshold brightness of a point source as related to brightness of the background:

Threshold brightness [glare], µlux	0.0203	0.0225	0.025	0.0288	0.0571
Brightness of background, µcd/m^2	0.032	0.32	3.2	32.0	320.0

Stars could be viewed in space against a background other than absolutely black when, for example, there is an "atmosphere" around the spacecraft that is formed by exhaust from jet engines with angular orientation. The brightness of these gases in the sun's rays could, in extreme cases, be of the order of 100 cd/m^2 or more, and could hinder viewing stars even of the first stellar magnitude. In view of the possibility of poorer visibility of stars, one should effect the angular orientation of the spacecraft in sufficient time for the above-mentioned atmsophere to dissipate before undertaking astronomic measurements.

Spacecraft illuminated by the sun and viewed from great distances may not necessarily differ in any way from stars with regard to their appearance. Indeed, if the spacecraft is 10 m in size, already at a distance of 35 km it cannot be distinguished from a star, and its glare will be determined by the phase of illumination by the sun and aspect , in addition to dimensions and reflective properties of its surface. Let us consider a spacecraft in the form of a sphere 10 m in diameter with a diffuse coefficient of reflection of 0.3 and illumination by the sun's lateral light (1/4 phase). For this case, its brightness will have the values listed below:

Threshold glare of spacecraft, μlux	10,000	2500	800	400	100	4	1	0.01
Distance to spacecraft, km	10	20	35	50	100	500	1000	10,000

As we see, the glare [brightness] of the spacecraft at a distance of several tens or even hundreds of kilometers will be many times greater than the brightness of navigational stars. This warrants the statement that there must be several neutral filters in sextants to equalize the brightness needed for reliable and accurate measurement of angles between a star (planet) and the spacecraft. This applies in particular to the case of measuring angles when the distances to the object are less than 20 km, when it would appear elongated to the viewer. It must be stipulated that, for distances of 35...100 km such an object could also appear elongated, even though the angular dimension is considerably smaller than the eye's resolution. This phenomenon occurs due to irradiation of stimulation of retinal regions of the eye that are adjacent to the one on which there is the image of the star. It is known that the greater the irradiation, which also means the size of the luminous object, the greater its brightness. Let us try to estimate the visible angular diameter of a star as a function of its brightness. Let us consider that the following are the main causes of irradiation: diffraction of light on the margin of the pupil; aberration of optical media of the eye, particularly the marginal regions of the cornea and lens; scatter of light in media of the eye; scatter of light in layers of the retina; additional expansion of the circle of scatter due to the large receptive fields of the retina.

The large number of factors causing the irradiation phenomenon warrants the assumption that the most probable law of distribution of illumination from a star on the retina according to its angular diameter will be the normal law, i.e.:

$$E(\gamma)=\frac{E}{\sigma\sqrt{2\pi}}e^{-\frac{\gamma^2}{2\sigma^2}},$$

where γ is angular distance from the center of the image of the star and σ is the parameter of the normal law.

Let us assume that there is a threshold level of illumination of the pupil E_0, below which there is no sensation of light in the eye. We can then write down the following equation:

$$\frac{E}{\sigma\sqrt{2\pi}}e^{-\frac{\gamma^2}{2\sigma^2}}=\frac{E_0}{\sigma\sqrt{2\pi}},$$

from which we obtain the angular diameter of the circle of irradiation in the form of:

$$\gamma_1=2\sigma\sqrt{2\ln E/E_0}.$$

In view of the fact that the diameter of the irradiation circle is close to 1' for a star of the sixth magnitude and taking E_0 = 5 nlux, we obtain σ = 0.4'. Under these conditions, we shall have:

$$\gamma_1 = 0{,}8\sqrt{2\ln\frac{E}{5\cdot10^{-9}}}.$$

Calculations using this formula yielded the following results:

Illumination on the pupil, μlux	0.011	0.07	0.17	0.45	1	10	100	1000
Diameter of irradiation circle, angular min	1	1.84	2.12	2.4	2.6	3.12	3.55	3.95

As we see from the submitted data, the angular diameter of the circle of irradiation increases, though slowly, to values that could yield an inadmissibly high magnitude of astronomical measurement error. This confirms the desirability of reducing glare of the object for more accurate superposition of the image of the object in the sextant over the star. However, it should be borne in mind that marked reduction of brightness of stars, the distance between which is being measured, makes it difficult to work with a sextant and increases measuring error. One could therefore believe that there is an optimum level of brightness that leads to minimal reading error. Its specific level will depend, to some extent, on the design of the sextant, operator working conditions and other factors. Nevertheless this level is of the order of 10 μlux. In conclusion, let us mention that all of the foregoing refers to the naked eye. However, inclusion in the sextant system of diopter systems, calculation of their optimum parameters, transfer functions, coefficients of absorption of light filters, etc., should be based entirely on the above comments.

We shall now cite a few photometric characteristics of the moon as an object of astronavigational measurements. The moon does not have an atmosphere, and this makes it much easier to measure angular distances between stars and the moon's horizon. However, it must be borne in mind that the brightness of the moon's surface illuminated by the sun (full moon) constitutes about 5000 cd/m^2, i.e., it is to great for astronomical readings.

The increase in angular dimension of the moon during flight elicited the subjective impression of increase in its brightness. Thus, one should consider it quite desirable to use an absorbing light filter in astronomical measuring instruments.

The lunar luminous constant, i.e., illumination of the full moon at a distance equaling the mean distance between the earth and moon, is 0.3 lux. Hence, the dark side of earth illuminated by a full moon would have a mean brightness of 0.03 to 0.07 cd/m^2, depending on the cloud cover over the earth's surface. At this level of brightness, there is 5-3-fold reduction of resolution of vision, as compared to the usual level. However, use of rapid diopter instruments in angle measuring instruments makes it possible to measure angles between space objects and objects on the dark side of earth illuminated by a full moon rather effectively for 1-2 days a month.

The lunar disk illuminated by earth, the so-called earthshine, can be used with even more success. The brightness of the moon's earthshine can constitute up to 0.4 cd/m^2, i.e., about 10 times greater than that of earth. There is reason to believe that use of the moon's horizon illuminated by earth for astronomic measurements may be wiser in many cases than the horizon illuminated by the sun.

Let us discuss some of the parameters of the sun as an object of astronomic measurements. The brightness of its surface constitutes a mean of about 2000 Mcd/m^2. It is higher in the center of the solar disk, where it reaches 2500 Mcd/m^2, whereas on the margins it is somewhat lower--1300 Mcd/m^2. The sun is surrounded by an atmosphere, the thickness of which is so small that it does not affect accuracy of readings at distances equaling the average distance to earth, Venus and even Mercury. During interplanetary flights, the brightness of artificial space vehicles at different distances from the sun can be readily calculated, considering the fact that the spherical intensity of solar light is $3.0 \cdot 10^{27}$ cd, whereas absorption of light in space equals zero. The dimensions of such objects, the phases of their illumination by the sun, foreshortening and mean brightness coefficients of their surfaces should be known.

When designing astronavigation systems for a spacecraft, it should also be borne in mind that astronavigational observations aboard a spacecraft are difficult because of the diverse background spots. The sources of these spots could be the sun, moon and earth. In addition, the inside light sources and reflection from parts of the spacecraft also make astronavigational observations difficult.

The magnitude of background spots reflected by radiation from the earth's atmosphere is determined by the equation $\Phi = 3.14\ SB\tau\gamma^2$, where S is the area of the instruments input aperture of the instrument, B is background brightness at the input of the instrument, τ is the transmission coefficient and γ is the angle of the instrument's field of vision.

Hence, we see that the magnitude of background spots Φ increases proportionately to the square of angle of visual field γ. Thus, background spots have the most substantial effect on observations dealing with identification of navigational reference points, when the width of the astronavigation instrument visual field is at a maximum.

The navigation instruments must have a visual field of at least 40° for certain identification of navigational landmarks. With such width of the visual field, the spot from earth's atmosphere could be so large that some navigational stars would not be distinguished against its background.

A laboratory experiment was conducted to assess the effect of light reflected from earth's atmosphere on discernibility of stars. During the experiment, a background spot from earth's atmosphere was simulated and an astronavigation instrument used with 40° width of visual field. Maximum discernible stellar magnitudes were obtained as a function of their angular distance from earth's horizon. Thus, with 20, 30, 40 and 50° angles between the star and earth's horizon, the maximum discernible stellar magnitudes constitute +0.7, +1.5, +2.0 and +2.5, respectively.

According to the foregoing, only stars of the first order of magnitude or brighter are discerned at angular distances of less than 30° from earth's horizon. If we consider that it is desirable to use stars of the third and second magnitude for high accuracy of astronavigational readings, it becomes apparent that optimum accuracy of astronavigational measurements is possible at angles of at least 40-50° from earth's horizon.

Foreign specialists believe that, because there is no atmosphere near the moon, conditions would be more favorable for astronavigational readings near its horizon.

However, when landing on the illuminated side of the moon near the terminator, there is a rather high probability of lateral glare [spot] from the Sun in the window [porthole]. Such exposure makes it substantially more difficult to identify navigational landmarks. Attenuation of the effect of lateral exposure [spots] is achieved, as shown by missions on the Apollo program, by using navigational instruments of the periscope type which have a rather large aperture ($S \geq 600$ cm^2). Such instruments make it possible to exclude the intermediate environment of the window from the optical system.

A dirty window pane has an adverse effect on astronomic observations.

The outside panes are most often soiled by the waste from propulsion systems, particularly the attitude engines that are usually situated in the immediate vicinity of windows. According to the report of the crew of Apollo 7, discharge of liquid waste caused formation of crystal clouds that made astronomic observation very difficult for several minutes.

According to the studies of American specialists, outgasing of the silicone seal of panes was the chief cause of a dull film on the window panes. The size of the dull spot on the window can change over a wide range, including complete coverage of the window. The size of the spot diminishes when the window is illuminated by solar rays. This phenomenon was used by the crew of Apollo 8 to improve observation of landmarks on the moon's surface. In preparing for subsequent missions aboard the Apollo, all seals for window panes were submitted to prior outgasing on the ground, and this was quite effective in preventing dirty windows.

2.4. Motor Analyzer and Operative Memory of Cosmonauts in Flight

During space flights, weightlessness is a specific factor that affects the cosmonaut's motor analyzer. It can be maintained that no other analyzer system of man is subject to such changes in weightlessness as the motor analyzer.

Studies of coordination of movements and motor activity in weightlessness were started on man long before the first manned space flight. At first, experiments were conducted in so-called Roman towers, high-speed elevators and in water. The subjects' task was essentially to superimpose images of observed objects. Different data were obtained by different authors. Thus, according to the findings of Lomanako [92], drastic increase in scattered hits was observed at the moment of weightlessness, whereas this was not observed in the experiments of V. S. Gurfinkel' and P. K. Isakov [32]. We must believe that the brief duration of weightlessness did not enable different authors to analyze performance under identical conditions. The test conducted by L. A. Kitayev-Smyk [45] during weightlessness in an aircraft revealed that the accuracy of superposition diminished, the shift occurring upward and to the right.

A. A. Leonov and V. I. Lebedev described the results of studies of coordination during brief weightlessness, in which they used a special coordinograph instrument [51]. They found that the speed of motor acts diminished in some cosmonauts in weightlessness. In subsequent flights, the speed of performance of this test was the same as obtained on the ground.

Authors who studied the effects of stable weightlessness devoted much attention to writing skill, the stability and individual distinctions of which are well-known, in the study of fine coordination. Thus, according to Yu. M. Volynkin [19], who analyzed the handwriting of B. B. Yegorov during flight, there was a 51% increase in time of writing some complex elements, whereas the increase constituted about 12% for simpler ones (numbers, signature).

Operations involved in manual control of the spacecraft were found to be the most impaired. For this reason, during the first missions, all manual control systems were backed up by automatic ones to improve reliability.

At the same time, analysis of the time spent on these operations revealed that it was longer at the start of a flight than in subsequent passes or training on the ground.

It is known that operating a telegraph key is the basis of radiotelegraphic communication. This activity involves finely coordinated hand movements. In this case, the quality of transmission of information depends on proprioceptive sensibility and time predicting [gauging?] function. Analysis of this form of cosmonaut activity during actual flight could contribute much to the demonstration of the distinctions of motor analyzer function in weightlessness.

Let us analyze the radiograms of P. I. Belyayev during his flight aboard Voskhod-2 spacecraft. Figure 22 illustrates the time graphs of different symbols in the Morse code taken from radiograms referable to the first passes and those sent shortly before the end of the flight [75]. For the sake of comparison, also illustrated are the same values selected from radio texts transmitted by P. I. Belyayev during training on the ground. As can be seen from the graphs, the motor part of the skill of radiotelegraphic communication underwent considerable changes, particularly at the first stage of the flight.

Experiments dealing with the dynamics of motor function of cosmonauts were started during the flight of the Voskhod-2 spacecraft and were continued aboard all spacecraft of the Soyuz type and Salyut orbital station.

Incidentally, let us note that, with increase in requirements of accuracy of man-machine systems, the means of relaying command information is becoming increasingly complicated, with increase in number of display equipment, and in structure of data decoding. Analysis of command motor impulses of cosmonauts pertaining to control of the spacecraft and navigation systems leads us to assume that the tracking reaction (pursuit and compensatory), simple operator reactions, reactions of choice and complex associative forecasting reactions could serve as the psychophysiological correlates of these movements. For this reason, the experimental psychophysiological part of the scientific programs of space flights was planned on the basis of these considerations [80, 30, 41]. The results of studies of man's dynamic characteristics are particularly important for further optimization of control systems of future, maneuverable spacecraft, making soft landings on other planets, docking, etc. For this reason, a model control system was used for the first time aboard Voskhod-2. The object of the studies consisted of the above-mentioned operator functions included in the model control (tracking) system during exposure to space flight factors and, first of all, prolonged and stable weightlessness.

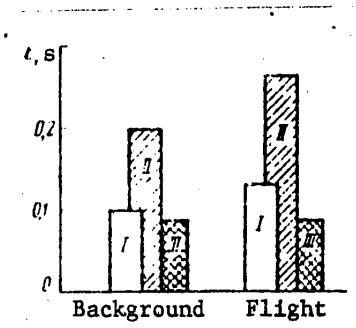

Figure 22.
Main parameters of radio messages of P. I. Nelyayev on the ground (background) and in space
I) duration of interval
II) duration of dash
III) duration of dot

Usually, one uses visual displays and, less often, audio indicators in studies of the tracking process. The difference between input and output signals expressed in different ways is always considered the quantitative gauge of the tracking process, while the operator's task is to reduce to a minimum the mismatch between signals. The function of this error over a specific period of time is a characteristic of operator performance.

There is particularly broad coverage in the literature (unrelated to space flights) of studies of human behavior in tracking systems as related to number of control levers, characteristics of input signal, damping of regulatory units, effects of some noises, etc. In describing tracking systems, many authors refer to theory of communication in closed servosystems, considering them as models of the man-machine tracking system. This thesis was very convenient for psychologists, who had difficulties in their studies in offering accurate descriptions of the system, while servomechanism theory is a method of mathematical analysis where the output of a complex system is described as a function of input signals, so that its functional characteristics can be established.

Thus, examination of the relation of input signal to output signal (change of input signal by the system) or transfer functions of the system is the subject of such studies. However, this generally involves the use of very complicated and cumbersome equipment, which is difficult to use on spacecraft. For this reason, the authors developed a functional system of a tracking process recorder (TPR) and designed a special miniaturized recorder.

In order to create a self-contained tracking system, we used the method of visual display with graphic recording of the output signal. The input signals were put on the tape of a tape-feeding mechanism, in the form of a sinusoid differing in frequency and other curves. The output signal was recorded by a pen recorder--finder, which was closely linked with the control lever. It was possible to study the operator's reactions during immediate and deferred feedback, i.e., there was simulation of an inertial control system. The contrast of the presented curve constituted about 0.85. The shape of the curves, their order and duration were the same at all stages of the experiment. The tape was fed at a stable rate of 5 mm/s.

Each measurement of a reaction consisted of 50 sinusoidal signals, 12 square-wave pulses collected in alternating order and signals of random processes in two segments, i.e., there was sufficient digital material for statistical processing on a computer. The study of dynamic characteristics of the operator in these experiments made it possible to define the following, which we know from automatic control theory: amplitude-frequency characteristic $A(\omega)$; phase-frequency characteristic $\phi(\omega)$, autocorrelation function R, coefficient of reciprocal correlation r, transfer function and certain other characteristics of the operator as a dynamic element of a control system.

The cosmonauts worked with a TPR under laboratory conditions, in a training spacecraft to fulfill a flight program, in a spacecraft during the prelaunching period and in flight. Reactions were measured 3-4 times at all stages of the study, with the exception of those conducted in flight. Each measurement of the reaction consisted of 50 sinusoidal signals and 22 square-wave pulses gathered in random order.

Analysis of all of the obtained data, as well as of frequency characteristics, led us in virtually all cases to describing the dynamic properties of an operator engaged in tracking by means of the following equation:

$$W(p)=\frac{ke^{-p\tau}(aT_1p+1)}{(T_1p+1)(T_2p-1)},$$

where $W(p)$ is the operator's transfer function, τ is operator reaction time, T_1 is the time constant characterizing the lag in the operator's oculomotor system, a is the coefficient characterizing the degree of participation of psychophysiological mechanisms of anticipation, T_2 is the time constant for delay in operator's decision making, k is the amplification factor and p is the Laplace transform argument.

According to analysis of transfer function, the damping coefficient changes in flight in the range of 0.1-1.0. Its optimum value is 0.7.

Analysis of amplitude-frequency and phase-frequency characteristics of the operator as a dynamic element of a control system revealed that the quality of tracking higher frequency sinusoid signals worsens, particularly in flight. For example, noticeable changes in amplitude-frequency characteristics during flight occurred already when working with a signal having a frequency of 3-4 rad/s. Analysis of phase-frequency characteristics showed that changes start at input signal frequency of the order of 1-2 rad/s, and in this case the magnitude of change was greater. Experiments revealed that there was an increase in duration of the transient process by a mean of 1.5-2.0 times for the operator to adjust a solitary mismatch during space flight. It is not possible to define this time more accurately because of substantial dispersion, which increased even more in flight, constituting 0.35 s^2, which corresponds to 45% in relation to mean value of the transient process and almost 75% according to standard measurement error. Moreover, in the course of the flight we observed a tendency toward monotonous increase in duration of the transient process, which was apparently related to progressive fatigue and adaptation of the neuromotor system to weightlessness, when its overall tonus diminished more and more with increase in duration of the flight. This occurred in particular when no intensive physical exercise was performed.

It should be noted that the above-mentioned high dispersion of duration of the transient process, which occurred during space flight, was attributable to some extent to the less convenient conditions of working with the instrument than on the ground. For this reason, the design of astronomic measuring instruments must meet several special conditions to assure better and faster work with them. In particular, an important prerequisite is to have the astronomic measuring instrument well-secured aboard the spacecraft. The gear ratios of lever movements, magnification of the sighting telescope and its luminous power will have an appreciable effect on accuracy of astronomic readings. As shown by the results of experimental studies, the brightness of stars or space vehicles [objects] between

which the angles are measured should be at least +1 stellar magnitude, otherwise there could be a marked increase in lag [value of τ in the expression for $W(p)$] and hence in work time. Such an effect can be the result of a wide difference between brightness levels of two stars, the images of which are superimposed for the measurements. In this case, adaptation of the eye becomes established at a certain mean level between the two stars, and for this reason the less bright star would be perceived as being dimmer than if it were alone in the field of vision. For this reason, by virtue of the well-known law [54], the inertial properties of the eye would be more pronounced.

To sum up the analysis of our experimental data, we can see that there are two types of changes in nature of oculomotor coordination which is the most responsible for accuracy of astronomic measurements during a space flight, as compared to terrestrial conditions: in the first place, extension of all processes occurring in the operator's motor sphere and, in the second place, increased instability of work, which is manifested by increase in dispersion of mistakes in oculomotor coordination. These two factors together would, of course, diminish accuracy of astronomic readings in flights. This decline constitutes a mean of ~50%. It must be borne in mind that further refinement of the design of astronomic measuring instruments, as well as of methodology of conditioning and training cosmonauts before flights could improve substantially the accuracy of astronomic measurements.

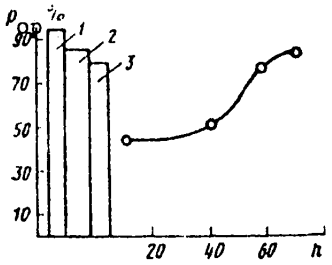

Figure 23.
Change in reliability of operative memory P_{op} as a function of duration of space flight (mean data)
1) background data obtained from laboratory experiments
2) data obtained in training spacecraft
3) data obtained during training

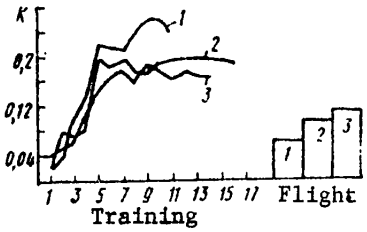

Figure 24.
Change in reliability of operative memory during training and 1-day space flights (K--general coefficient of quality of operative memory)
1) data for cosmonaut A
2) data for cosmonaut B
3) data for cosmonaut C

As has been shown previously [73], operative memory is the structural basis of operator performance in an extrapolation system. For this reason, during the flights aboard Voskhod-2 and Soyuz-6 spacecraft we studied the dynamics of cosmonauts' operative memory, comparing it to the parameters obtained on the ground and in a training spacecraft.

Figure 23 illustrates the mean results of testing operative memory of subjects while fulfilling programs of long-term space flights (8 experiments, 16 subjects,

240 measurements). Analysis of the submitted data confirmed the assumption we previously expounded that there is an adaptation phase in dynamics of psychophysiological functions. It was demonstrated that, under the experimental conditions, operative memory diminished on the first day of flight and held, with some variation, at 35-45% of the control level to the end of the experiment. Longer experiments did not alter the previously obtained data. Thus, in the course of a 70-day experiment, it was also possible to single out the adaptation phase of changes in operative memory and persistent change in this function in the next phases.

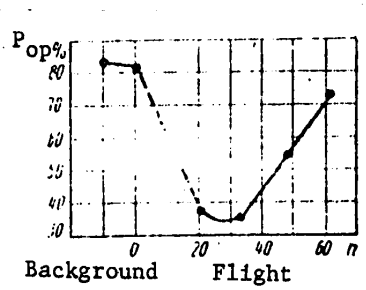

Figure 25.
Comparative characteristics of operative memory at different stages of many-day space flight (P_{op}--reliability of operative memory)

During preparations for performing the scientific research program in flight, each cosmonaut participated in 12-16 training sessions, during which 70-100 measurements were taken of tests characterizing the functional level of operative memory [75]. In all cases, a stable "plateau" was reached for this form of activity, which served as the control background. Figure 24 illustrates the findings referable to a 1-day flight (B. B. Yegorov, P. I. Belyayev and A. A. Leonov) and Figure 25 to a many-day flight (G. S. Shonin, V. N. Kubasov).

As can be seen from the results illustrated in these figures, starting with the fifth and sixth training sessions the general coefficient of performance quality became set at one level and did not undergo appreciable changes thereafter. The highest coefficient was found for B. B. Yegorov, The same figure illustrates results obtained during a space flight (using mean data for the flight as a whole). A decline was inherent in this coefficient (most marked in B. B. Yegorov) during the flight.

In the case of the multiday flight, there was fluctuation of reliability of operative memory characterizing the adaptation phase of flight and phase of established work capacity. The results indicate that space flight factors, particularly prolonged weightlessness, diminish lability of memory, which can be classified as operative according to all of its characteristics. The fact that operative memory diminishes should also be taken into consideration when forecasting performance of tasks dealing with identification of navigational stars and orientation in the process of taking astronomic readings.

CHAPTER 3. PROBLEMS OF ENGINEERING PSYCHOLOGY IN DEVELOPMENT OF VISUAL OPTICAL MEANS OF SPACE ASTRONAVIGATION

3.1. Use of Optical Visual Devices

At the present time, increasing preference is being given to self-contained navigation equipment for space flights. As the programs of space exploration grow more complicated, the importance of autonomous navigation systems will increase, the class of problems solved with use thereof will expand, and there will be an increase in requirements of their accuracy, speed and reliability.

Several specialized visual optical navigation instruments for manned spacecraft have already been developed, both in our country and abroad. Some of our instruments have undergone trials aboard Soyuz series spacecraft and the Salyut orbital station. Some experience in using opticovisual navigation instruments was gained during preparations for and participation in space flights. For this reason, we are able to solve problems of navigation using existing optical devices and work out the main specifications for future instruments and systems.

In developing opticovisual means of space astronavigation, it is very important to take into consideration the experience gained during actual space flights. For example, considerable attention was devoted to testing astronavigation systems and observation of navigational landmarks during flights aboard American spacecraft on the Gemini program.

Several navigation experiments were conducted.

1. Observing setting of stars beyond earth's horizon on the dark side of the orbit.

The experiment was conducted by the crews of Gemini 7, Gemini 10 and Gemini 11. It was established that stars of less than 1.5 stellar magnitude could not be seen in open space through the light filter of the space suit.

2. Photography of objects on earth's surface.

In this experiment, the crew of Gemini 5 (Conrad and Cooper) detected rather small objects (individual ships, aircraft) on earth.

3. Measurement of "star--star" and "star--object" (carrier rocket stage) angles.

This experiment was performed by the crews of Gemini 4, Gemini 6 and Gemini 7. It was also conducted during the flight aboard Apollo 7 in 1968. The crew of this

spacecraft succeeded in viewing the last stage of the carrier rocket by means of a sextant at a distance of up to 550 km.

4. Observation of special markings laid out on earth. As such markings, 16 white strips were used, which were paved with plaster (Laredo, Texas), as well as shell-rock (Carnarvon, Australia). The target indication of these signs was performed by means of smoke signals. The crew of Gemini 5 and Gemini 6 were able to observe these signs at a distance of 640 km.

The program of astronavigation experiments performed by the crew of the Apollo included most of the experiments that had been previously conducted aboard Gemini.

The technical tasks included the following: elimination of spots; development of devices that would permit observation of navigational stars on the day side of orbit; providing for high light transmission.

When methodological problems are solved, it will be possible to make the final choice of observation objects (navigation landmarks) and methods for processing the obtained information in order to assure optimum efficiency of the astronavigation system.

The statements of the cosmonauts also revealed that they set up many engineering psychological problems, the solution of which would permit development of an optimal ergatic operator--instrument system. The following tasks should be included here: choice of optimum coefficient of magnification; determination of size of visual field for certain identification of navigational landmarks; providing for the necessary accuracy of readings; development of optimum system to stop the image from "wandering" [running], and generally speaking developing a piece of equipment that takes into consideration the dynamics of the object (manned spacecraft), etc.

3.2. Specifications for Space Sextants

The effects of space flight factors on man, as part of the system of space astronavigation, the accumulated experience with space flights, as well as ground-based studies, enable us to formulate, even now, several specific requirements of opticovisual instruments for space astronavigation.

Let us discuss several general requirements of space sextants.

1. Presence of two sighting lines. The fact of the matter is that one cannot use pendulum verticals to create the datum point base in sextants. Use of other types of verticals leads either to great errors and increase in dimensions and weight that are not acceptable for opticovisual equipment, or loss of autonomy of the system. For this reason, stars are used as the datum base in developing space sextants, since they are an excellent datum base because of their very distant location [35]. But stars carry no information about the location of a manned spacecraft. As a result, it is necessary to add a second sighting channel to the sextant to measure the direction of the navigational landmark (nearest celestial body). We shall call such a two-channel sextant a sight-sextant (SS). The angle measured with the SS between directions to the star and landmark defines the surface of the spacecraft position and constitutes primary navigational information.

Thus, a two-channel optical system, which permits simultaneous viewing of two sighted objects, must be used in a space sextant.

2. Visual field of sextant. It was established experimentally that the sextant's field of vision should be about 40° for certain detection and identification of navigational stars and landmarks. If a small visual field is chosen for some reason or other, there must be provisions for high viewing speed.

3. Sextant magnification. We know that sighting is improved with increase in sextant magnification. However, it is necessary to reduce the sextant's visual field to increase magnification with retention of dimensions of the instrument within a wise range. As a result, the task of detecting navigational stars and terrestrial landmarks, and to measure angles between them from a spacecraft could become quite difficult. For this reason, in preparing the specifications for the sextant, it is necessary to search for compromises in selecting magnification and field.

Below are the results of laboratory studies of accuracy of astronomic readings as a function of sextant magnification [82]:

Sextant magnification	2.5	6	8	12	16	20
Root mean square error of sighting, angular s	22	15	12	8	6	5

The more precise results of astronomic readings are attributable mainly to increase in angular distance between images of the sighted objects.

These data indicate that accuracy of readings increases by almost 32% when magnification is increased from 2.5 to 6. On the other hand, an increase in magnification from 10 to 20 increases accuracy by only 15%, but worsens significantly the conditions for identifying stars, which we mentioned above, and makes measurement difficult due to the high angular rate of movement and shaking of the image of the stars in the eyepiece when taking readings with a sextant that is not secured. Analytical studies revealed that to assure encounters of spacecraft in orbit, the permissible error of readings when using a sextant as a self-contained means of navigation would be of the order of 10' [35]. For this reason, there should be over 8-fold magnification of the sextant telescope for these purposes.

4. Multifunction. There are many natural sensors of navigational information (stars, sun, moon, earth, etc.) in space. For this reason, a space sextant must make it possible to observe and sight them, in spite of the wide scatter of their illumination characteristics. The cosmonaut must be able to adapt to changes in flight conditions. This makes it necessary to provide filters differing in optical density.

5. Multimodality. Since the space sextant could be used, on the one hand, as a means of correcting the inertial navigation system and, on the other hand, as a spare navigation tool, it must have provisions for automatic and manual collection of navigational information. For automatic collection, precision sensors of angles of rotation of the main mirrors of the space sextant must be installed, and they must be linked with an alphanumeric computer.

To increase the reliability of the navigation system, there must also be provisions for the feasibility of reading data by man, directly from dials [dial devices].

6. Mechanism to stop image "wandering." As shown by different studies, the dynamic characteristics of the manned spacecraft affect the accuracy of measuring navigational parameters. This has the most adverse effect when sighting landmarks on the surface of a planet in near-planet navigation. In this case, "wandering" of the image must be compensated by means of some sort of electromechanical drive operating automatically from signals computed by an alphanumeric computer on the basis of information from the INS [inertial guidance system?]. In this case, the operator would work under conditions where the visible "wandering" [or running] of the image is determined solely by errors of compensation. The reading accuracy then increases significantly.

7. Connection with timer [time sensor, clock]. The high speed of the spacecraft makes it necessary to be extremely accurate in checking the time of taking angular measurements. While, for example, timing errors of 1 s could lead to an error of several tens or hundreds of meters in determining the location of a ship or aircraft, the same error would cause a difference of 7000-8000 m in locating an orbiting spacecraft. For this reason, space sextants must be connected to a chronometer that permits fixing the time of taking angle measurements.

8. Compensation of systematic sighting errors. This requirement means that there must be thorough examination of each instrument during exposure to factors that affect its characteristics.

For example, the uneven surface of the window glass, presence of a wedge-like angle between two surfaces of window glasses, as well as distortion of glass surface due to pressure difference on both sides of the cabin, are factors that affect distortion of object sighting lines. The difference in refraction coefficient of the environment in which light spreads (space, interior of spacecraft) is a fourth factor that is not directly related to the window.

Distortion of the surface of window glass, a wedge-shaped angle and pressure gradient can be demonstrated both analytically and experimentally. Knowing the characteristics of glass, angle of incidence and location of beams hitting the glass, one can eliminate such errors within a range of up to 1".

One can estimate the correction for the difference in refraction if one knows the measured angle, pressure and temperature in the spacecraft, as well as direction of sighting lines in relation to the surface of the window glass.

Other similar errors must be evaluated and compensated in an analogous fashion.

9. Utmost simplicity, reliability and long operating time.

10. Minimum dimensions, weight and energy consumption. Specific requirements for sextants can be formulated only with due consideration of the functions they perform on a specific manned spacecraft.

For example, the requirements for the sextant used to conduct experiments aboard Gemini 12 were formulated as follows:

Precision	+10'
Maximum weight	6 pounds
Maximum length along main sighting line	7.5 inches
Eyepiece use	normal and away from eyes when working with space helmet visor closed

Information obtained in the course of experimental studies enabled the NASA Research Center in Ames to define the specifications for a space sextant to be used for orbital flights around earth and to the moon [99, 101]. These requirements were as follows:

Magnification	8× (normal eyepiece)
Magnification	4.6×(eyepiece with attachment)
Telescope visual field angle	7°
Sextant's margin of error (overall)	no more than +10'
Moving mirror actuation	1 and 5° per turn of handle
Range of measurements	6 to 70°
System of sextant	with two lines of sight
Weight of sextant	2.7 kg (selected rather arbitrarily)

In addition, there were several requirements, such as a chronometer on the sextant with a button to start it and delivery of a synchronizing pulse at the moment of reading the angle on the onboard recorder or computer, filters of different optical density for simultaneous sighting of objects differing in brightness, need to illuminate the angle counter and eyepiece hairs, mechanical angle counter. There was special mention of the fact that the cosmonaut must be able to work with the sextant when the space helmet is closed, as well as with a guard-filter used in an emergency situation. The latter required an additional attachment for the eyepiece, so that it could be at a distance of at least 5-7.5 cm from the eye.

New space sextants are being developed on the basis of the above requirements. At first such work was pursued on the basis of existing aviation and maritime sextants. The changes made in their design were usually directed toward making work easier with them for cosmonauts during flight and increasing sextant accuracy [1, 88]. However, there are already some original instruments that are based on new principles.

The functional diagram and main design features of a special type of space sextant have been published [88]. It was indicated that use of a mirror made of beryllium, which precluded the effect of temperature fluctuations on accuracy of readings, as well as high quality of manufacturing the drive gears for the mirror, resulted in a margin of error in the sextant not exceeding 10". Moskowitz et al. [95] describe the design and drawings for a space sextant consisting of 3 telescopes with visual field angles of 40, 7 and 1°. The sextant is equipped with a spectrometer that permits measurement of Doppler shift of spectral lines in the radiation from sighted stars, which permits calculation of radial velocity of the spacecraft. The weight of such a sextant is estimated at about 2.7 kg, while the margin of error does not exceed 1".

Let us consider the construction of one type of space sight-sextant, which was developed with consideration of the above-formulated requirements and is a visual optical instrument for autonomic determination of the coordinates of the craft's location [99, 101].

The space sight-sextant, a diagram of which is illustrated in Figure 26, is a combination in one instrument of an optical sight and sextant, and it consists of the following: a) Optical mechanical sight consisting of the main sight mirror 3 with sensors of directional angles of terrestrial (lunar) landmarks, sight window (*4*), optical system of sight (*5* and *7*), mechanism for controlling position of main sight mirror and automatic setting of "wandering" of image of earth's (moon's) surface (*8*), binocular viewing system (*9*), eyepieces of binocular system of sight (*10* and *11*); b) mechanical optical sextant instrument consisting of sextant window (*1*), main sextant mirror (*2*) with sensors of angles of direction to celestial bodies, stationary semitransparent mirror (*17*), optical system of sextant (*15* and *16*), mechanism for controlling position of main sextant mirror (*14*), monocular system of viewing the sky (*13*), sextant eyepiece (*12*).

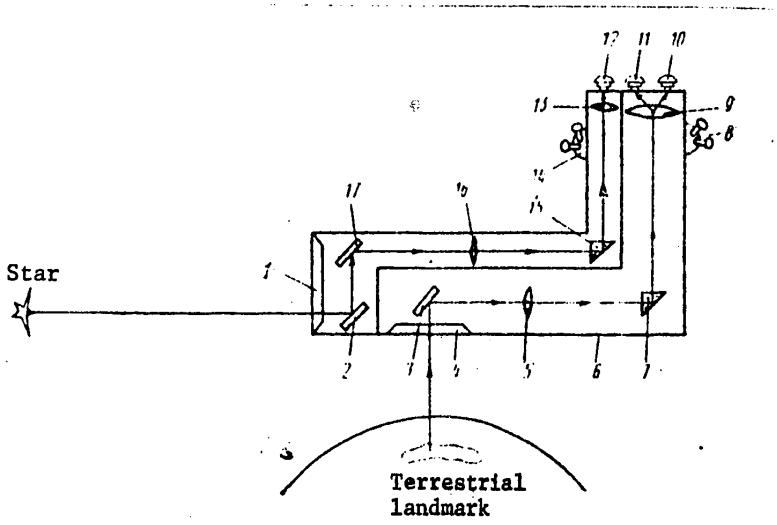

Figure 26. Diagram of space sight-sextant

1) sextant window
2) main mirror of sextant
3) main mirror of sight
4) sight window
5) optical system of sight
6) housing
7) optical system of sight
8) mechanism to control position of main sight mirror
9) binocular viewing system
10, 11) eyepieces of binocular vision system
12) sextant eyepiece
13) monocular system for viewing sky
14) mechanism to control position of main mirror of sextant
15, 16) optical system of sextant
17) stationary semitransparent mirror

The task for the operator-astronaut is to superimpose identified images of navigational heavenly bodies and the terrestrial (lunar) landmark over the center of the visual field of the space sextant. When these images are visually superimposed over the center of the instruments field and a special button is depressed, there is automatic reading and storage of readings of sensors of the angles of position of main mirrors of the sextant, and the time of the measurement is recorded.

During a space flight, astronomic measurements are made when the "wandering" of the image in the field of the sextant is stopped in order to facilitate the process of identification by the operator-astronaut of navigational stars and landmarks. Image "wandering" is stopped automatically by using the algorithms for selection of navigational stars and landmarks on the onboard digital computer and adjusting the main mirrors of the sextant in the direction of specified stars and landmarks.

In this mode of work, the operator-astronaut is given only the task of eliminating mismatch and superposing the images of the star and terrestrial (lunar) landmark over the center of the sextant's field.

To work with such instruments, the astronauts must be able to correctly choose the navigation parameter to be measured in a given situation, i.e., he must know approximately what their characteristics are and have stable professional skill, developed on earth, in taking measurements.

3.3. Navigational Parameters Measured With Space Sextants and Measurement Errors

At the present time, the following navigational parameters can be measured with space sextants: angle between directions of navigational star and landmark on a planet's surface; angle between directions of navigational star and artificial satellite of planet, as well as probe released from a spacecraft; angle between directions of navigational star and centers of planet or its satellite (vertical of earth, moon, etc.); angle between directions of navigational star and visible planet horizon; angle between directions of two landmarks on surface of planet, in the centers of two artificial satellites or two planets; angle between vertical to the planet and landmark on its surface; angular diameter of celestial body (sun, earth, moon and other artificial or natural bodies).

In addition, other angular values can be measured, as well as the rate of change in these values, Doppler shift of spectral lines in radiation from sighted stars, etc.

We shall discuss navigational measurements involving the use of an artificial problem on the basis of foreign investigations.

Astronomic measurements of "probe--star," "probe--terrestrial landmark" and "probe--lunar landmark" are based on releasing an artificial probe from a spacecraft and subsequent measurement by the astronaut, using a sextant, of the angular position of the probe in relation to identified navigational stars or terrestrial (lunar) landmarks. The method of self-contained navigation, which is based on the release of an artificial probe, makes use of the effects of the gravity fields of earth and the moon on movement of the artificial probe and spacecraft.

In view of the fact that this method does not require mandatory viewing of terrestrial (lunar) landmarks, astronomic readings can be taken when the earth's surface is covered with clouds. However, when taking astronomic measurements by this method, some time is required for stabilization of the probe by the gravity field of earth (moon). For this reason, when there is a shortage of time for astronomic readings, use is made of other stars and landmarks.

Thus, the use of an artificial probe combined with natural navigational stars and landmarks solves the problem of astronavigation aboard manned spacecraft, not only in orbital flight, but in flights from the earth to the moon and back, in the absence of visibility of terrestrial landmarks.

Any of the above-mentioned navigational parameters measured from a manned spacecraft determines the surface, in each point of which it will be the same at a given point in time. To put it differently, the measured parameter determines the surface of the position of the spacecraft or geometric location of points of its possible position characterized by constancy of the measured parameter.

Since measurements of a parameter are made with some element of error under the influence of different causes, the position surfaces obtained in measuring navigational parameters deviate from the actual ones. One can determine the link between navigation measurement errors and errors in determining position surfaces by using the concept of gradient of measured function.

As we know [20], the linear displacement of position surface in the direction of the normal is determined by the equation $\Delta n = \Delta\Theta/g$, i.e., it depends on error of measuring parameter Θ and modulus of gradient g.

If function Θ is specified analytically in a rectangular system of coordinates, $\Theta = \Theta(x, y, z)$, the numerical value of the gradient modulus is determined with the formula:

$$g = \sqrt{(\partial\theta/\partial x)^2 + (\partial\theta/\partial y)^2 + (\partial\theta/\partial z)^2}.$$

Analogously, the error of determining the surface of the spacecraft position and error manifested by change in navigational parameter Θ are related by the equation $\Delta p = \Delta\Theta/g$. By using this correlation, one can estimate the error of determination of surfaces of the spacecraft position when measuring various navigational parameters.

When measuring angle Θ between a navigational star and landmark on a planet's surface, the equation for surface of spacecraft position in a topocentric system of coordinates OXYZ, whose Z axis coincides with the direction to the star and the beginning of the coordinates is at the location of the selected navigational landmark (Figure 27) will be written in the form of $x^2 + y^2 - z^2 \tan^2\Theta = 0$; the gradient of this position surface is $g = \cos\Theta/z$; the error of determining the position surface is:

$$\Delta p = \frac{\Delta\Theta}{g} = z\Delta\Theta/\cos\Theta$$

Measurement of angle Θ_1 between the direction of the navigational star and artificial earth satellite also determines the conical surface of position. The difference is that the apex of this cone is at the location of the artificial earth satellite at the time of the measurement. In the rectangular system of coordinates $O_1X_1Y_1Z_1$ (Figure 28) related [linked] to the artificial earth satellite (the axis of this system is oriented along the line that connects the satellite and star), the equation for this surface will be written down as $x_1^2 + y_1^2 - z_1^2 \tan^2\Theta_1 = 0$. The error of determining position surface of the spacecraft when measuring this parameter with error $\Delta\Theta_1$ will be determined from the equation $\Delta p_1 = \Delta\Theta_1/g_1 = z_1\Delta\Theta_1/\cos\Theta_1$.

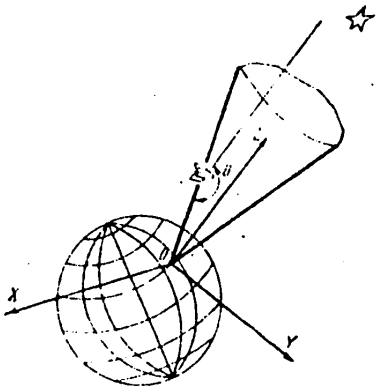

Figure 27.
Surface of spacecraft position determined by angle between directions of landmark on planet's surface and star

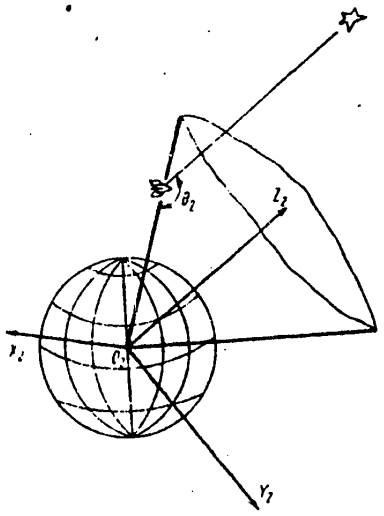

Figure 29.
Surface of spacecraft position determined by angle between vertical to planet and direction of star

The angle between the vertical to the planet and direction of navigational star Θ_2 also determines the conical surface of position. The apex of this cone will be in the center of the planet, while the axis of rotation coincides with the line that connects the star with the center of the planet.

In a geocentric system of coordinates $O_2X_2Y_2Z_2$ (Figure 29), axis Z_2, of which coincides with the direction of the star from the center of earth, the equation for this surface will be written down as:

$$x_2^2 + y_2^2 - z_2^2 \operatorname{tg}^2 \theta_2 = 0.$$

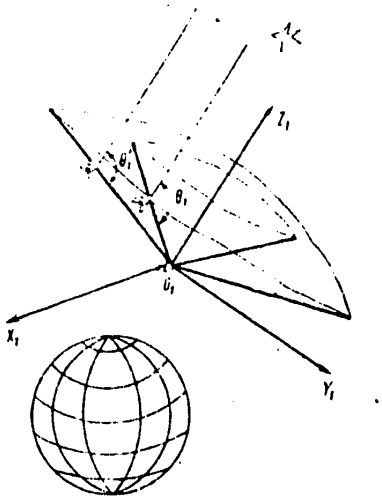

Figure 28.
Surface of spacecraft position determined by angle between direction of navigational artificial earth satellite and star

is also a right circular cone (Figure 30). The apex of this cone is on the line connecting the star with the middle of the planet at distance z_0 from its center:

The error of determining the surface of spacecraft position will be found with the equation $\Delta p_2 = \Delta\Theta_2/g_2 = z_2\Delta\Theta_2/\cos\Theta_2$.

The surface of spacecraft position, when measuring the angle between the navigational star and visible planet horizon Θ_3

$$z_0 = \frac{R_П}{\sin \Theta_3}$$

where $R_П$ is planet radius.

The equation for this surface in a rectangular system of coordinates $O_3X_3Y_3Z_3$, the start of which coincides with the apex of the cone and whose Z_3 axis is in the direction of the line connecting the planet center to the star, has the following appearance: $x_3^2 + y_3^2 - z_3^2 \tan^2 \Theta_3 = 0$. The gradient of this position surface is determined with the equation $g_3 = \cos \Theta_3 / z_3$, while error of determining position surface is

$$\Delta p_3 = \frac{\Delta\theta_3}{g_3} = \frac{z_3 \Delta\theta_3}{\cos\theta_3}.$$

When measuring angle Θ_4 between the directions of two landmarks O_1 and O_2 on the surface of a planet or angle between directions of centers of two planets $П_1$ and $П_2$, the distance between which is commensurable to the distance to the spacecraft, determination is made of the position surface that is a cyclide obtained by rotating the arc of the circumference about axes O_1O_2 (Figure 31a) or $П_1П_2$ (Figure 31b), which connect either two landmarks on the surface of a planet or the centers of two planets (celestial bodies).

The cyclide equation is $l^2 = R_1^2 + R_2^2 - 2R_1R_2 \cos \gamma$, where R_1, R_2 are distances from centers of celestial bodies (landmarks) to the spacecraft, l is the distance between centers (landmarks). The coordinates of the landmarks or centers of celestial bodies and distances between them are known.

In a rectangular system of coordinates $П_1X_4Y_4Z_4$, related to one of the planets П (for example, earth), $l^2 = x_П^2 + y_П^2 + z_П^2$, where $x_П$, $y_П$, $z_П$ are coordinates defining the position of $П_2$ (for example, the moon) in relation to $П_1$ (earth) at the time of measuring parameter Θ.

The distances between $П_1$ and $П_2$ and the spacecraft are determined accordingly by the following equations:

$$R_1^2 = x_4^2 + y_4^2 + z_4^2;$$
$$R_2^2 = (x_4 - x_П)^2 + (y_4 - y_П)^2 + (z_4 - z_П)^2.$$

after differentiation, we shall have the equation for the value of gradient $g_4 = l/R_1R_2$. The error of determining position surface is:

$$\Delta p_4 = \Delta\theta_4 g_4 = R_1R_2\Delta\theta_4/l.$$

Analogously, when measuring angle Θ_5 between navigational landmarks on a planet's surface and the vertical to it, determination is made of position surface in the form of a cyclide, which is obtained by rotating the arc of the circumference about the axis that links the center of the planet with the landmark (Figure 32).

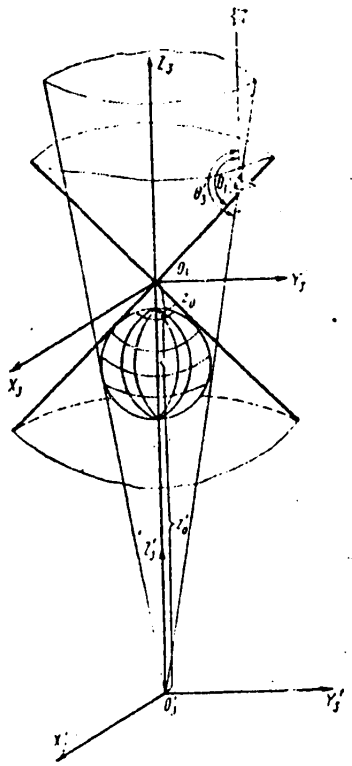

Figure 30.
Surface of spacecraft position determined by altitude of star in relation to visible horizon of planet

The equation for this surface has the following appearance: $R_П^2 = R_3^2 + R_4^2 - 2R_3R_4 \cos \Theta_5$.

For earth in a geocentric system of coordinates $O_5X_5Y_5Z_5$, this equation can be written down on the basis of the fact that

$$R_3^2 = x_5^2 + y_5^2 + z_5^2;$$
$$R_4^2 = (x_5 - x_m)^2 + (y_5 - y_m)^2 + (z_5 - z_m)^2;$$
$$R_0^2 = x_m^2 + y_m^2 + z_m^2,$$

where R_0 is the earth's radius in the following form:*

$$x_m^2 + y_m^2 + z_m^2 = x_5^2 + y_5^2 + z_5^2 + (x_5 - x_m)^2 + (y_5 - y_m)^2 + (z_5 - z_m)^2 - 2\sqrt{(x_5^2 + y_5^2 + z_5^2)[(x_5 - x_m)^2 + (y_5 - y_m)^2 + (z_5 - z_m)^2]} \cos \theta_5.$$

After differentiation, we shall have the equation for determining the gradient: $g_5 = R_0/R_3R_4$.

The error of determination of position surface is:

$$\Delta p_5 = \frac{\Delta \Theta_5 R_3 R_4}{R_0}$$

Measurement of angular diameter of cosmic body Θ_6 determines the position surface in the form of a sphere with its center in the center of the cosmic body (Figure 33). The radius of this sphere is:

$$R = \frac{R_T}{\sin \Theta_6/2} = R_T \operatorname{cosec} \Theta_6/2.$$

If we measure the angular diameter of earth, the equation for surface of spacecraft position corresponding to this navigational system of coordinates will have the following appearance: $x_6^2 + y_6^2 + z_6^2 = R_0^2 \operatorname{cosec}^2 \Theta_6/2$.

The flaw of determining the surface of spacecraft position when measuring angular diameter of earth Δp_6 is determined with the formula:

*Subscript "m" in formulas may refer to landmark ("or" in Russian).

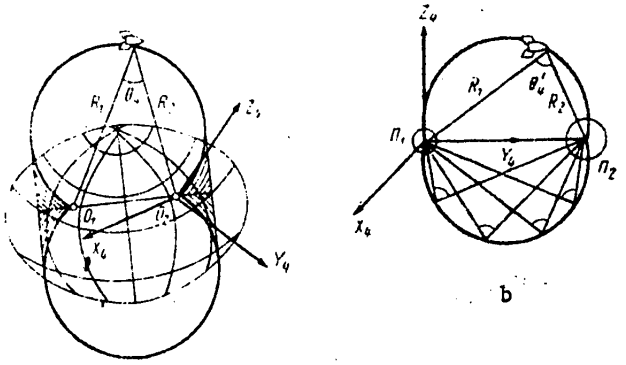

a b

Figure 31. Surface of spacecraft position determined by angle between directions of two terrestrial landmarks or centers of two planets

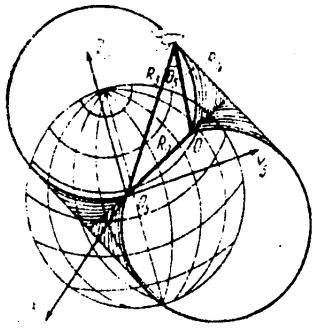

Figure 32. Surface of spacecraft position determined by angle between vertical to planet surface and direction of navigational landmark

$$\Delta p_{\theta} = \frac{\Delta\theta_{\theta}}{g} = \frac{R\Delta\theta_{\theta}}{2\,tg\,\theta_{\theta}/2} = \frac{R_{r}\,\mathrm{cosec}\,\frac{\theta_{\theta}}{2}\,\Delta\theta_{\theta}}{2\,\mathrm{tg}\,\frac{\theta_{\theta}}{2}}.$$

The errors of determination of surfaces of spacecraft position when measuring any other navigational parameters can be defined in an analogous manner.

The above equations for errors of determination of postition surfaces when measuring various navigational parameters enable us to conduct a comparative analysis of the potential accuracy of readings made under different conditions. It must be borne in mind that the choice of a given navigational parameter in each specific instance should be made not only on the basis of the condition of maximum gradient of the surface of spacecraft position determined by this parameter, but of the requirement of minimum error of the measured navigational parameter. The latter could include various components for any parameter. For example, when measuring the angular diameter of earth, measurement error would include operator error, instrument error, errors appearing because earth is not spherical and the line of the visible horizon is blurred, etc. Thus, use of a specific navigational parameter should be preceded by comprehensive analysis thereof. It must also be taken into consideration that at least three navigational parameters must be measured for direct determination of spacecraft coordinates with the use of position surface.

3.4. Methods of Evaluating Potential Accuracy of Solving Astronavigation Problems With a Space Sextant

As we have already stated, the accuracy of solving astronavigation problems when using a space sight-sextant is affected both by error of sextant reading and type of reading taken. Moreover, accuracy of solving problems of space navigation also depends on the selected set of types of angular measurements and geometric location of the manned spacecraft in relation to sighted stars and landmarks.

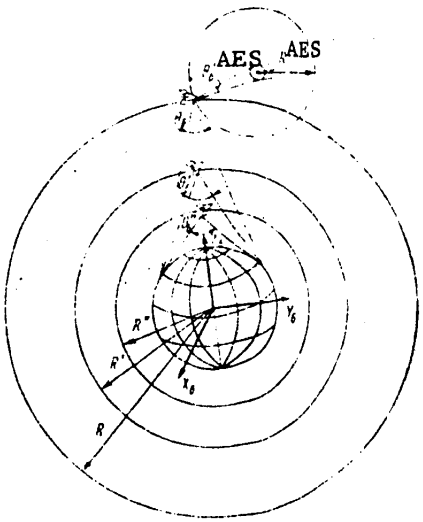

Figure 33.
Surface of spacecraft position determined by angular diameter of planet (celestial body) [AES--artificial earth satellite]

We shall discuss below the methods of estimating the potential accuracy of solving astronavigation problems with a manual [hand-held] space sextant.

In processing the astronomic measurements, we shall assume that the approximate location of the spacecraft is known; then the astronavigation problem is reduced to finding deviations of the spacecraft from the base orbit of flight. For this reason, for any type of astronomic measurement, the matrix equation of link between deviations of measured parameter q with location $\bar{r}$ can be written down in the following form [10]:

$$dq = \bar{h}d\bar{r} \qquad (3.1)$$

where $\bar{h}$ is the vector-row [or line] that depends on the type of astronomic measurement and characterizes the correlation between measurement errors and errors in determining the coordinates of the space vehicle. Let us demonstrate this for different types of astronomic measurements.

"Star--terrestrial landmark" type of measurement

According to Figure 34, we can write down:

$$\bar{n}\bar{r} = -r\cos(A_1 + \Theta) \qquad (3.2)$$

where $\bar{r}$ is the vector of the location of the spacecraft in relation to the center of the earth; $\bar{n}$ is the unit vector of direction of identified navigational star, A_1 is the angle between the lines of sighting the star and terrestrial landmark, Θ is the angle between the direction of the landmark and local vertical.

By differentiating (3.2.), we shall obtain

$$\bar{n}d\bar{r} + \bar{r}d\bar{n} = -\cos(A_1 + \Theta)dr + r\sin(A_1 + \Theta)(dA_1 + d\Theta). \qquad (3.3)$$

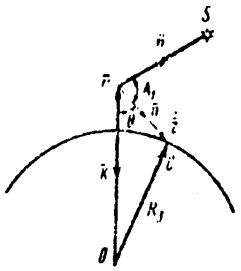

Figure 34.
For measurement of "star--terrestrial landmark" type

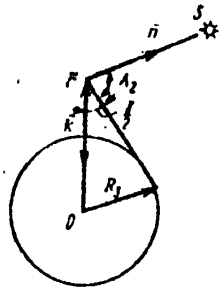

Figure 35.
For measurement of "star--visible horizon of earth" type

We find angular deviation $d\Theta$ from the equation:

$$\overline{rz} = -rz\cos\theta, \tag{3.4}$$

where $\bar{z}$ is the vector of inclined distance between the spacecraft and terrestrial landmark.

Differentiating equation (3.4), we shall obtain:

$$d\theta = \frac{(\bar{z} + \bar{z}\cos\theta\bar{k})\,d\bar{r} + (\bar{r} + \bar{r}\cos\theta\bar{m})\,d\bar{z}}{rz\sin\theta}, \tag{3.5}$$

where $\bar{m} = \bar{z}/z$ is the unit vector of direction of inclined distance z, $\bar{k} = \bar{r}/r$ is the unit vector of direction of earth's center.

In view of the fact that $d\bar{r} = -d\bar{z}$, $d\bar{n} = 0$, and inserting (3.5) in (3.3), we shall have:

$$dA_1 = \left[\frac{1}{r\sin(A_1+\theta)}\bar{n} + \left(\frac{\cos(A_1+\theta)}{r\sin(A_1+\theta)} + \frac{1-\cos\theta}{r\sin\theta}\right)\bar{k} + \left(-\frac{\cos\theta}{z\sin\theta} - \frac{1}{r\sin\theta}\right)\bar{m}\right]d\bar{r}, \tag{3.6}$$

where dA_1 is a value determined by the difference between measured and calculated angle of sighting the star and terrestrial landmark.

Let us rewrite (3.6) in the following form:

$$dA_1 = \bar{h}_1 d\bar{r}, \tag{3.7}$$

where

$$\bar{h}_1 = \left[\frac{1}{r\sin(\theta+A_1)}\bar{n} + \left(\frac{\cos(A_1+\theta)}{r\sin(A_1+\theta)} + \frac{1-\cos\theta}{r\sin\theta}\right)\bar{k} + \left(\frac{\cos\theta}{r\sin\theta} - \frac{1}{r\sin\theta}\right)\bar{m}\right] \tag{3.8}$$

is the vector characterizing the "star--terrestrial landmark" type of astronomic measurement.

"Star--visible horizon of earth" type of measurement

According to Figure 35, we have:

$$\bar{n}\bar{r} = -r\cos(A_2+\gamma/2), \tag{3.9}$$

where γ is the angular diameter of earth.

Calculating in (3.9) the first order differentials, we shall obtain:

$$\bar{n}d\bar{r} = -\cos(A_2+\gamma/2)dr + r\sin(A_2+\gamma/2)dA_2 + d\gamma/2. \tag{3.10}$$

We find angular deviation $d\gamma$ from the equation:

$$\sin\gamma/2 = R_3/r, \tag{3.11}$$

where R_3 is earth's radius.

Taking in (3.11) the first order differential, let us write down

$$d\gamma = -\frac{2R_3}{r^2\cos\gamma/2}\bar{k}d\bar{r}. \tag{3.12}$$

Substituting (3.12) in (3.10), we shall have:

$$dA_2 = \frac{1}{r}\left\{\frac{1}{\sin(A_2+\gamma/2)}\bar{n}_1 + [\operatorname{ctg}(A_2+\gamma/2) + 2\operatorname{tg}\gamma/2]\bar{k}\right\}d\bar{r}, \tag{3.13}$$

where dA_2 is determined by the difference between measured and calculated sighting angle for the star and visible horizon of earth.

If we write (3.13) in the form of (3.11), we shall have:

$$dA_2 = \bar{h}d\bar{r}, \tag{3.14}$$

where

$$\bar{h}_2 = \frac{1}{r}\left\{\frac{1}{\sin(A_2+\gamma/2)}\bar{n} + [\operatorname{ctg}(A_2+\gamma/2) + 2\operatorname{tg}\gamma/2]\bar{k}\right\} \tag{3.15}$$

is the vector characterizing the "star--visible horizon of earth" type of astronomic measurement.

"Visible angular diameter of earth" type of measurement

In accordance with Figure 35, we find the visible angular diameter of earth with the equation

$$\sin\gamma/2 = R_3/r,$$

which is analogous to (3.11). Then, on the basis of (3.12), we can write down:

$$d\gamma = \bar{h}_3 d\bar{r}, \tag{3.16}$$

where $d\gamma$ is determined by the difference between measured and calculated visible angular diameter of earth

$$\bar{h}_3 = -\frac{2R_\odot}{r\cos\gamma/2}\bar{k}, \tag{3.17}$$

where $\bar{h}_3$ is the vector characterizing the "visible angular diameter of earth" type of astronomic measurement.

Equations of the (3.1) form can be obtained analogously for other types of astronomic measurements.

Thus, while q is a parameter that has to be measured and dq is the difference between its measured and approximately known estimated value, regardless of the type of astronomic measurement, there is a correlation between dq and deflection of spacecraft position $d\bar{r}$ in the form of (3.1).

As a rule, three independent and accurate astronomic measurements taken at a known point in time are sufficient for unequivocal determination of the coordinates of the spacecraft's location. Since the equations linking dq and $d\bar{r}$ are linear for each of the different types of measurements, the result of the three readings can be submitted in the following matrix form:

$$d\bar{q} = \bar{H} d\bar{r}, \tag{3.18}$$

where $d\bar{q}$ is the three-dimensional vector-column composed of deviations of the observed values; $\bar{H}$ is the 3×3 matrix, each line of which consists of components of vector $\bar{h}$ in the specified system of coordinates XYZ, which correspond to a separate atronomic measurement and can be submitted in the following form:

$$H = \begin{Vmatrix} h_x^{\mathrm{I}} & h_y^{\mathrm{I}} & h_z^{\mathrm{I}} \\ h_x^{\mathrm{II}} & h_y^{\mathrm{II}} & h_z^{\mathrm{II}} \\ h_x^{\mathrm{III}} & h_y^{\mathrm{III}} & h_z^{\mathrm{III}} \end{Vmatrix}.$$

If all three vectors characterizing different types of astronomic measurements, from which matrix H was formed, are indeed independent, the vector of deviation of the spacecraft from nominal orbit at the moment of taking the measurement can be calculated with the formula:

$$d\bar{r} = H^{-1} d\bar{q}, \tag{3.19}$$

where H^{-1} is the matrix that is the reciprocal of H.

The above-described process of determining deviation $d\bar{r}$ of the position of the spacecraft implies the use, for unequivocal determination of vector $d\bar{r}$, of only

the sufficient number of astroreadings (at least three). To assess the accuracy of solving an astronavigation problem with a space sextant, let us introduce an analytical expression for errors of determination of location coordinates. For this purpose, let us consider the following:

$$\begin{aligned} \hat{d\bar{q}} &= d\bar{q} + \bar{\alpha}; \\ \hat{d\bar{r}} &= d\bar{r} + \bar{\varepsilon}, \end{aligned} \tag{3.20}$$

where $\hat{d\bar{q}}$ is the measured deviation, $d\bar{q}$ is the real deviation, $\hat{d\bar{r}}$ is estimation or assumed deviation of spacecraft from nominal orbit, $d\bar{r}$ is true deviation of spacecraft position from nominal orbit, $\bar{\alpha}$, $\bar{\varepsilon}$ are errors made in measurements and estimation of location of spacecraft, respectively.

Evidently, the true deviations $d\bar{q}$ and $d\bar{r}$ satisfy equation (3.1). Then, if we consider only the sufficient number of measurements, the following formula must be fulfilled for an unshifted [?] evaluation:

$$d\bar{r} = \bar{H}^{-1} \hat{d\bar{q}}. \tag{3.21}$$

Consequently, error vectors $\bar{\alpha}$ and $\bar{\varepsilon}$ must also be linked through this matrix $\bar{H}$, i.e.,

$$\bar{\varepsilon} = \bar{H}^{-1}\bar{\alpha}, \tag{3.22}$$

hence we shall find that the mean square error of determination of coordinates of the spacecraft's location is:

$$\varepsilon^2 = \bar{\varepsilon}^T\bar{\varepsilon}, \tag{3.23}$$

where $\bar{\varepsilon}^T$ is transposed matrix $\bar{\varepsilon}$.

As an example, let us discuss one set of the above-mentioned three astromeasurements and determine the error in defining the coordinates of the location of the spacecraft.

"Star--terrestrial landmark," "star-terrestrial landmark" and "visible angular diameter of earth" types of measurements

For the sake of convenience in obtaining the necessary mathematical functions, let us select a system of OXYZ coordinates related to the spacecraft and direct its axis to the local vertical (Figure 36).

Let us orient unit vectors $\bar{n}_1$ and $\bar{m}_1$ so that they are in plane XZ, where $\bar{n}_1$ would coincide with the direction of the X-axis and $\bar{m}_1$ with the direction of terrestrial landmark C_1. Let us set vectors $\bar{n}_2$ and $\bar{m}_2$ accordingly in plane YZ. We shall pick two navigation stars S_1 and S_2 in the direction of the axes of coordinates X and Y, respectively. Let the angles between the direction of terrestrial landmarks and navigation stars be A_1 and A_2. Then, according to (3.7), the projections of vector $\bar{h}_1$ on the axis of XYZ coordinates for two astromeasurements will have the following appearance:

$$h^{I}_{1x}=a_1+c_1\cos A_1;\ h^{I}_{1y}=0;$$
$$h^{I}_{1z}=b_1+c_1\sin A_1; \tag{3.24}$$

for the first "star--terrestrial landmark" astromeasurement, and:

$$h^{II}_{1x}=0;\ h^{II}_{1y}=a_2+c_2\cos A_2;$$
$$h^{II}_{1z}=b_2+c_2\sin A_2, \tag{3.25}$$

for the second "star--terrestrial landmark" measurement, where:

$$a_{1,2}=\frac{1}{r\sin(A_{1,2}+\theta_{1,2})};\ b_{1,2}=\frac{\cos(A_{1,2}+\theta_{1,2})}{r\sin(A_{1,2}+\theta_{1,2})}-$$
$$-\frac{1-\cos\theta_{1,2}}{r\sin\theta_{1,2}};\ c_{1,2}=\frac{\cos\theta_{1,2}}{r\sin\theta_{1,2}}-\frac{1}{r\sin\theta_{1,2}}.$$

For the third measurement of "visible angular diameter of earth," we shall have, according to (3.16):

$$\bar{h}^{III}_{1x}=0;\ \bar{h}^{III}_{1y}=0;\ \bar{n}^{III}_{1z}=1\ s,$$
$$\text{where}\qquad s=-\frac{r^2\cos\gamma/2}{2R_3}. \tag{3.26}$$

According to (3.18), (3.24), (3.25) and (3.26), matrix H will take on the following appearance:

$$H=\begin{vmatrix} a_1+c_1\cos A_1 & 0 & b_1+c_1\sin A_1 \\ 0 & a_2+c_2\cos A_2 & b_2+c_2\sin A_2 \\ 0 & 0 & 1\ s \end{vmatrix}, \tag{3.27}$$

hence, the value of the reciprocal matrix will be:

$$H^{-1}=\begin{vmatrix} \frac{1}{a_1+c_1\cos A_2} & 0 & -\frac{(b_1+c_1\sin A_1)\,s}{a_1+c_1\cos A_1} \\ 0 & \frac{1}{a_2+c_2\cos A_2} & -\frac{b_2-c_2\sin A_2}{a_2+c_2\cos A_2} \\ 0 & 0 & s \end{vmatrix}. \tag{3.28}$$

Using (3.18) and (3.28), we shall obtain the following analytical expressions for errors of determination of coordinates of the location of a manned spacecraft:

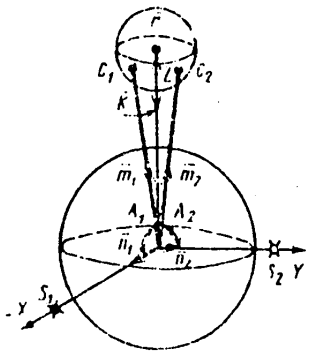

Figure 36.
For measurement of the "star--terrestrial landmark," "star--terrestrial landmark" and "visible angular diameter of earth" type

$$\varepsilon_x = \frac{1}{a_1 + c_1 \cos A_1}\alpha_x - \frac{(b_1 + c_1 \sin A_1)\, s}{a_1 + c_1 \cos A_1}\alpha_z;$$
$$\varepsilon_y = \frac{1}{a_2 + c_2 \cos A_2}\alpha_y - \frac{(b_2 + c_2 \sin A_2)}{a_2 + c_2 \cos A_2}\alpha_z; \qquad (3.29)$$
$$\varepsilon_z = s\alpha_z.$$

where α_x, α_y, α_z are errors in measurement of astronavigation angles with a hand-held sextant.

Analysis of functions (3.29) shows that errors of determination of coordinates of spacecraft location ε_x, ε_y, ε_z depend not only on errors in measuring angles with the sextant α_x, α_y, α_z, but on the parameters characterizing a different set of astronomic measurements and geometric location of the spacecraft in relation to sighted stars and navigational landmarks.

If we assume that, in (3.29), the maximum values of the angles are $A_1 = A_2 = 90°$ and $\alpha_z = 0$, we shall have:

$$\varepsilon_x = r\alpha_x;\ \varepsilon_y = r\alpha_y;\ \varepsilon_z = 0 \qquad (3.30)$$

We see from (3.30) that the obtained errors in determining the spacecraft coordinates correspond to the known errors in aircraft astronavigation. Thus, with $\alpha_x = \alpha_y = 1'$ and $r \cong 6372$ km, we shall find that $\varepsilon_x = \varepsilon_y \cong 1.8$ km.

CHAPTER 5. MODELING CONDITIONS OF OPERATOR-ASTRONAUT PERFORMANCE IN SOLVING ASTRONAVIGATION PROBLEMS

5.1. Methods of Simulating the Celestial Map

The reliability of experimental data is largely determined by fullness of simulating observation conditions. Several simulators of the celestial map [stellar sky] were developed and tested for this purpose.

In one of the simulators, stars were modeled by means of orifices made in one of the glass walls of a space illuminated from the inside.

A thin layer of metallic silver was applied to the glass. An electric discharge was used to make holes in it. The diameter could be regulated over a wide range by the voltage delivered to the punch. Provided several photometric conditions are met, this can be used to simulate the stellar background, since it is the most available and simple.

In another variant, the stellar sky was simulated by means of shining spheres attached to a surface covered with black velvet and properly illuminated. If illumination is such that the background brightness does not exceed the permissible level, the reflection of the light source on the shiny surface of the spheres will simulate stellar brilliance.

Calculation of radii of the spheres and background illumination when simulating stars with brightness of the first to 11th star magnitude, as well as conditions of illumination of spheres, is made in accordance with the diagram illustrated in Figure 51.

If the distance to the light source $l = 1$ m, which is quite advantageous from the standpoint of construction since the light source could then fit within the tube [barrel] that shields the background of the stellar sky from extraneous light, we shall obtain different angular dimensions of simulated stars, depending on the dimensions of light source S (Table 5.1). Using the data listed in this table it is easy to determine the illumination of the spheres as a function of sight magnification.

One can also simulate the stellar sky by means of light guides, one end of which is attached to the flat background surface of the simulator and the other illuminated with a light source.

The following method is handier and rather simple to execute. Stars are simulated with either a dot (when the mirror surface of the sheet is impaired) or white

Table 5.1. Angular dimensions of simulated stars (in angular seconds) for different radii of light source

Radius of light source, mm	Required source brightness cd/m^2	Stellar magnitudes of simulated stars											
		0	1	2	3	4	5	6	7	8	9	10	11
2	0.25	37.4	22	15	9.4	5	3	2.2	1.2	0.9	0.4	0.3	0.2
1	1	18.7	11	7.5	4.7	2.5	1.5	1.1	0.6	0.45	0.2	0.15	0.1
0.5	4	0.35	5.5	3.75	2.35	1.25	0.75	0.55	0.3	0.22	0.1	0.07	0.05
0.35	8.2	0.6	3.8	2.5	1.6	0.8	0.5	0.38	0.21	0.15	0.07	0.05	0.03
0.25	16.4	4.7	2.73	1.83	1.15	0.6	0.35	0.27	0.15	0.11	0.05	0.037	0.025

paint on a sheet of plexiglass illuminated from the end. For the light not to dissipate, the edges of the plexiglas sheet have a light-proof covering, the width of which is determined by the maximum angle of total internal reflection. With an ideal mirror surface of the plexiglass, the brightness of the stellar background will be determined by the brightness of the screen located in the back. When the technique for applying the dots is worked out well, this method is the simplest and most accessible.

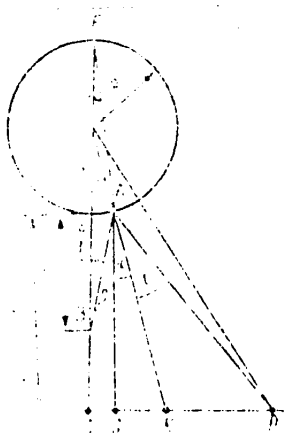

Figure 51.
Diagram of simulation of a star with a shiny sphere (∈C = L--distance from surface of sphere to light source; CD = S--radius of light source; R--radius of of sphere; DA--direct beam from source to sphere; AB--beam reflected from sphere; AK--BAD bisector)

The method of applying luminophore particles exposed to ultraviolet rays was also used. Luminescence of such particles simulated stars rather well.

At any rate, regardless of which method is given preference, the simulator must recreate a stellar map that is as close to the real one as possible in order to obtain reliable results. The resemblance can be considered adequate if the simulated stellar sky is on a plane and there is equality of the following parameters: density of stellar background, distribution of stars according to stellar magnitudes, visible brightness of stars, angular dimension of stars, brightness of background and a few others.

5.2. Photometric Conditions for Simulating Earth's Surface

The task of adequately modeling the conditions under which the cosmonaut-operator works in a system of self-contained astronavigation is one of the principal ones in conducting studies under ground-based conditions. Providing photometric conditions of operator work should be considered one of the elements of such modeling; along with others this must be taken into consideration in developing and building simulators of earth's

surface. The choice of the basic plan [flowchart?] of the viewing unit or simulator may be determined by a number of specified conditions: size of the room in which experiments will be conducted, electricity supplied to lights, viewing angle, etc. Thus, in developing one variant of the viewing unit, the above-mentioned requirements resulted in constructing the earth simulator in the form of a panel on a cylindrical surface with a large radius of curvature (R = 10 m). The surface of this pannel was tilted toward the operator (angle of the order of 10°) so that the image of earth's horizon and segment of the sky reproduced in the top part would be about 2.20-2.30 m away from the operator.

Geometric, photometric, scalar, foreshortening [aspect] and other parameters of the picture viewed by the operator of the sunlit surface of earth were selected for the most probable viewing conditions from space.

The following were the base data that were used to develop a simulator of earth's surface: angle of operator's vision of earth's surface constituted 55° directed toward the nadir; altitude of spacecraft flight 200 km; distance from sun to local horizon h = 45°; azimuth of the sun counting from the vertical plane in the direction of viewing constituted 90°; solar light constant E_0 = 135 klux; angle of visual field when viewing terrestrial landmarks through a window 55°; mean reflectivity of earth's surface 39% with clouds (in visible part of spectrum and 15% without clouds.

Because of the perspective nature of the image of earth's surface, geometric, photometric, scalar, foreshortening and other altitude parameters must be variable. Bearing this in mind, calculation was made of parameters for nine belts that we distinguished, which separated the underlying surface on the simulator according to altitude. Figure 52 illustrates a diagram of location of the belts over the height of the panel.

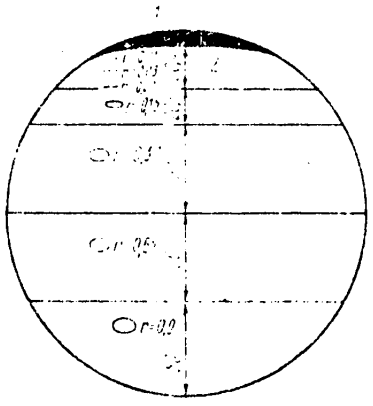

Figure 52.
Diagram of location of belts on simulator of earth's surface

1) window 2) earth's horizon

Scale M and foreshortening [angle of approach r of terrestrial formations for different angles of inclination of viewing in relation to direction of nadir Θ are determined using the following equations:

$$M = \frac{2l \sin \beta}{R \sin\left[\arcsin \frac{(R+H)\sin \beta}{R} - \beta\right]};$$

$$l = \sec\left[\arcsin \frac{(R+H)\sin \beta}{R}\right],$$

where R is the radius of earth, H is altitude of craft over earth's surface, l is distance at which the operator views panel under training conditions (l constituted 2 m).

As can be seen from the above equation, angle of approach referred to the degree

of visible shortening of the object in the viewing direction, considering that terrestrial landmarks were flat.

Calculation of photometric parameters of the underlying surface was made for a standard atmosphere, which is characterized by horizontal visibility of 20 km and optical thickness $\tau = 0.299$ (for light wavelength $\lambda = 550$ μm) for the known spectral coefficients of brightness of terrestrial formations [58].

Calculation of optical characteristics of the atmosphere, which could constitute the overall brightness of terrestrial landmarks and clouds, was made by the system of K. S. Shifrin and I. N. Minin using the tables given by K. Ya. Kondrat'yev [47].

Table 5.2. lists the values of overall brightness of terrestrial formations calculated by this method when viewing them from space. After selection of the system of lighting the underlying surface, calculation was made of brightness of formations (objects) in different belts. We took into consideration the actual illumination of various segments of the underlying surface.

Table 5.3. lists the brightness coefficients of formations (objects) on the simulated surface of earth in different belts.

Table 5.2. Overall brightness of terrestrial formations observed from space, in cd/m^2

Formation (object)	Belt No							
	Nadir	9	8	7	6	5	4	3
Wet chernozem soil	7500	7770	8045	9176	11865	14046	14762	20000
Dry chernozem	7900	8150	8420	9500	12120	14220	14893	20000
Coniferous forest	8300	8540	8790	9840	12374	14400	15024	20000
Leaf forest	8700	9000	9160	10170	12630	14565	15155	20000
Succulent meadow	9100	9400	9530	10500	12890	14740	15285	20000
Wet loamy soil	9100	9400	9530	10500	12890	14740	15285	20000
Dry loamy soil	9100	9400	9530	10500	12890	14740	15285	20000
Stubble [fields]	10700	11000	11020	11850	13910	15430	15810	20000
Dry yellow sand	12700	13000	12900	13500	15190	16300	16460	20000
Dry white sand	14700	14700	14750	15200	16470	17160	17120	20000
Clouds	5400	5300	5100	50000	46000	35000	30000	20000

It should be noted that the image of the clouds on the panel could be changed, since it was applied to polyethylene film stretched over the image of the underlying surface.

With the selected illumination and relative areas of different formations (objects), overall adaptational brightness of the image of earth's surface was of the order of 7500 cd/m^2, which is an average of one-fifth natural brightness under such conditions. However, in view of the great compensatory capabilities of the visual analyzer, it can be maintained that neither resolution nor acuity of vision differed under the experimental conditions from those present under natural ones ($\Delta J/J \leq 0.012$, $\Delta V < 0.06$ ... 0.09, respectively [48]).

Table 5.3. Brightness coefficients of formations (objects) on simulated surface of earth

Formation (object)	Belt No						
	9	8	7	6	5	4	3
Wet chernozem soil	0.141	0.158	0.183	0.258	0.40	0.491	0.67
Dry chernozem soil	0.154	0.165	0.29	0.264	0.406	0.497	0.67
Coniferous forest	0.161	0.172	0.197	0.279	0.411	0.502	0.67
Leaf forest	0.17	0.179	0.203	0.275	0.417	0.505	0.67
Succulent meadow	0.177	0.186	0.21	0.28	0.421	0.509	0.67
Wet loamy soil	0.177	0.186	0.21	0.28	0.421	0.51	0.67
Dry loamy soil	0.177	0.186	0.21	0.28	0.421	0.51	0.67
Stubble [fields]	0.208	0.216	0.237	0.302	0.431	0.528	0.67
Yellow dry sand	0.245	0.253	0.27	0.33	0.465	0.550	0.67
White dry sand	0.277	0.29	0.304	0.358	0.491	0.571	0.67
Clouds	1.0	1.0	1.0	0.9	0.8	0.7	0.67

Other characteristics of sight, just like effective [adjusted?] sensitivity to light, temporary [time-related?] processes of visual perception, color vision and other brightnesses for the indicated gradient, present even less deviation.

Operators were trained to find and identify landmakrs on the illuminated side of earth in several stages, and some physiological parameters (pulse rate, respiration, etc.) were recorded at that time. After the "ready" signal, which the operator himself gave, an image of landmarks was displayed to him on the illuminated side of earth and, simultaneoulsy, a stopwatch was started. Physiological parameters were recorded concurrently. Upon detection of a landmark and determination of its range, the operator turned off the lighting of the simulator by depressing the proper key. the electric stopwatch equipment that recorded physiological parameters were turned off and the window covered [shut]. Data about the site of detection of the landmark, its range and foreshortening were entered in the operator's log.

At the same time, the experimenter set a new variant of underlying surface for searching for terrestrial landmarks. During one training session, the operator worked on 4 variants with 10 displays in each variant. The variants were marked by the background features (underlying surface) against which the landmarks were selected (shoreline, boundaries of mountain formations, river deltas, etc.).

Daily training lasted an average of 1 h.

The results of the tests conducted on 12 operators for detection of landmarks on the illuminated side of earth were characterized by the following parameters. As can be seen in Figure 53, average time required to detect terrestrial landmarks diminished significantly in the course of training. Thus, while the operator needed about 40 s to search and detect a landmark at the early stage of the training processes, after 25-30 displays search and detection time was reduced to 5-7 s. There was virtually no further change in time spent on the tested operation in subsequent training sessions.

In the course of the studies it was found that the time required to search and find landmarks depends on their range. Figure 54 illustrates time of detection of some space landmarks as a function of their distance. An appreciable difference

in time of detection of these landmarks was observed as a function of characteristics of the background against which the operator saw them. Figure 55 illustrates landmark detection time as a function of background.

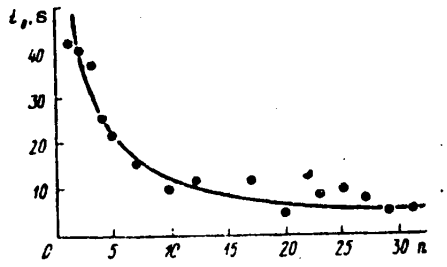

Figure 53.
Time t_0 of detection of manned spacecraft as a function of number n of training sessions (mean data for all operators, range 5000 m)

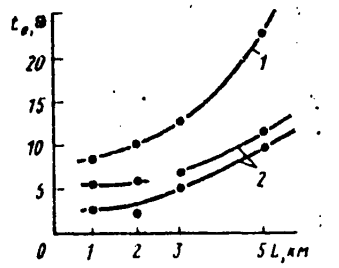

Figure 54.
Time t_0 of detection of manned spacecraft as a function of distance L
1) first training session
2) subsequent training sessions

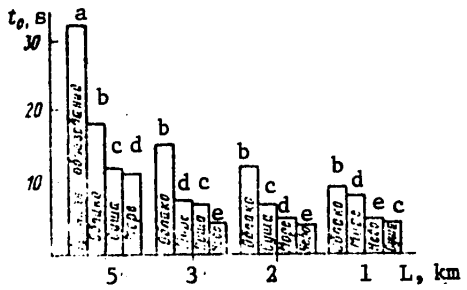

Figure 55.
Time of detection of manned spacecraft as a function of its background

Key:
a) boundary of formations
b) cloud
c) land
d) sea
e) sky

On the whole, it can be noted that the method of training operators to solve problems of detecting landmarks on the illuminated side of earth, as well as the simulator developed for this purpose, were beneficial and able to improve achievement with such problems in actual flights.

There were some curious reports by the cosmonauts after flights concerning the laboratory simulator: "The segment of earth's surface was well-rendered on the "isoplan" [isochart, isomap?], the brightness of terrestrial formations without clouds was close to natural," etc. At the same time, there were comments such as: "Clouds and some terrestrial formations appeared much brighter from space than on the panel, it would be desirable to add the dynamics of motion of our spacecraft," etc.

5.3. Modeling the Visual Situation When Flying to the Moon

It is known that ground-base services make the necessary calculation to control a spacecraft, while the onboard equipment is used as a back-up [reserve]. For this reason, American programs for professional training of crews for the Apollo spacecraft included 40 h of work in a planetarium [97], about 50 h on a special simulator imitating approximation to the moon and traveling away from it [65]. Some time was spent on studying 37 navigational stars, data about which were inputted

in an alphanumeric computer, as well as comprehensive instruction of the astronauts with respect to elements of the lunar topography at the proposed landing sites.

Unquestionably, the flights to the moon and then landing of spacecraft crews on its surface required concrete knowledge about the topography, its forms, names of different elements, relative location of main details and chioce of main navigational landmarks on the surface. Without these conditions, it would be inconceivable for an astronaut to orient himself, not only on the lunar surface, but with regard to guiding the spacecraft in a selenocentric orbit, taking navigational measurements, selecting the specified landing site, etc.

There were other matters involved in training crews, the most important of which were: determination of volume of information gathering about the lunar topography; determination of groups of objects of lunar topography remembering which would present no difficulties; determination of reliability of remembering formations of lunar topography for the purpose of singling out the main landmarks and zones; retaining skill in identifying lunar landmarks as they approach the moon (with decrease in number of objects in the field of vision).

The study of these matters required additional research and methods developed for this purpose, as well as special simulators and mock-ups. Various methods and equipment have been described in the foreign literature for the study of human characteristics in the course of observing and identifying lunar objects (digital data for Section 5.3 [65, 97]).

Slides of the moon, photographed in different phases and scales, were used to study the psychophysiological capacities of astronaut-operators. In the course of the work, the slides were projected on a round white screen with black masking around it. Total brightness of the image of the moon on the screen constituted a mean of 200 cd/m^2. This brightness is sufficient for testing the process of identifying lunar formations but, as it was established in the course of the experiment, far from adequate for taking angular measurements.

Of course, the choice of stellar sky simulator is one of the factors that could affect reliability of "lunar landmark--star" type of astronomic readings. It was observed that it is desirable to simulate stars, the moon and lunar formations between which angular distances were measured on a plane that is approximately perpendicular to the sighting line. The actual value of measured angles was calculated on the basis of measurements of distances between the objects to be measured and distances to the apex of the measured angle. Collimation error was taken into consideration by means of base reference points.

The dynamics of the process of flying to and around the moon were simulated by projecting on the screen some specially taken slides and film. The base data for them were obtained from examining several typical flight trajectories, for example the trajectories of the flight of Apollo 8 and others (Figure 56).

Estimates revealed that, starting at a distance of 10,000-15,000 km between the spacecraft and moon, its movement in relation to the stellar background would not be observed by astronauts. Viewing this phase of the "flight," which lasted about 9-10 h, was performed by means of slides taken in the proper scales, phases of illumination by the sun and foreshortening. It was found that 30 slides of the moon were sufficient to similate flight at this stage [65].

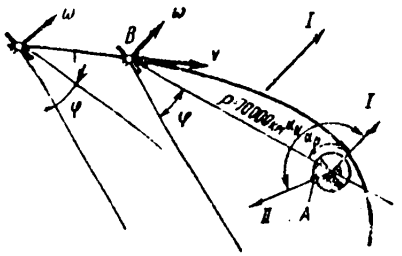

Figure 56.
Calculation of conditions of viewing moon while flying toward it (v--vector of linear speed of spacecraft; ω--vector of angular rotation of spacecraft about direction of sun; ϕ--angle of astronaut's field of vision through spacecraft window; α_N--angle between directions of sun and earth; α_n--angle between directions of sun and spacecraft; ρ--distance between spacecraft and center of the moon

I) direction of sun
II) direction of earth
A) point where moon's longitude is 0
B) point of trajectory at which astronaut begins to see the moon through spacecraft window

The conditions of viewing the moon can be calculated for different trajectories at any stage of flight. Figure 56 illustrates the calculation of conditions of viewing the moon while flying about 70,000 km away from it. During each turn of the manned spacecraft about the direction of the sun, i.e., every 20 min, the astronauts will have the moon in their visual field for 2 min. In the experiments, each successive slide was shown to the subjects every 20 min, like in actual flight, which saved time and made it possible to use considerably more slides. At distances of about 10,000 km from the moon, the astronaut begins to see movement of the moon in relation to the stellar background. Figure 57 illustrates the results of calculating the angular velocity of this movement as a function of angle Θ between the direction of the periselene and observer, as compared to threshold angular speed ω_{thr} observed by the astronaut. Under such conditions, the astronaut must identify a specified object in the topography, and this was included in the training program. These data correspond to reliability of the astronaut's sight equal to its usual norm on earth. However, at the time of approaching the moon, vision would undergo certain changes under the influence of prolonged weightlessness, and this could lead to some corrections in the calculations.

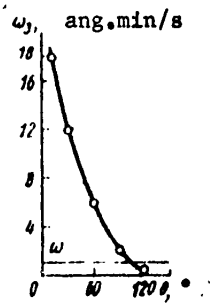

Figure 57.
Angular velocity ω_3 of the moon's movement in relation to stars as a function of angle Θ (according to data in foreign publications)

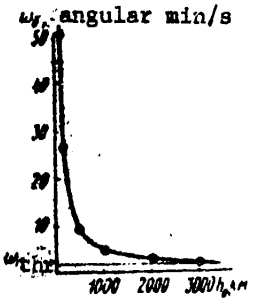

Figure 58.
Angular velocity ω_6 of "running" of lunar surface as a function of altitude h_0 of periselene (according to data in foreign publications)

Finally, "backward running" of the moon's surface will be observed while flying over it. The angular velocity of movement of lunar surface ω, which is observed from a spacecraft stabilized with its window in the direction of the center of the moon, will depend on flight altitude.

Figure 58 illustrates the results of calculating the angular velocity of "running" of the lunar surface as a function of the altitude h_0 of the spacecraft above the moon.

Many foreign authors assumed that the changing brightness of the underlying surface of the moon would make it difficult to identify specified landmarks. For this reason, the amount of astronaut training was increased, as we have already mentioned [97].

Moreover, the results of calculations, on the basis of which the curves of Figure 58 were plotted, served as the basis for making a film simulating a flight toward the moon and over its surface. However, for this method of visualization to be used under laboratory conditions, it is necessary to make several changes in the optical system of the film projector. In particular, a special optical attachment for the lens was developed and built to increase the angle of the image field.

On the whole, the described (according to data in foreign publications) methods of simulating the visual situation in space made it possible to conduct extensive studies, under laboratory conditions, of the psychophysiological capacities of an astronaut-operator with regard to solving astronavigation problems.

5.4. Modeling of Mental States of Operators

Most laboratory experiments in aviation and space psychophysiology, which explore the capabilities of an operator, yield a somewhat unilateral idea about the level of these capabilities.

The specifics of working conditions at different stages of space flights will definitely affect work capacity. For this reason, finalization of existing and future navigation systems should be based on studies, in which not only adequate performance conditions, but corresponding mental states of operators are simulated. It is relatively easy to experimentally simulate stress factors of a physical nature, such as accelerations, vibration, temperature, changes in gas atmosphere, etc. At the same time, the problem of purposeful and adequate modeling of emotional states caused by psychogenic factors (great responsibility, danger to life, etc.), as well as prolonged sensation of weightlessness, present serious difficulties.

The following main procedures are used in experimental psychology for purposefully affecting a subject's emotional sphere: strong and unexpected audio, photic, nociceptive or other unpleasant stimuli to form negative emotions and, on the contrary, pleasant audio and visual images to create positive emotions; performance of tasks that appear simple at first glance but actually difficult or unsolvable, performance in the presence of interference, fatigue and shortage of time; use of pharmacological agents that alter the emotional state; direct electrostimulation of primary brain structures using microelectrode techniques; recreating real working conditions that cause great emotional stress in the operator (controller, pilot, etc.).

It can be maintained that the most suitable method of studying emotions is to examine them in a real situation (for example, sports competitions and performances, during intensive industrial work) when the experimenter accompanies the subject through the stages of a real activity and records, in some way or other, data about his mental and physiological state. A. R. Luriya selected expressly this route for the study of emotional states [56]. Emotional tension of a pilot related to performance of his professional activities is studied by simulating flights on simulators, as well as real situations.

More and more works are being published that deal with the study of emotional states of cosmonauts at different stages of space flights [35, 49, 72]. The importance of such research is just as great in our times, while the results thereof are quite valuable in gaining understanding of human behavior under psychological stress.

There are different difficulties involved in modeling the state of an operator that is caused by the sensation of weightlessness. The substantial change in performance characteristics, including locomotor ones, of an operator in weightlessness compels specialists in space medicine and psychology to continue research thereof, including studies using various modeling methods.

The methods of modeling states of partial and total weightlessness are largely determined by the researchers' objectives. However, all of the methods can be reduced to several main groups.

Biomechanics of man's motor activity in weightlessness were studied with the use of special stands, where the general center of gravity of the body and of different parts of the limbs were weighted by means of a system of weights and blocks.

In many cases, an immersion medium was used to simulate the effects of diminished gravity, into which the subject submerged with a special life-support system. Under these conditions, there was refinement, for example, of the actions of American cosmonauts to perform some work operations within a spacecraft, as well as during extravehicular activity.

Lockheed Aircraft (Georgia department) developed an original device for simulating the physiological effect of weightlessness involving the use of immersion [75].

Stands on air pillows with different degrees of freedom were developed to study some of the biomechanical characteristics of man's motor activity in weightlessness [in a support-free state].

Finally, the last method of simulating weightlessness best meets the requirements of research problems. It makes use of the state of weightlessness that occurs in a free-falling body. It is expressly in this state that only gravity affects the body, but no gravity force ["force of weight"] occurs in the body [32, 44, 85 and others].

The planning and execution of prolonged space flights actualized, to a significant extent, the problem of readaptation after long-term weightlessness. Comprehensive investigation of this problem and development of effective measures to prevent the adverse signs of the readaptation period also require a search for adequate models.

Modeling Emotional States

Of all the above-listed methods of modeling emotions, only a few are suitable for experimental aerospace psychology. Thus, procedures of purposefully influencing the emotional state of subjects, which involve the use of potent and unusual stimuli, cannot be used repeatedly, since a healthy body adjusts to them very rapidly and the severity of emotional reactions diminishes. The emotional reaction to a strong stimulus may also be mild at the very beginning when the subjects' attitude toward this stimulus is critical enough.

The study of emotional states of operator-cosmonauts during actual work involves, first of all, technical difficulties, which arise in connection with the recording of objective parameters at the work place. One must also take into consideration the fact that awareness that one is the object of a study could turn out to be a stronger emotiogenic factor than customary activities. This circumstance often distorts substantially the nature of reactions, which is not acceptable, not only from the standpoint of purpose of the studies, but safety of work.

In our studies, we used the method of hypnosis to simulate emotional states of operators. The method of reproducing emotions under hypnosis has been used since 1959 to study the emotional reactions of parachutists [26, 27, 29]. Physiological changes related to suggested or reproduced emotion were studied during hypnotic sleep. Of course, this method cannot be used to solve problems of experimental psychology. Inhibition of the subjects' cerebral cortex, selectivity of verbal contact, marked functional disturbances referable to the motor and other analyzers render it unsuitable for psychological studies. The latter require ["imply"] that there be satisfactory and coordinated function of mental and physiological components of activity inherent only in the waking state.

On the basis of experimental experience, it can be stated that suggested emotional states are expressed more fully when they are motivated by the appropriate suggested situation. In such cases, they are productive reactions and formed on the basis of the subject's own life and emotional experience, as well as his characterological traits.

The above method of investigation is certainly not among simple and easy methods. Use thereof is limited by availability of specialists in hypnosis and the proper group of subjects. However, when these conditions are available, use thereof is quite promising for simulating specified emotional states in the study of operator reliability in control systems.

Modeling States Related to Sensation of Diminished Body Weight

The stability of the gravity field is one of the most important constants that determine normal vital functions of man, which were formed in the course of phylogenesis. The role of gravity in functional development of organisms has been repeatedly described in the works of classics in natural science--C. Darwin, I. M. Sechenov, K. A. Timiryazev, I. P. Pavlov. "Gravity," wrote A. A. Ukhtomskiy, "is the most persistent ["hard to get rid of"] and constant field, that no being on earth can rid itself of (along with the electromagnetic field)" [70].

As a rule, weightlessness elicits a primary reaction in all systems of the body (sensory, motor, autonomic and mental changes), which may become significantly

attenuated as one adjusts to new conditions. Prolonged weightlessness elicits secondary functional changes.

A distinction is made of three types of primary sensory reactions, according to nature and severity thereof. Individuals presenting the first type of reaction show now decrease in work capacity in weightlessness, and there is no change in their well-being. The second type of reaction is related to experiencing the experience of free fall, sensation of upturned position, rotation of the body, being suspended head down, etc. These spatial illusions are often associated with restlessness, disorientation and sensation of discomfort. The third type of reaction is characterized by the "space form of motion sickness" [78, 79].

The data obtained from orbital flights performed in the Soviet Union and the United States revealed that there are some important distinctions to function of the motor analyzer during both the period of adaptation to weightlessness and period of stabilization of functions. Studies of motor activity during space flight revealed that the changes in speed of motor reactions occurred in different directions.

Slower performance of a test was noted in Yu. A. Gagarin and V. F. Bykovskiy in weightlessness, whereas G. S. Titov, A. G. Nikolayev and P. R. Popovich presented a faster pace of movement than in the background demonstrated on the ground [43].

I. I. Kas'yan et al. [43] studied the muscular strength of subjects submitted to brief weightlessness (35-45 s) during flights in laboratory aircraft in a Keplerian parabola. It was established from 266 readings on 26 subjects that the muscular strength of the hand decreased by 4-22 kgf in 82% of the cases, from the base level of 45-65 kgf. However, in some cases (up to 9%), when the readings were taken with the subject attached to a chair, we also observed an increase in strength of the hands. The authors believe that generalized decrease in tonic tension of muscles is one of the causes of diminished muscular strength.

L. A. Kitayev-Smyk [45], who studied coordination of movements during brief weightlessness by means of target shooting tests, demonstrated that precision was diminished due to a typical error--overshooting upward and to the right.

There were also distinctions to oculomotor activity in cosmonauts A. G. Nikolayev, P. R. Popovich, V. F. Bykovskiy and V. V. Tereshkova during space flights [4]. At the start of the flight there was persistent increase in oculomotor activity, from 40 movements/min on earth to 300-400 during the first passes. At the start of the flight there was prevalence of wide-amplitude movements ("leading" of the eyes). As adaptation progressed, the eye movements became better coordinated, faster and completely normal on the 2d-3d day.

A large amount of information about autonomic functions in weightlessness was obtained during space flights. Much attention was devoted to the study of parameters of the cardiovascular and respiratory systems during all manned orbital flights. It was established that the heart rate slows down in orbital flight in all cosmonauts. Measurement of arterial pressure during the flights revealed that there was a drop of systolic pressure and a tendency toward insignificant elevation of diastolic pressure, which led to appreciable drop of pulse pressure.

The existing data enable us to refer to different types of EEG changes during space flights. Thus, A. G. Nikolayev and V. F. Bykovskiy presented a tendency toward predominant replacement of low-frequency waves (less than 8 Hz) by high-frequency oscillations with gradual decline of amplitude of bioelectrical rhythms in weightlessness. V. V. Tereshkova presented chiefly an increase in low-frequency potentials.

Biochemical studies of the cosmonauts following orbital flights revealed more or less marked weight loss (3 kg for B. B. Yegorov). It is believed that inadequate replacement of fluid loss is the main cause of weight loss in flight [6].

According to all of the foregoing, there are changes in sensory, as well as motor and autonomic components, of the systemic reaction in weightlessness. Of course, this cannot fail to be associated with a change in work capacity.

Studies of sensorimotor coordination during prolonged weightlessness during flights of single and multipassenger spacecraft revealed that sensorimotor coordination worsened at the start of the flight, but was significantly restored as adaptation to weightlessness progressed.

Evaluation of general locomotor activity in weightlessness and open space was made by means of biomechanical analysis of the process of exiting from the spacecraft into space by A. A. Leonov [67]. A comparison of the generalized criterion of quality of this action in space to the same criterion obtained during brief weightlessness aboard a laboratory aircraft revealed that it was significantly decreased (39.7%, versus 57-60%).

Simulation through hypnosis of states related to sensations of both diminished and increased body weight implies that the sensation of actual change in body weight, in either direction, is also encountered in man's everyday life.

Engrams with imprinted experience of subjective experiences elicited by weight fluctuations and corresponding autonomic reactions are retained in long-term memory. It can be stated that each adult man has some experience in subjective evaluation of his state when there is a change in his body weight.

Persistent illusions of weightlessness are also not uncommon in patients with depersonalization syndromes, and this enabled R. Ya. Golant [24] to single out a depersonalization syndrome, in which the sensation of weightlessness is the prime sign.

It is logical to assume that the above cases of hypogravity illusions occur as a result of temporary activation in the cerebral cortex of the engrams imprinted by life experience in subjective sensations related to brief changes in body weight. Impaired control and regulation by higher mental functions at a given time must be a mandatory condition for such activation. However, direct indications that "... the clinical signs of any disease, particularly at its early stages, are formed from the material referable to prior life experience" [71] are considered to be sufficient grounds for such assumptions.

All of the subjects presented rather typical changes in static posture with reproductive suggestion of partial weight ("gravity hyposthesia"): the spine is straightened out, not infrequently the subject stands on his toes, his arms are

somewhat bent at the elbow and are moved away from the body. These postural distinctions persist when walking, which is performed at a slower pace with limited biodynamic participation of the arms in this process.

Figure 59 illustrates the typical changes in vertical components of the test movement of "elevating hands to shoulder level and dropping them" at a comfortable pace. The analyzed movements were made in a hypnotic state, with sensation of usual weight, as well as reproductive suggestion of 1/g G hypogravity. Table 5.4 lists mean changes in movement parameters.

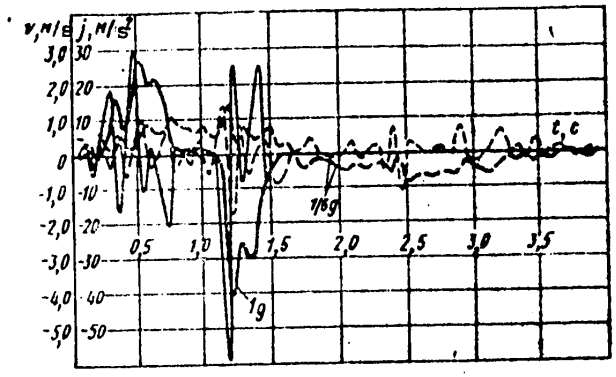

Figure 59. Changes in vertical velocity (boldface lines) and accelerations (thin lines) while raising and dropping hands in the ordinary state (——) and with suggestion of diminished body weight (---)

Table 5.4. Main parameters of test movement in a state of hypnosis

Movement	Experimental condit. G	Movement time, s	Mean speed m/s	Maximum speed m/s	Mean acceleration m/s²	Maximum acceleration m/s²
Raising arm	1 1/6	1,0 1,7	0,9 0,5	27,4 14,0	6,6 3,6	31,0 13,5
Dropping arm	1 1/6	0,56 2,3	1,7 0,35	41,0 8,8	13,8 1,8	58,5 11,5

As can be seen in this table, with reproductive suggestion of partial gravity there was 1.7-fold increase in speed of the active part of the test movement and 4.1-fold increase in the passive part (dropping the hand). Mean and maximum speed decreased by 1.8 and 1.9 times, respectively when elevating the arm and by 4.8 and 4.6 times when dropping it; in the former case, mean and maximum acceleration decrease by 1.8 and 2.2 times and in the latter case by 7.3 and 5.0 times. According to these figures, the initial biomechanical effect of partial gravity (longer movement time) is manifested to a greater extent in the passive part of the locomotor act and to a lesser extent in its active phase, which is voluntary [77]. A comparative analysis of horizontal elements is not made here on the grounds that

they reflect to a considerably lesser extent interaction between the motor analyzer and exogenous force field, i.e., demonstrate to a lesser extent the functional role of the muscular system in interaction with gravity forces [9].

Typically enough, progressive "increment" of body weight is associated with progressive increase in pulse rate. This is manifested the most when the factor is real: reproductive suggestion elicits considerably less increment of pulse rate than a real influence.

There were no physical factors of gravity in the form of deformation and displacement of internal organs, change in pressure in blood vessels, etc., in this experiment. Consequently, the observed cardiovascular reaction to reproductive suggestion of gravity is attributable to increase in general mental tension, as well as accentuation or redistribution of general muscle tone. The data referable to the galvanic skin response and actography are an indirect confirmation of this finding. However, only special myographic studies can offer a direct reflection of functional state of different muscle groups exposed to the above factors.

Functional reorganization of the motor analyzer in the course of decline of afferentation associated with subjective sensation of diminished weight also had a specific effect on the electroencephalogram (Figure 60).

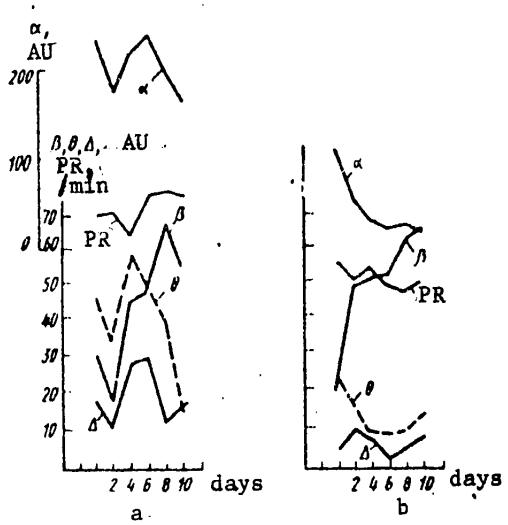

Figure 60.
Change in EEG spectrum when gradual decrease of body weight to 5 kgf is suggested to subject (PR--pulse rate)
a) subject 1; b) subject 2; AU--arbitrary units

The results of studies of biomechanical and autonomic reactions of man to whom the reproductive suggestions are made during hypnosis of different gravity states revealed that the functional and locomotor changes that occur are similar to those that are observed under actual conditions of partial weight loss, as well as with the use of other modeling methods.

Bearing this in mind, it was deemed quite interesting to explore the possibility of continuous retention of suggested "gravity hyposthesia" for a long time in the posthypnotic period (3-10 or more days), during which the subjects would be able to perform the complete set of tasks stipulated in standard programs for space flights. Experiments following a specific program were conducted twice for 3, 5 and 10 days (repeated after 15-20 days) on the same subjects. The experiments were preceded by a period of instruction and training of subjects in all of the techniques simulating operator work. The widely used parameter, "establishment of a functional plateau," served as a criterion of degree of readiness of operators for these experiments dealing with quality of performance of test work.

In the first (control) experiments, the subjects were in their ordinary state and the main factor affecting the body consisted of 3-, 5- or 10-day relative hypodynamia. At the start of repeated (main) 3-, 5- and 10-day experiments, the subjects were submerged into a deep hypnotic state, after which similar suggestions were made of partial loss of sensitivity to gravity factors. In group experiments, the suggestions were made to all subjects at the same time. After appearance of objective signs ("floating" of the arms, electrophysiological parameters) and verbal account of the subjects confirmed that the suggestion was effective, they were brought out of hypnosis 5-7 min later and began to perform programs of the appropriate multiday experiments with new gravity sensations.

Upon completion of the experimental programs at the end of the 3d, 5th and 10th days, the subjects were again hypnotized. Weight "was restored" under hypnosis by means of using a suggestion with opposite meaning. There was gradual "increase" in weight to the usual level over a period of 10 min, with constant monitoring of physiological functions, after which the subjects were brought out of the hypnotic state just as slowly.

The most typical mental reaction in the first few hours of hypogravity was some degree of euphoria, associated with excessive motor activity, talkativeness and laughter. Such signs were also seen in cosmonauts who first experienced real weightlessness in orbital flights.

The second common [general] distinction of mental sensations during simulation of decreased body weight is absence of pressure of the chair and tension of dorsal muscles while keeping a constant position for several days. The subjective sensations of hypogravity are associated with corresponding objective manifestations, which usually have a tendency to accumulate with time and become fixed.

Figure 61 illustrates some of the characteristics of movements when walking at different stages of 10-day experiments (the data were averaged for three subjects). As can be seen from this figure, the biomechanical changes when walking in a state of diminished weight, as well as at the first stage of the readaptation period, lead to appearance of the so-called "sailor's gait." The decreased stability in vertical position causes shortening of steps and placement of the feet at a considerably greater distance from the axial line of movement than is normally the case. The gait disorder is even more marked at the readaptation stage.

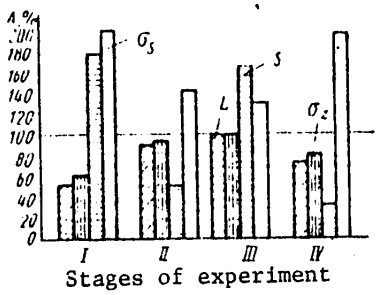

Figure 61.
Plantography data at different stages of long-term experiments (A--level of change in function in relation to base readings; L--length of step; S--deviation from midline)
I) 1st day, hypogravity
II) 10th day, hypogravity
III) 10th day, hypodynamia
IV) 10th day, readaptation

The disturbances referable to coordination with the suggestion of diminished weight are very graphically demonstrated on oculograms. There is drastic change in shape of the EOG [electrooculogram], with appearance of irregular additional waves. As time passes, these signs disappear; however, the amplitude of the EOG continues to increase over the

entire period of suggested diminished weight. In the readaptation period, however, there was drastic decrease in EOG amplitude (Figure 62).

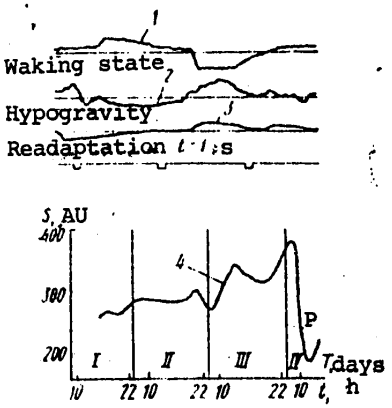

Figure 62.
EOG during simulation of diminished body weight (P--readaptation, AU--arbitrary units)
1) waking state
2) hypogravity
3) readaptation
4) averaged data for area circumscribed by amplitude and isoline in hypogravity state

These changes were associated with fluctuations of some characteristics of visual functions, particularly acuity and contrast sensitivity. These data are illustrated in Figure 63, as compared to data obtained during an actual space flight when performing the same visual tests.

Figure 64 illustrates data characterizing the pulse rate dynamics during 3-, 5- and 10-day experiments (curves 1, 2 and 3, respectively). In all cases, simulated states of diminished weight (hypogravity) elicited considerably greater slowing of the pulse (by 5-10%) than relative hypodynamia, which was present in the control experiments. The most marked decline of pulse rate in such a state was observed at rest, particularly nocturnal sleep, and it was less marked when performing work operations. Exercise in a state of diminished weight was associated with relatively greater increment of pulse rate than in control experiments.

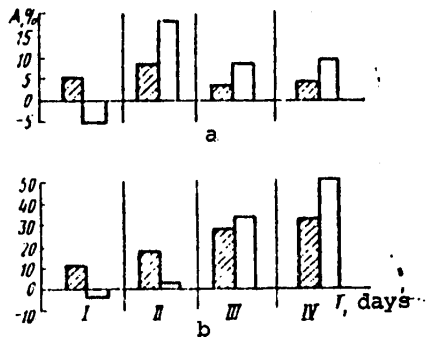

Figure 63.
Change in visual functions during simulated hypogravity (white columns) and actual space flight (striped columns)
a) visual acuity
b) contrast sensibility

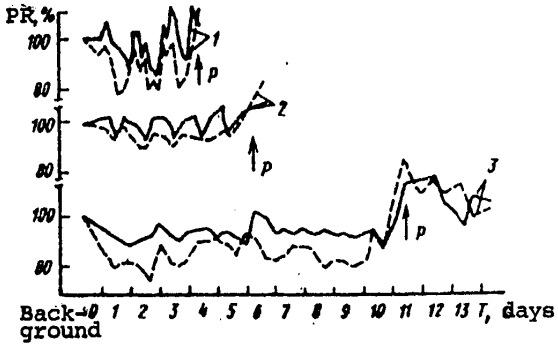

Figure 64.
Changes in pulse rate [PR] (mean data) in many-day experiments
1) 3-day experiments ——) control experiment
2) 5-day experiments
3) 10-day experiments ---) hypogravity

Orthostatic tests, which were conducted before and after control experiments, as well as experiments where the suggestion of hypogravity was made, revealed that the reactions of the cardiovascular system were less favorable in the latter case (Figure 65).

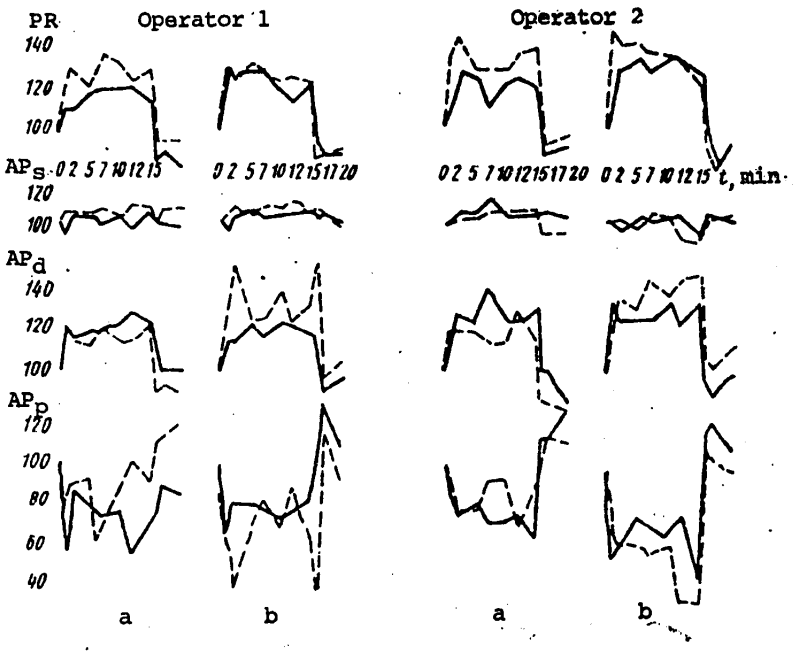

Figure 65. Orthostatic reactions after 5-day control experiments (a) and experiments with suggested hypogravity (b)

AP_s) systolic arterial pressure
AP_d) diastolic arterial pressure
AP_p) pulse arterial pressure

1st-15th min--orthostatic position
15th-20th min--horizontal position
—— before, --- after experiment

Marked cardiovascular and motor reactions were demonstrated in the period of readaptation to usual weight, which lasted 1 day after the 3-day experiment, 2 days after the 5-day one and 5 days after the 10-day one.

Thus, it was proven that the effectiveness of a single hypnotic suggestion of subjected sensation of diminished body weight can persist for 5-10 days.* As time passes, not only does the hypnotized state fail to regress, on the contrary, it shows a tendency toward "further completion of expression," of becoming firmly fixed and eliciting adequate physical changes in the body.

*At the present time there are experimental data indicating that such a state may persist for 30 days.

CHAPTER 6. EVALUATION OF EFFECTIVENESS OF ASTRONAVIGATION SYSTEMS WITH A HUMAN OPERATOR

6.1. Research-training astronavigation unit

Modern systems of space astronavigation are systems of the man-machine type. In such systems, the operator emerges in the role of the most important, most responsible element. For this reason, it is impossible to design such systems without consideration of the "human factor." At the present times, problems that arise in designing systems including man, as well as studies of the effectiveness [or efficiency] of such systems, involve essentially experimentation [22].

Experimental studies of systems of the man-machine type require the use of a diversified approach, since it is only possible to obtain reliable results if there is full enough recording of both the parameters characterizing the performance and psychophysiological state of the operator and parameters of dynamics of the machine and state of the environment.

For this reason, at the present time there has been broad development of experimental research based on dynamic complexes [units]. They are intended for half-scale ["seminatural"] modeling of systems of the man-machine type, objective evaluation of the efficiency of such systems with the use of various algorithms, demonstration of statistically reliable characteristics of the operator as part of the system under study as affected by the environment, as well as for offering work training with specific equipment, with concurrent evaluation of training achievement.

We shall discuss below an astronavigational research-training unit (ARTU), which consists of the following (Figure 66): system operator and consoles, with which he works (model of sensorimotor field)--I; sensors and recorders (including sensors of psychophysiological parameters)--II; combination computer system--III; experimenter's monitoring and control consoles.

The computer system (CC) of this ARTU consisted of a Minsk-32 digital computer (DC), Dnepr-1M multipurpose control computer (MCC) and MN-18 analog computer (AC), which were all interconnected.

The MN-18 AC makes it possible to preset [preselect] the model of the object, change its dynamic properties easily and can serve as the matching element between the operator's console and inputs of the Dnepr-1M MCC; it also solves problems of modeling the dynamics of the sensorimotor field of the operator and filtration task.

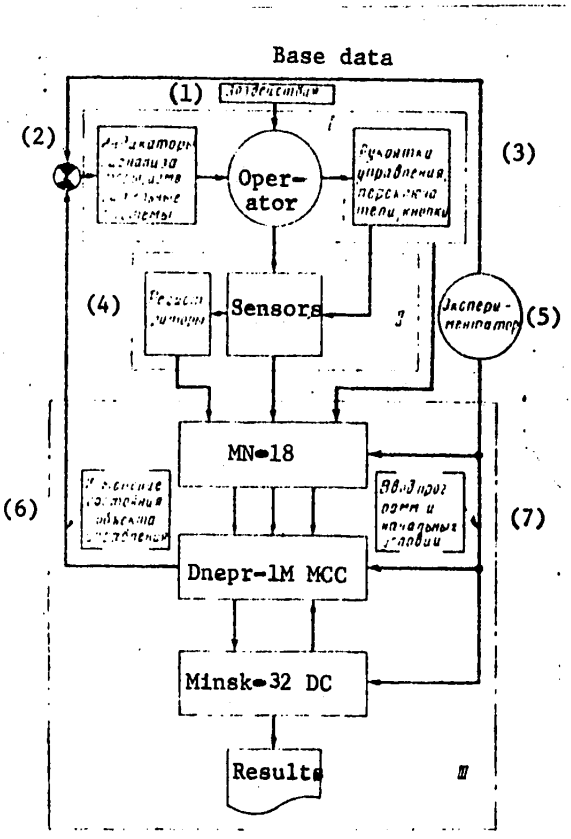

Figure 66.
Block diagram of astronavigational research training complex (ARTU)

Key:
1) actions
2) display signals of measuring systems
3) control handles, switches, buttons
4) recorders
5) experimenter
6) change in state of object of control
7) input of programs and initial conditions

The Dnepr-1M MCC performs the functions of a translator transmitting information from the operator's console and sensors to the Minsk-32 DC. It can perform the following tasks: convert analog signals and submit them to preliminary statistical processing (obtaining mean values and dispersions, computing criteria and estimates of various types of work, averaging the results of psychological tests, etc.); form an array of electrophysiological parameters and evaluations of performance; convert data into a form that is convenient for input in the Minsk-32 DC; produce control signals and voltage for the AC.

The Minsk-32 DC is used for final processing of experimental data by means of specified algorithms, mathematical modeling of the system (subsystem) under study, printing out the results of running the programs, etc. It is known that computations made on an analog computer are notable for high speed but low accuracy. At the same time, it is quite difficult to use precise digital methods when processing rapid phenomena, particularly if many parameters of a given process, as well as various processes, are being recorded. For this reason, it is logical to combine digital and analog computers in the CC. The use of different types of computers in the CC expands significantly the capabilities of the entire unit.

Converters (analog-digital--ADC, and digital-analog--DAC), multichannel switches and decoders, synchronizers and controlling devices, buffer devices, memory, etc., are required to make joint use of analog and digital computers.

Multichannel switches [commutators] and decoders are used so that the converters, which translate a continuous signal into a discrete digital code and vice versa, could function in a time-sharing mode. The memories are needed to store the values of continuously changing signals for a time that is sufficient to effect the conversion. The buffer devices are needed to match the levels of amplitudes,

shapes and duration of pulses that provide for the joint operation of digital and analog computers. Finally, the synchronization and control circuits are needed to synchronize processes in the different units that form the system.

The functions of all of the above devices can be assumed by an intermediate digital computer additionally connected into the system as a mediator beween the base DC and AC. Of course, the intermediate digital computer must be small and have adequate elementary software, but broad capabilities with regard to control of input and output devices. The small digital computers of the Dnepr type meet these requirements in full; each unit thereof contains a device for communication with the object, which has a large enough number of analog and relay inputs, as well as relay outputs. For this reason, one can easily connect the MN-18 AC with the Dnepr-1M computer in the described ARTU, making direct use of analog and relay inputs of the latter. The MN-18 AC and Dnepr-1M MCC function together automatically by means of a program with the use of a control unit (CU) and device for communication with the object (DCO) in the Dnepr-1M and its relay inputs (RI).

In order to perform the task of combining the Dnepr-1M MCC with the base DC, which is a series produced computer of the Minsk-32 type in the ARTU, special devices are also required that are quite complicated when communicating via the fast channel (they are not included with these computer units). It would be much simpler to use one-way communication via the slow channel. Thus, in the ARTU under discussion, information is transmitted from the Dnepr-1M to the Minsk-32 in a binary code over the coded read lines using a buffer cascade, tape input (UVvL-23) of the Minsk-32 and special programs for transmitting data, which function synchronously in both computers.

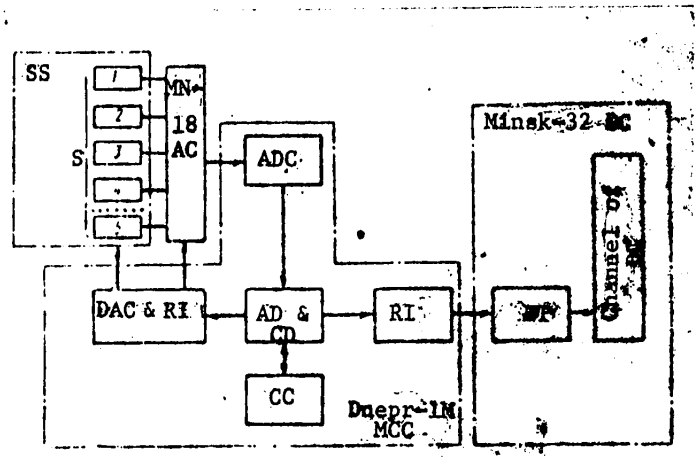

Figure 67. Block diagram of computer system of ARTU

S) data sensors
DAC) digit-analog converter
ADC) analog-digital converter
IO) input-output device
SS) space sextant
CC) control console
DT) device for input from papertape
CU) control unit
AD) arithmetic device
RI) relay input device

Figure 67 illustrates the block diagram of a combined CC in the ARTU. This figure shows that the obtained system has both two-way (MN-18--Dnepr-1M) and one-way

(Dnepr-1M--Minsk-32) communication. For this reason it is possible to control progress of the experiment only on the basis of intermediate results. Further development of this CS is to create two-way communications between the Minsk-32 and Dnepr-1M computers.

Current information from different sensors can be transmitted to the computer system over the communication cable. This permits making fuller use of the CS by connecting to it various models of the operator's sensorimotor fields (or real field). For this reason, the operator, system and consoles with which he works can be located in a separate room, which expands the capabilities of the complex with respect to studying the effects of different factors on operator work capacity. In addition, this creates beneficial conditions for simulating cosmonaut performance as a whole, on a manned spacecraft in our case. Not only performance, but rest, diet, etc., conditions can be simulated, i.e., concrete programs of short- or long-term flights can be modeled. From the standpoint of obtaining reliable data, the optimum approach to studies of psychophysiological capacities of man when working in an astronavigation system is one where the work under study is included in the overall "flight" program.

The model of the operator's sensorimotor field is designed to simulate systems, consoles that the operator works with and conditions of his work. It is the most expedient to use combined models in the complex [33], which include elements of a general and detailed model. The composition of the model can be changed, depending on the purpose of the study. However, the model must always include a sensory field (displays, signals, viewfinders [sights], etc.) and a motor field (control handles, buttons, switches, etc.).

The following are included in the model of sensorimotor field of the above-described ARTU (which determines its specialization): functional mock-up of space sextant (SS) with its control console and simulator of earth's surface (detailed models), as well as a mock-up of a manned spacecraft cockpit (general model).

The block diagram of linkage of elements of functional SS model with the ARTU computer system is illustrated in Figure 68. Sensors D_1, D_2 and buttons K and H can serve also to obtain the time characteristics of the process of directing the SS (time spent on solving the entire problem, reaction time, decision making time, etc.), while R_1, R_2, R_1' and R_2' are precision characteristics (amplitude of error, its integral, etc.).

Work with the functional model of a space sextant was done in a special simulation chamber (mock-up of manned spacecraft cockpit). A model of the operator's work place was installed in this chamber, where he took navigational readings with a space sextant.

The operator's work with an SS model consisted of the following:

1) Identifying the specified sighting objects (for example, a star and terrestrial landmark) upon receiving the signal to "start working," viewing their images concurrently in the stationary eyepiece of the SS model.

2) Guide the specified sighting objects into the crosslines of the eyepiece of the SS model by manipulating control handles.

3) Fix the end of the measurement and depress button for input of information. The obtained angles of deflection of the main mirrors of the sextant and sight are automatically read by the computer.

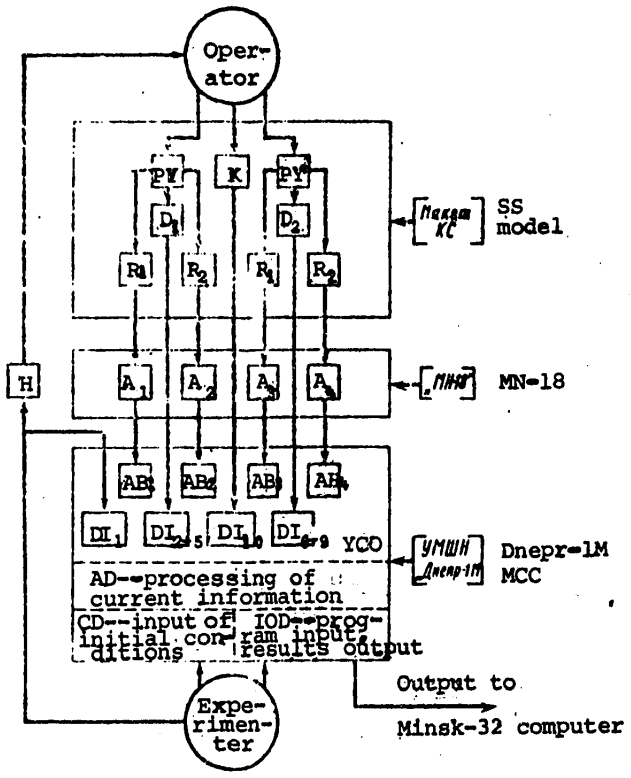

Figure 68. Block diagram of communication between model of space sextant and computer system

PY, PY') handles [knobs] of sextant and sight
SS) space sextant
R_1, R_2, R_1', R_2') SS electric sensors from which information is taken to calculate angle between direction of sighted objects
A_1, A_2, A_3, A_4) amplifiers of matching unit
K) button for input of data into digital computer
D_1, D_2) discrete sensors of position of control handles
YCO) device for linkage with object
AB) analog inputs of YCO
CD) control device
IOD) input-output device
AD) arithmetic device
DI) discrete inputs of YCO

Thus, this model of the sensorimotor field made it possible to include a real operator in the astronavigation system and thereby enabled us to study it as a whole.

The sensors and recorders are designed to receive and issue to the CS information that is required to assess the efficiency of the system as a whole or its different elements, as well as to determine the psychophysiological state of the operator. Signals, buttons, contact strips and other position sensors and devices on the operator's console, as well as various sensors attached to the operator and connected to biopotential amplifiers (in the ARTU a type TR-60 8-channel encephalograph was used), can serve as sensors of parameters of efficiency of the system. This equipment makes it possible to input in the CS and use for evaluation of operator performance such psychophysiological parameters as reaction time, decision making time, encephalogram, pneumogram, electromyogram, oculogram, electrocardiogram, etc.

Such physiological parameters as mathematical expectation and dispersion of the operator's heart rate are quite informative in studies of efficiency of operator performance in a man-machine system. The general algorithm for obtaining them in the ARTU are: 1) recording the electrocardiogram (EKG) by means of biopotential sensors and the TR-60 unit; 2) amplified biopotentials (EKG) are fed to the MN-18 input from the output of the TR-60; 3) EKG R waves are singled out on the MN-18 and fed to the relay input numbered K of the Dnepr-1M MCC in the form of pulses with negative polarity; 4) the Dnepr-1M MCC interrogates input K following the set program and, upon appearance of a pulse, stores time t_1 by means of the time pulse counter. Upon appearance of the next pulse, time t_2 is stored, then t_3, ..., t_i, ..., t_n; 5) in the arithmetic device (AD) of Dnepr-1M determination is made of $T_j = (t_i - t_{i-1})$, which is the time between two cardiac contractions (in seconds), where $i = 1, 2, 3, \ldots, n$ is the number of transmitted pulses, $j = i-1$ is the number of recorded periods; 6) from the T_j stored in Dnepr-1 M, calculation is made of mathematical expectation--$M(f)$--and dispersion--$D(f)$--of heart rate within the specified time (minute) using the equations:

$$M(f) = \frac{60(n-1)}{\sum_{j=1}^{n-1} T_j}; \quad D(f) = \frac{\sum_{j=1}^{n-1}\left[\frac{60}{T_j} - M(f)\right]^2}{n-2},$$

where f is the frequency of cardiac contractions, beats/min.

Using analogous algorithms, we can process other psychophysiological parameters (for example, respiratory rate).

It should be noted that the program for processing psychophysiological parameters is executed together with other programs inputted in the ARTU computer system. This makes it possible to evaluate, in the course of the experiment, the state of the operator and his psychophysiological "expenditures" as an element of some system or other.

Thus, one can do the following using the above-described astronavigational research-training unit: teach operators various types of work with concurrent evaluation of

how well they were learned; study the effects of different factors on efficiency of the ergatic system, and these factors may vary in nature (for example, technical executation of some elements of the system, effect of simulated weightlessness, distribution of functions between the operator and automatic equipment, etc.); evaluate dynamic parameters of different systems of navigation and control; evaluate time and precision characteristics of the process of taking astronomic readings; evaluation of efficiency of the astronavigation system as a whole with the use of some quantitative criteria or other; obtain generalized estimates on the basis of psychophysiological and technical parameters.

This complex also permits solving many other problems. An important distinction of using the complex for investigations is that it is possible to solve several problems simultaneously, with concurrent recording of many diverse parameters (psychophysiological, technical, state of the environment).

Such a method of evaluating a man-machine system is complex (polyeffector) [33]. The reliability and informativeness of results obtained by this method are determined by the fact that it is based on reproduction of the actual dynamics of the control process, simulation of external operator working conditions, consideration of quantitative and qualitative characteristics of the control process, as well as recording and analyzing psychophysiological parameters of the operator.

6.2. Evaluation of Dynamic Characteristics of Navigation and Control Systems

After analyzing cosmonaut performance referable to solving interrelated navigation and control problems, it is not difficult to arrive at the conclusion that these activities include tracking functions in the closed control circuit.

Modern control theory has comprehensively developed methods for analysis and synthesis of tracking systems of different types. Use of this theory to study ergatic systems is possible if we have a mathematical description of the work of an operator in the system. It is desirable for this description to be of the same type as used to describe machine elements of the system.

Along with other types of models, wide use is made in control theory of transfer function, which is the input-output correlation in the Laplace image space [transform?], as a mathematical model of various objects (systems).

There has already been development for several decades of studies of ergatic tracking systems by methods of automatic control theory with the use of transfer functions as operator models. Man is a complex biological system, so that a mathematical model thereof, which would take into consideration of the entire diversity of distinctive features in man's controlling activities, would be tremendously complicated. Obviously, development of an operator model should be based on the optimum compromise approach, taking into consideration as many factors as possible that reflect the specifics of man's performance in a tracking system and the need to design a relatively simple model, which would be suitable for analysis and synthesis of an ergatic system.

At present, we know of a considerable number of various mathematical models of man's performance in the tracking mode. Thus, 20 variants of mathematical models of man as an element in a closed tracking system have been listed in [58]. Their diversity is attributable not only to various methods of construction, but primarily

the fact that the reactions and functional characteristics of an operator depend appreciably on many factors: type of controlled object, nature of input signal, type of display [indicator], degree of operator fatigue, level of his training, emotional state, etc. In the case in question, when the cosmonaut is the operator, one must also bear in mind factors that are related to the specific conditions of space flights.

The variability of characteristics of the operator and their dependence on many different conditions move to the fore the task of evaluating the ergatic system on a real time scale when controlling a specific object under concrete conditions. In other words, it becomes necessary to identify the system, i.e., form an adequate mathematical model on the basis of processing input signals and the system's reactions to them.

Identification involves two tasks: 1) determination of the structure and parameters of the model; 2) determination of parameters of the model of an object when a given structure applies.

Since availability of information about the structure of the model or choice of a rather general structure as the base to start the identification process speeds up this process significantly, it is easier to make the identification on a real time scale within the framework of the second task.

The so-called quasilinear model has gained wide popularity as the model of man as an element of a tracking system. Such a model, which is more general in form than the one described in Chapter 2, has a linear part in the form of a transfer function and a "remainder" [11]. One can obtain sufficient generality [or similarity] of a quasilinear model, required to take into consideration the variability of human traits, by virtue of the fact that transfer function of the operator (W(p) is given in the form of relationship between two polynomials without stipulating a priori the number of terms in either the numerator or denominator:

$$W(p)=\frac{\sum_{i=0}^{m} b_i p^i}{\sum_{i=0}^{n} a_i p^i}=\frac{Y(p)}{U(p)}, \qquad (6.1)$$

where a_i and b_i are parameters of the model of the operator which take into consideration the linear component of man's reaction to an input signal presented to him on a display. The "remainder" in the quasilinear model reflects the degree of inadequacy of a linear model for man's actual characteristics when working in a given system, under given concrete conditions.

After choosing the structure of the mathematical model of an ergatic system to be of the (6.1) type, the task of identification is reduced to experimental determination of its parameters, evaluation of parameters. It must be noted that, although we know of many different identification methods, most of them were not developed to the stage of concrete algorithms for estimation of parameters and structure of an object on a real time scale; for this reason, it is still a pressing task to

conduct research to upgrade these methods in the direction of improving accuracy and speed of evaluation, particularly as related to ergatic systems.

We shall describe one of the effective methods of identification that is used on a real time scale. This method amounts in essence to conversion of a differential equation equivalent in the time area to a transfer function (6.1) to a system of linear algebraic nonstationary equations and then to recurrent solution of this system.

In the time area, transfer function (6.1) corresponds to a differential equation of the following appearance:

$$\sum_{i=0}^{n} a_i \frac{d^i y(t)}{dt^i} = \sum_{j=0}^{m} b_j \frac{d^j u(t)}{dt^j}, \tag{6.2}$$

where $u(t)$ and $y(t)$ are input and output signals of the object, respectively; a_i and b_j are unknown parameters of the object, one of which, for example a_0, can be considered to equal one. In this case, the vector of unknown parameters h is an l-dimensional vector ($l = n+m+1$):

$$h^{\mathrm{T}} = [a_1, a_2, \ldots, a_n, b_0, b_1, \ldots, b_n] \tag{6.3}$$

The task at the first stage of identification is to form algebraic equations in relation to coordinates of unknown vector h. When there are unknowns, the coefficients should be the observed coordinates of the object.

Let us introduce the following designations:

$$\begin{gathered} y(t) = \psi(t); \\ -\frac{dy(t)}{dt} = \varphi_1(t), \ldots, \quad -\frac{d^n y(t)}{dt^n} = \varphi_n(t); \\ u(t) = \varphi_{n+1}(t); \\ \frac{du(t)}{dt} = \varphi_{n+2}(t), \ldots, \quad \frac{d^m u(t)}{dt^m} = \varphi_l(t); \\ \varphi^{\mathrm{T}}(t) = [\varphi_1(t) \ldots \varphi_l(t)] \quad (l = n+m+1). \end{gathered} \tag{6.4}$$

With consideration of designations (6.4), the differential equation (6.2) for discrete points in time k can be submitted in the form of an algebraic equation:

$$\psi(k) = \phi^{\mathrm{T}}(k)h \tag{6.5}$$

Let us call such a transformed model the ideal canonical model. It does not take into consideration conversion and measurement errors. These errors can be taken into consideration in a canonical model of the following appearance:

$$\psi(k) = \phi^{\mathrm{T}}(k)h + \eta(k) \tag{6.6}$$

where $\eta(k)$ is discrepancy, which is also called noise. The discrepancy could be attributable to measurement errors, errors of approximation of a real object in a linear model and other factors.

By measuring $\psi(k)$ and $\phi(k)$ at successive points in time and using one of the iterative computing algorithms, we can estimate parameter vector h, the coordinates of which are, according to (6.3), coefficients of differential equation (6.2). The difficulty lies in the fact that we need to know the derivatives of the input (to the m order) and output (to the n order) signals. Under real conditions, repeated direct differentiation is not effective because of the interference superimposed on input and output signals.

To avoid direct differentiation of signals, let us turn to the other observed coordinates of the object on the basis of the method of additional filtration [21]. For this, let us use certain ancillary operator-filters with the same transfer functions $F(p)$ on the observed input $u(t)$ and output $y(t)$ signals of the object. With the proper choice of filters, all of the phase coordinates of signals are observable at their outputs and are found to be related in the fashion of (6.5) to vector h determined by equation (6.3).

Using the Laplace transform for equation (6.2) and then multiplying it by function $F(p)$, all poles of which are to the left of the imaginary axis of plane p, we shall have:

$$F(p)\left\{\sum_{i=0}^{n} a_i\left[p^i Y(p)-\sum_{q=1}^{i} p^{i-q}\left(\frac{d^{q-1}y(t)}{dt^{q-1}}\right)_{+0}\right]\right\}= =F(p)\left\{\sum_{j=0}^{m} b_j\left[p^j U(p)-\sum_{r=1}^{j} p^{j-r}\left(\frac{d^{r-1}u(t)}{dt^{r-1}}\right)_{+0}\right]\right\}. \tag{6.7}$$

where $(\ )_+$ refers to the initial conditions of variables. In this equation, the terms that depend on base conditions of variables $y(t)$ and $u(t)$ and their derivatives are extinguished [damped] in the time region, and the less the time of the transfer processes of filters $F(p)$, the faster this damping occurs:

$$\lim L^{-1}\left\{F(p)\sum_{q=1}^{i} p^{i-q}\left(\frac{d^{q-1}y(t)}{dt^{q-1}}\right)_{+0}\right\}=0$$

and $$\lim L^{-1}\left\{F(p)\sum_{r=1}^{j} p^{j-r}\left(\frac{d^{r-1}u(t)}{dt^{r-1}}\right)_{+0}\right\}=0 \quad \text{with } t\to\infty,$$

where L^{-1} is the symbol for the inverse transform of Laplace.

Thus, by performing the inverse Laplace transform in equation (6.7) and disregarding the influence of base conditions, we shall obtain the main equation for the method of additional filtration:

$$\sum_{i=0}^{n} a_i \left[\frac{d^i y(t)}{dt^i}\right]_{F(p)} = \sum_{j=0}^{m} b_j \left[\frac{d^j u(t)}{dt^j}\right]_{F(p)}, \tag{6.8}$$

where $$\left[\frac{d^i y(t)}{dt^i}\right]_{F(p)} = L^{-1}\{Y(p)p^i F(p)\}$$

and $$\left[\frac{d^j u(t)}{dt^j}\right]_{F(p)} = L^{-1}\{U(p)p^j F(p)\} \tag{6.9}$$

are the phase coordinates at the output of the additional filters when signals $y(t)$ and $u(t)$, respectively, are fed to their inputs.

We assume that in equation (6.8) $a_0 = 1$ and introduce the following designations:

$$\begin{gathered} [y(t)]_{F(p)} = \varphi_1(t); \\ \left[\frac{dy(t)}{dt}\right]_{F(p)} = \varphi_2(t), \ldots, \left[\frac{d^n y(t)}{dt^n}\right]_{F(p)} = \varphi_n(t); \\ [u(t)]_{F(p)} = \varphi_{n+1}(t); \\ \left[\frac{du(t)}{dt}\right]_{F(p)} = \varphi_{n+2}(t), \ldots, \left[\frac{d^m u(t)}{dt^m}\right]_{F(p)} = \varphi_l(t); \\ \ldots \end{gathered} \tag{6.10}$$

With consideration of these designations, equation (6.8) for discrete points in time k is put into canonical form (6.5):

$$\psi(k) = \phi^{\mathrm{T}}(k)h$$

Here, $\psi(k)$ and vector coordinates $\phi(k)$ are converted phase coordinates of model (6.2) observed at the outputs of the filters $F(p)$ at discrete points in time k.

Let us discuss the requirements of the structure and parameters of the additional filters.

In order to obtain estimates of all l coefficients of the object's transfer function by the method of additional filtration, we must observe the appropriate number of phase coordinates at the outputs of the additional filters. This condition is satisfied if the order of the transfer function of additional filters $F(p)$ is not lower than the order of the object's transfer function. Thus, taking into consideration the requirement that execution must be simple, we determine the structure of the additional filters. In selecting the parameters of these filters, one should proceed from the level of high-frequency interference. The higher this level, the narrower the bandpass of the filters must be. One must also bear in mind that reduction of the bandpass prolongs the transient processes due to the nonzero base conditions.

Figure 69 illustrates, as an example, the block diagram for conversion of phase coordinates for parametric identification of an object, the model of which is

described by a second order transfer function. For such an object, the order of transfer function of additional filters should be at least two. The block diagram illustrates third order filters $F(p)$.

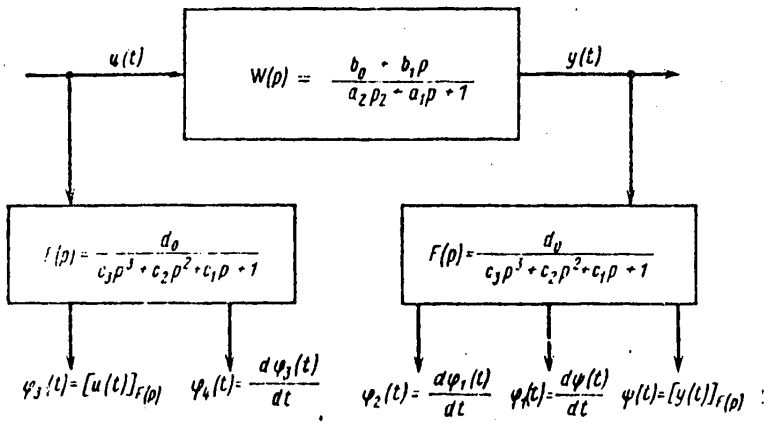

Figure 69. Block diagram for conversion of second order model of a dynamic object to canonical form

Output signal $\psi(k)$ of the transformed model (6.5) is formed by measuring at successive points in time k the output signal of filter $F(p)$ connected to the output of the object. To form the coordinates of four-dimensional vector $\phi(k)$ one uses discrete measurements of two phase coordinates of the filter connected to the object's output and two phase coordinates of input filter $F(p)$. Additional filters can be executed in analog or digital form.

The second stage of solving the problem of parametric identification is to calculate the parameters of a nonstationary object when the structure of its model is specified. In the general case, we shall discuss the model reduced to canonical form (6.6). The algorithms for calculating estimates of parameters of nonstationary objects must define the parameters of its model in the course of functioning of the object. Such models were named adaptive [76].

The adaptive approach to solving the estimation problem makes it possible to track the changing vector of object parameters as information is received about input and output variables of the object. The simplest way to do this is to use recurrence algorithms to calculate the estimates of parameters.

Recurrence algorithms, which do not require repeated processing of the entire sequence of observations at every step, permits evaluation of the object's parameters in real time. Recurrent or interative estimation provides a solution in the form of a sequence of vectors, which are formed by means of a uniform process--the iteration process.

In each calculation of estimates, iterative algorithms can make use either of only incoming information about input and output variables of the object, or of preceding information as well. In the latter case, the algorithm should retain

prior information (i.e., it should have a memory). The volume of information used to obtain a new estimate of parameters determines the depth of algorithm memory. Recurrence algorithms can be divided into three groups in relation to this feature.

The first group consists of algorithms without memory, which do not store the results of prior observations, and they are often called single-step ones. They use one--the last--set of measurements of input and output variables of the object to calculate estimates of parameters. The depth of their memory, which we shall refer to hereafter as S, equals one.

The second group refers to algorithm with memory of $2 \leqslant S \leqslant l$ (l--dimensionality of vector of object parameters). In these algorithms, each determination of estimates is made as a result of processing S of the last sets of measurements of object coordinates, so that (S-1) of sets of prior readings must be stored.

The third group will include recurrence algorithms for adaptive solution of the problem of estimating parameters with memory depth $S > l$.

The basic distinction of the third group of algorithms, as compared to the second group, is that l linearly independent equations are required to solve the system of equations (6.6) in relation to an l-dimensional stationary vector h. With $S < l$, the system is underdefined and with $S > l$ it is overdefined.

Both the second and third groups of algorithms are multistep ones in the sense that the results of many steps of measuring the object's coordinates are used for each successive evaluation of the parameter vector.

To stress this fact and, at the same time, set off different algorithms, we shall call the second group simply multistep algorithms and the third group multistep with redundant memory.

Analysis revealed that, of the recurrence algorithms, single-step ones have the best computer parameters; however, it is difficult to use them because of their low operating speed (rate of convergence). On the other hand, algorithms with redundant memory, which have good convergence, require a large volume of calculations for each iteration. This is suggestive of the conclusion that it is desirable to develop and use multistep algorithms, which have better machine characteristics than algorithms with redundant memory and operate faster than single-step ones.

There are several ways of forming algorithms for calculating estimates of parameters. In essence the differences lie in method of finding the extremum of a certain loss function. Use of methods of linear algebra makes it possible, in a number of cases, to avoid time-consuming analytical conversions and obtain algorithms in rather compact form, which is convenient for analysis and subsequent execution.

We assume that the equation of an object with l-dimensional parameter vector is reduced to canonical form (6.5):

$$\psi(k) = \phi^{T}(k)h$$

Let us consider this as an equation of a certain hyperplane consisting of a plane with dimensionality l-1 with a normal vector $\phi(k)$, in l-dimensional Euclidean space [17]. Apparently, with such an approach, vector h can be submitted as the

vector of intersection l of noncollinear hyperplanes described by equations of the (6.5) type. In the case where fewer than l equations are known, one cannot find the vector of object parameters h with them, and one can obtain only some approximation thereof, its estimate $c(k)$. When new information about the object is received, this estimate can be successively defined. Let us follow expressly this recurrent scheme, which is suitable for estimating parameters of both stationary and nonstationary objects. We shall search for the multistep algorithm in a certain general form, which is valid for different memory depth $S \leqslant l$.

Let us write equation (6.5) in the form of a system of equations obtained from measurement of converted coordinates of objects at S points in time, ending with $(k-\mu)$:

$$\psi(k-S+1)=\varphi^{T}(k-S+1)h;\ \psi(k-1)=\varphi^{T}(k-1)h;\ \psi(k)=\varphi^{T}(k)h. \tag{6.11}$$

These equations can be considered as a description of S hyperplanes of l-dimensional Euclidean space. We assume that at arbitrary point in time k-1 vector $c(k-1)$ is known, which satisfies the first S-1 equations of system (6.11). To correct estimate $c(k-1)$ at the kth point in time, another change is made in object coordinates, a reflection of which is the last equation in system (6.11).

By definition, in an S-step algorithm, at each step of determination of estimates of parameters there is processing of information about the object obtained as a result of S steps of measuring object coordinates. Let us search for maximum improvement of vector $c(k-1)$ according to information contained in equations (6.11). Improvement of the vector refers to reduction of the Euclidean norm of the vector of error of parameter measurement.

The new vector $c(k)$ must satisfy equations (6.11), and the Euclidean distance between vectors $c(k-1)$ and $c(k)$ must be minimal. Vector $c(k)$ satisfying these conditions can be found as the orthogonal projection of vector $c(k-1)$ on the hyperplane of $(l-S+1)$-dimensional space formed by intersection of hyperplanes (6.11) of l-dimensional space.

Proceeding from this, we can write the correlation between the new and old estimates in the following form:

$$c(k) = c(k-1) + z_S(k)f \tag{6.12}$$

where $z_S(k)$ is componant of vector $\phi(k)$ orthogonal to the hyperplane containing the first S-1 vectors of system (6.11). Vector $c(k)$ determined in this manner with arbitrary number f satisfies the first S-1 equations of system (6.11). The number f can be determined from the condition that vector $c(k)$ satisfies the last equation of system (6.11) also, and in this case it can be rewritten as:

$$\psi(k-S+1)=\varphi^{T}(k-S+1)c(k)+\varphi^{T}(k-S+1)z_S(k)f; \tag{6.13}$$

Inserting $c(k)$ from equation (6.12) in the last equation of system (6.13), we shall find f:

$$f = \frac{\psi(k) - \varphi^{T}(k)\, c(k-1)}{\varphi^{T}(k)\, z_S(k)}. \tag{6.14}$$

Inserting (6.14) in (6.12), we obtain the generalized multistep estimation algorithm, in which the preceding and following estimates of parameters are related as follows:

$$c(k) = c(k-1) + \frac{\psi(k) - \varphi^{T}(k)\, c(k-1)}{\varphi^{T}(k)\, z_S(k)}\, z_S(k). \tag{6.15}$$

The second summand in algorithm (6.15) is the vector-correction that is proportionate to prediction error $\varepsilon(k)$, which is calculated with the formula:

$$\varepsilon(k) = \psi(k) - \varphi^{T}(k)\, c(k-1). \tag{6.16}$$

Vector $z_S(k)$, which determines the direction of the vector-correction, is a component of vector $\phi(k)$ that is orthogonal to S-1 of the preceding input vectors of the object. Hence, to determine vector $z_S(k)$ we must subtract from vector $\phi(k)$ the components that coincide in direction with vectors $z_i(k\text{-}S+1)$ (i = 1, 2, ..., S-1). Thus:

$$z_S(k) = \varphi(k) - \sum_{i=1}^{S-1} \frac{z_i^{T}(k-S+i)\,\varphi(k)}{z_i^{T}(k-S+i)\, z_i(k-S+i)}\, z_i(k-S+i), \tag{6.17}$$

where

$$z_i(k-S+1) = \varphi(k-S+1). \tag{6.18}$$

Let us mention that formula (6.17) is based on the orthogonalization process of Gram-Schmidt for a system of vectors [34].

Let us convert algorithm (6.15) into a form that is more convenient to use. Considering equation (6.17), let us calculate the denominator of the vector-correction of algorithm (6.15):

$$\varphi^{T}(k)\, z_S(k) = \varphi^{T}(k)\,\varphi(k) - \sum_{i=1}^{S-1} \frac{\left[z_i^{T}(k-S+i)\,\varphi(k)\right]^2}{z_i^{T}(k-S+i)\, z_i(k-S+i)}; \tag{6.19}$$

$$z_S^{T}(k)\, z_S(k) = \varphi^{T}(k)\,\varphi(k) - \sum_{i=1}^{S-1} \frac{\left[z_i^{T}(k-S+i)\,\varphi(k)\right]^2}{z_i^{T}(k-S+i)\, z_i(k-S+i)}. \tag{6.20}$$

Indeed, since vectors z_i are orthogonal to (6.17), we need to subtract from the square of Euclidean norm of vector $\phi(k)$ the square of Euclidean norms of subtracted components to find the square of the Euclidean norm of vector $z_S(k)$.

According to comparison of (6.19) and (6.20):

$$\phi^{T}(k)\, z_S(k) = z_S^{T}(k) z_S(k) \tag{6.21}$$

Substituting (6.21) in (6.15), we shall have:

$$c(k) = c(k-1) + \frac{\varepsilon(k) - \varphi^{T}(k)\,c(k-1)}{z_S^{T}(k)\,z_S(k)}\,z_S(k). \qquad (6.22)$$

Equation (6.22), in which vector $z_S(k)$ is determined by equation (6.17), is the basic form of writing down the generalized algorithm for correction of parameter estimates in the next and S-1 preceding step of measurement of coordinates of the object. The algorithm is called generalized, since it is written in the same form for different memory levels, from S = 1 to S = l. Thus, the generalized algorithm is in essence the description of an entire class of multistep algorithms. What is in common in all algorithms in this class is the form of calculation of the vector-correction of error of prediction $\varepsilon(k)$ and vector $z_S(k)$. The differences between algorithms differing in memory depth are determined by (6.17), according to which vector $z_S(k)$ is calculated. A change in value of parameter S will yield different concrete algorithms.

For example, let S = 1; in this case system of equations (6.11) degenerates into one equation:

$$\psi(k) = \phi^{T}(k)h$$

Replacing in (6.22), in accordance with (6.18), $z_1(k)$ with $\phi(k)$, we shall have:

$$c(k) = c(k-1) + \frac{\psi(k) - \varphi^{T}(k)\,c(k-1)}{\varphi^{T}(k)\,\varphi(k)}\,\varphi(k),$$

which corresponds to the so-called Kaczmarz algorithm [68].

When processing this algorithm for the initial evaluation of the vector of object parameters an arbitrary vector of l-dimensional space can be selected, for example, zero. The preceding estimate $c(k-1)$ is defined more accurately here by using the orthogonal projection of vector $c(k-1)$ on the hyperplane, the equation of which was obtained as a result of the next measurement of object coordinates.

Then, let S = 2, and equation system (6.11) will consist of two equations:

$$\psi(k-1) = \varphi^{T}(k-1)\,h; \qquad (6.23)$$

$$\psi(k) = \varphi^{T}(k)\,h. \qquad (6.24)$$

By virtue of (6.16), (6.17) and (6.22), the two-step iterative algorithm can be written down as:

$$c(k) = c(k-1) + \frac{\varepsilon(k)}{z_2^{T}(k)\,z_2(k)}\,z_2(k), \qquad (6.25)$$

where

$$z_2(k) = \varphi(k) - \frac{\varphi^{T}(k-1)\,\varphi(k)}{\varphi^{T}(k-1)\,\varphi(k-1)}\,\varphi(k-1). \qquad (6.26)$$

In this case, the vector of preceding estimate $c(k-1)$ belongs to the hyperplane described by equation (6.23). A more definite estimate of $c(k-1)$ is obtained here by using orthogonal projection of vector $c(k-1)$ on the hyperplane of $(l-1)$-dimensional space, which is formed by intersection of hyperplanes of l-dimensional space described by equations (6.23) and (6.24).

If the depth of memory of the generalized multistep algorithm is increased there is an increase in needed volume of calculations at each step of the iterative

process and processing the algorithm is more difficult. The largest number of computing operations is required to determine vector $z_S(k)$.

As the depth of algorithm memory is increased, the process of determining vector $z_S(k)$ grows increasingly time-consuming ["cumbersome"]. It can be simplified by making it recurrent. The fact of the matter is that the simplicity of evaluation algorithms is determined primarily by the simplicity of algorithm coding, rather than number of calculating operations. We refer to the fact that, determination of vector $z_S(k)$ should be a recurrent procedure at each iterative step of an iterative multistep algorithm. Such a procedure can be obtained on the basis of the Greville method [23].

Let us assume that, as a result of measuring object coordinates, we shall have a system of equations of the (6.11) type. Let us rewrite it with simplification of designations:

$$\begin{aligned} \psi(1) &= \varphi^T(1)h, \\ \psi(2) &= \varphi^T(2)h, \\ &\cdots\cdots\cdots \\ \psi(S) &= \varphi^T(S)h. \end{aligned} \tag{6.27}$$

Let us consider vector $\phi(1)$ as a matrix Φ_1, $l \times 1$ in size, and find for it pseudo-inverse [reciprocal] matrix Φ_1^+, $1 \times l$ in size:

$$\Phi_1^+ = \frac{\varphi^T(1)}{\varphi^T(1)\varphi(1)}. \tag{6.28}$$

All subsequent correlations are recurrent for j = 2, 3, ..., S. They begin with calculation of ancillary vector

$$d_j = \Phi_{j-1}^+ \varphi(j), \tag{6.29}$$

where d_j is vector of dimensionality j-1 and Φ_{j-1}^+ is a matrix $(j-1) \times l$ in size.

Vector dj is used to find the vector

$$z_j = \varphi(j) - \Phi_{j-1} d_j, \tag{6.30}$$

where Φ_{j-1} is a matrix with dimensionality $l \times (j-1)$, the columns of which are the first to $(j-1)$th vectors $\phi(j)$.

We then check for fulfillment of the condition

$$j = S \tag{6.31}$$

If it is satisfied, the calculations to determine the vector are terminated and the found value of $z_S(k)$ is used to estimate $c(k)$ using formula (6.22). If, however, condition (6.31) is not fulfilled, calculations continue using the following formulas of the Greville method:

$$b_j = (z_j^T z_j)^{-1} z_j^T \tag{6.32}$$

$$\Phi_j = [\Phi_{j-1} \; d_j] b_j^T \tag{6.33}$$

where D_j is a matrix of dimensionality $(j-1)\times l$. This matrix, with b_j^T attached as the jth line of the vector, forms the matrix:

$$\Phi_j = \begin{vmatrix} D_j \\ \cdots \\ b_j \end{vmatrix} \qquad (6.34)$$

of dimensionality $j\times l$.

Matrix Φ_j^+ is used for a new cycle of recurrent calculations, which begins with equation (6.29) with values of S increased by one.

Let us discuss the distinctions of the generalized multistep algorithm with recurrent determination of vectors $z_S(k)$. The recurrent nature of calculation of vectors $z_S(k)$ simplifies the processing of multistep algorithms (6.22). With increase in depth of memory, the nature of calculations does not change; there is only an increase in number of calculations and, if the computer is rapid enough, this does not prevent use of the algorithm.

By changing parameter S, the same computer program can permit processing of algorithms differing in level of memory. For this reason, there is the possibility of simple processing of algorithms with variable memory, which is necessary, in particular, at the start of the iterative process of parametric identification, during the period of storing information about the object in the identifier.

The structure of the generalized estimation algorithm is illustrated in Figure 70. The first S steps of the estimate shaper with constant memory operates in the "run" [start] mode, i.e., in the mode of increasing depth of memory from 1 to S. At the first step of the iterative process, calculations are made with memory depth of 1, at the second step with memory depth of 2, etc., to S. Starting with the Sth step, depth of memory remains constant. This mode of function is implemented by conditional statements 3, 7, 9 and 11. Figure 70 does not show the estimate output statements; these statements follow states 4 and 8 and function after a specified number of steps.

When the algorithms of parametric identification are used under real conditions, the input and output variables of the object [process] are measured with errors, and this diminishes the accuracy of estimation of its parameters. One can improve the accuracy of estimates by means of recurrent determination of vector $z_S(k)$ (6.28)-(6.34), by using only the vectors whose length exceeds a certain value F, rather than all vectors $z_S(k)$. Let us call this process of gathering the most informative vectors $z_S(k)$ informational filtration.

Let us illustrate the order of determination of vectors with informational filtration.

1. The results of S steps of measurement of input and output variables of the object (6.27) are stored in the digital computer's memory.

2. Determination is made of pseudo-inverse matrix Φ_1^+ using formula (6.28).

3. The value of 2 is ascribed to parameter j.

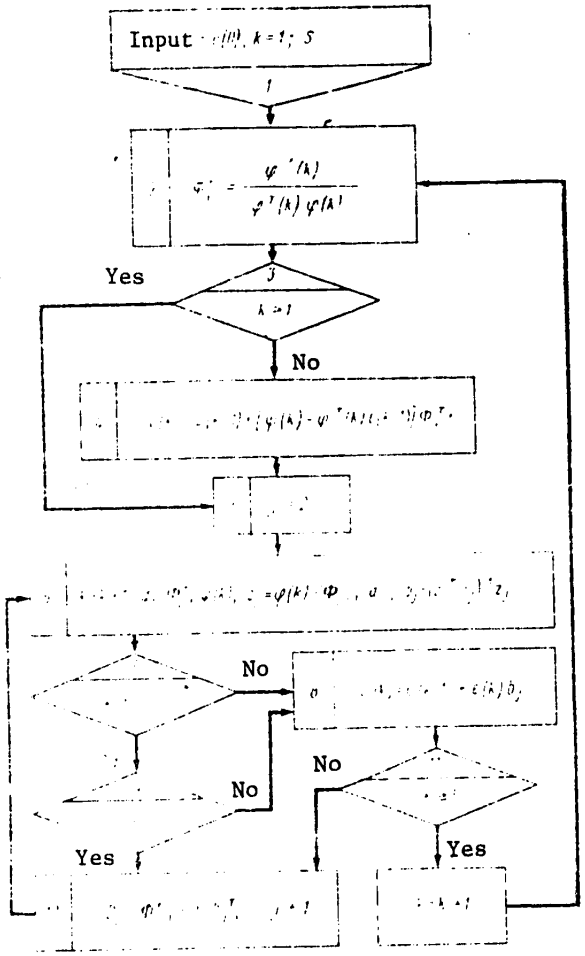

Figure 70. Structure of generalized multistep recurrence estimation algorithm

4. Ancillary vector d_j is calculated using equation (6.29).

5. Vector z_j is determined using equation (6.30)

6. The Euclidean norm of vector z_j is calculated and a check is made of fulfillment of the condition:

$$z_j^T z_j > F^2 \qquad (6.35)$$

7. If condition (6.35) is not fulfilled, vector $\phi(k)$ and scalar $\psi(k)$ are replaced on the basis of the data of the new step in measuring input and output variables of the object.

8. Calculations of items 2-6 [above] are repeated.

The values of ϕ and ψ are changed until a vector ϕ is found, with which condition (6.35) is fulfilled.

9. Calculations are made using equations (6.31) and (6.34).

The values of ϕ and ψ are also changed in subsequent cycles of the recurrent procedure for determining vector $z_S(k)$.

The above-described method for lowering the effect of noise [interference] on accuracy of estimation makes it possible to perform calculations for any input and output variables of the object, even when they are closely timed. It permits gathering only the signals that cause less influence of interference. Control of interference is effected without making the algorithm more complicated or increasing the digital computer memory required for processing it.

The astronavigational research-training unit described in the preceding section enabled us to conduct an experimental study of the method of identification of dynamic characteristics of navigation and control systems that we have discussed. This study was conducted in the form of solving several test problems. We shall discuss some of them.

Problem 1. Analysis of effect of depth of memory of estimation algorithm on its operating speed.

A comparison is made of identification time for algorithms differing in memory depth. Identification time is determined by the iteration number starting with which the normalized mean square errror of estimation does not exceed 1%. Input vectors $\phi(k)$ are formed from a noncorrelated pseudorandom sequence with unit dispersion. The zero vector is taken as the initial estimate of the vector of object parameters.

Table 6.1 lists the results of determination of identification time for a stationary object with parameter vector dimensionality $l = 5$. We used estimation algorithms with memory depth S = 1, 3, 3 and 4. We obtained 12 estimates of identification time k (0.01) for each algorithm with different processing of random input vector $\phi(k)$. The mean identification time k_m (0.01), which was calculated from 12 runs, is listed for each of the four algorithms in the last column of Table 6.1. Table 6.2 lists analogous data on identification time, but for a process with dimensionality $l = 4$ of the vector of parameters.

Table 6.1. Results of determining identification time (s) of stationary process with $l = 5$ dimensionality of parameter vector

S	1	2	3	4	5	6	7	8	9	10	11	12	k_m (0.01)
1	41	35	38	39	33	36	55	52	41	43	29	28	38
2	20	20	34	25	31	27	24	38	39	30	30	26	29
3	17	10	20	14	18	26	23	31	23	15	22	16	20
4	13	5	9	8	7	9	9	10	6	10	12	9	9

Table 6.2. Results of determining identification time (s) of stationary process with $l = 4$ dimensionality of parameter vector

s	1	2	3	4	5	6	7	8	9	10	11	12	$k_{m(0.01)}$
1	22	16	25	35	30	21	29	22	31	22	21	33	26
2	14	12	19	19	16	13	22	14	18	14	23	20	17
3	6	8	11	5	10	8	11	7	13	12	16	10	10

Table 6.3. Results of determining mean identification time (s) for processes with $l = 5$ and $l = 4$ dimensionality of parameter vector

Correlation time	Mean identification time $k_{m(0.01)}$						
	l				$l-1$		
0	[illegible]	[illegible]	[illegible]	9	26	17	10
[illegible]	[illegible]	[illegible]	[illegible]	11	30	14	7
[illegible]	[illegible]	[illegible]	[illegible]	7	71	11	6

The obtained data are indicative of monotonous increase in speed of running estimation algorithms with increase in depth of their memory and decrease in dimensionality of the vector of estimated parameters.

Problem 2. Analysis of the influence of statistical characteristics of input signal on operating speed of estimation algorithms.

The set-up of this problem is the same as the first, but in addition there is change in time of correlation of the pseudo-random sequence, from which input vectors $\phi(k)$ are formed.

Table 6.3 lists the results of determination of mean identification time for processes with $l = 5$ and $l = 4$ dimensionality of parameter vector. These data enable us to derive an important conclusion: correlation time of input sequence has very little influence on operating rate of multistep algorithms. Expressly this property of multistep algorithms determines, to a significant extent, the success of using them under conditions of passive identification.

Problem 3. Identification of dynamic process with optimization of the structure of model thereof.

This problem was formulated to check the efficiency [work capacity] of identification algorithms when the structure of the model of the process

is not rigidly set. It is only known that the model is described by a transfer function of the (6.1) type and its maximum possible order n_{max} is known. In this case, the identification system functions as follows.

For all variants of models in the range of $n \leqslant n_{max}$ and $m \leqslant m_{max}$, determination is made of established values of estimates of parameters. The minimum mathematical expectation of square of discrepancy between process output and model output is a criterion for choice of optimum model structure. In practice, calculation is made of the sum of squares of discrepancy for each possible structure over a certain finite interval of time. The minimum of these values indicates the structure and parameters of the optimum model of the process.

Table 6.4.lists the results of defining the structure and parameters of a process described by transfer function

$$W(p) = \frac{Y(p)}{U(p)} = \frac{6 + 3p}{1 + 2p + p^2}.$$

Identification is made on the assumption that $n_{max} = 2$.

Table 6.4. Results of determining structure and parameters of process

Model $W(p)$	Optimality criterion	Remarks
3,71	$1{,}35 \cdot 10^{2}$	
$\frac{6{,}43}{1+1{,}66p}$	$1{,}10 \cdot 10^{0}$	
$\frac{6{,}06+0{,}9p}{1+1{,}43p}$	$1{,}48 \cdot 10^{-1}$	
$\frac{6{,}04}{1+1{,}56p+0{,}252p^2}$	$8{,}74 \cdot 10^{-2}$	
$\frac{6+3{,}01p}{1+1{,}99p+1{,}04p^2}$	$2{,}95 \cdot 10^{-5}$	Optimum model
$\frac{6{,}01+2{,}51p+0{,}072p^2}{1+1{,}99p+0{,}993p^2}$	$1{,}38 \cdot 10^{-4}$	

Analysis of the data listed in Table 6.4 shows that it is possible to define parameters of the process with adequate accuracy even when the structure of its model is not rigidly specified.

Problem 4. Parametric identification of a two-coordinate ergatic tracking system.

The purpose of the experiment was to determine the effect of operator proficiency ["degree of training"] on the dynamic parameters of a tracking

system of which he is a part. The tracking system had two channels, horizontal and vertical. Determination was made of time constants for each channel (T_h, T_v) during work of three different operators.

The results of parametric identification of the two-coordinate ergatic tracking system are illustrated in Figure 71. This figure shows that the estimates of time constants of the system are localized in region *1* with the best trained operator, and this corresponds to the lowest time constants. Evaluation of the system with the least trained operator corresponds to the highest values for time constants, and they are localized in region *3*. The region of localization of evaluation of the system with the average operator, *2*, corresponds to average time constants. In addition, this figure shows two regions for each operator, the one that is farther away from the start of the coordinates corresponding to the first performance of the tracking problem, while the region situated closer to the start of the coordinates corresponds to performance of the task after 10 training sessions.

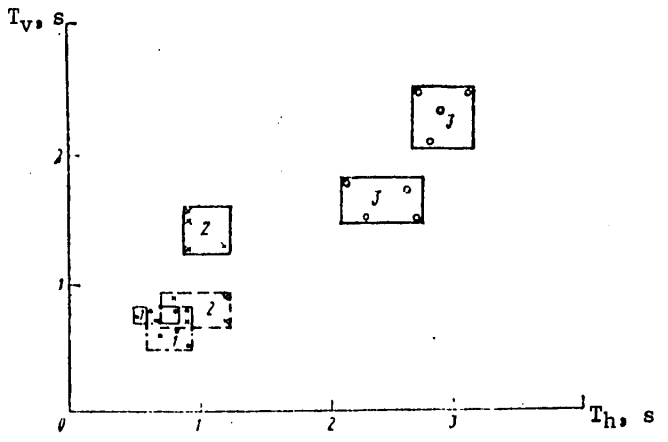

Figure 71. Results of parametric identification of two-coordinate ergatic tracking system

The results we obtained enable us to conclude that it is possible to use parametric identification to obtain estimates of efficiency of ergatic tracking systems.

6.3. Methods of Estimating Time Characteristics of the Process of Taking Astronomic Measurements

Time criteria can be used to evaluate level of operator training for astronomic readings by means of a space sextant. The time required for an operator to take astromeasurements is a random parameter, and to estimate it one can use the law of distribution of probabilities, which yields numerical characteristics--mathematical expectation, dispersion, etc.

The operator--sextant element of the system of autonomic navigation is characterized by extreme complexity of internal and external correlations. For this reason,

statistical data about the time and accuracy of astromeasurements during a real space flight would be the most reliable. However, there are some difficulties involved in obtaining such statistical data. For this reason, the most expedient thing is to obtain the necessary statistical characteristics of astromeasurements with simulation of a space flight.

The algorithm for processing time parameters of operator's astromeasurements could be based on the mathematical model of R. Bush [16], in which time τ of performance of astromeasurements by an operator is described by gamma distribution:

$$f(\tau) = \frac{\rho^R}{(R-1)!}[\rho p_n(\tau-\tau_{min})]^{R-1} e^{-\rho p_n(\tau-\tau_{min})} \qquad (6.36)$$

with $\tau \geqslant \tau_{min}$, where R and ρ are parameters of gamma distribution, τ_{min} is minimum time of astromeasurement by the operator determined by the technical capabilities of the sextant and physiological parameters of the operator and p_n is a parameter that depends on the number of operator training [practice] sessions.

To determine the values of R, ρ, τ_{min} in equation (6.36), let us put $p_n = 1$ and introduce the designation:

$$x = \rho(\tau - \tau_{min}). \qquad (6.37$$

Then equation (6.36) can be written down in the following form:

$$\varphi(x) = \frac{\rho x^{R-1}}{(R-1)!} e^{-x}, \quad x > 0 \qquad (6.38)$$

On the basis of (6.38), let us write the integral distribution of observed values in the form of an incomplete gamma function:

$$P = \int_0^x \varphi(x)\,dx. \qquad (6.39)$$

Integral (6.39) is solved on the basis of tables [62]. Since the value of x here depends on three unknown parameters, as a rule there are three set values for the upper range of the integral (6.39) in the form of percentage points of distribution.

Let us propose, for example, a 10% u_{10}, 25% u_{25} and 75% u_{75} shares of integral distribution. Then, using the tables [62] with the selected R, we find the values of integral distribution (6.39) for u_{10}, u_{25}, u_{75} and solve the equation:

$$\varepsilon = \frac{u_{25} - u_{10}}{u_{75} - u_{10}}. \qquad (6.40)$$

Let us select from the experimental data the time of operator performance of astromeasurements that equals three values of percentage shares of τ_{10}, τ_{25} and τ_{75}, and calculate:

$$\bar{\varepsilon} = \frac{\tau_{25} - \tau_{10}}{\tau_{75} - \tau_{10}}. \qquad (6.41)$$

Searching for the value of ε (obtained from the table for a given R) that is closest to the result of calculating $\bar{\varepsilon}$ from experimental data, we find the sought parameter R of gamma distribution. The values of parameters ρ, τ_{min} and p_n of gamma distribution (6.36) are calculated from the following equations:

$$\begin{gathered} \varrho = \frac{u_{75} - u_{25}}{\tau_{75} - \tau_{25}}; \\ \tau_{min} = \tau_{75} - \frac{u_{75}}{u_{75} - u_{25}} (\tau_{75} - \tau_{25}) = \tau_{75} - \frac{u_{75}}{\varrho}; \\ p_n = \alpha^{n-1} p_1 + (1 - \alpha^{n-1}), \end{gathered} \tag{6.42}$$

where p_1 and α are constants determined from experimental data, n is the number of practice series (cycles).

To obtain parameter p_n, using (6.42) we determine in each training series the median time of performance of astromeasurements by the operator using:

$$u_{50n} = \varrho (\tau_{50n} - \tau_{min}), \tag{6.43}$$

where τ_{50n} is the median time spent by the operator on measurements in the nth training series. Then the estimate of parameter p_n for this training series will be:

$$p_n = u_{50n} / u_{50}, \tag{6.44}$$

where u_{50} is the median time spent by the operator on astromeasurements in the first training series.

We obtain parameter α from the equation:

[illegible] (6.45)

where j is the number of practice sessions in the series.

The value of p_1 is determined using formula (6.44) with consideration of (6.43) for values of time spent by the operator on astromeasurements in the first training cycles.

Knowing parameters R, ρ, p_n and τ_{min} of the law of distribution (6.36), we find mathematical expectation $m(\tau^*)$ and dispersion $\sigma^2(\tau^*)$ of time spent by operator on astromeasurements using the formulas:

[illegible] (6.46)

The time spent by the operator on astromeasurements corresponding to probability of 0.99 can be calculated on the basis of the following equation:

$$\tau_{99} = \tau_{min} + u_{99} \sigma, \tag{6.47}$$

where u_{99} is the value determined from tables corresponding to 0.99 probability and the calculated value of parameter R of gamma distribution.

The effects of different space flight factors on time spent by the operator on measurements using a sextant can be evaluated in the following manner. From the experimental results, we calculate median time $\tau_{50\phi}$ spent on astromeasurements by the operator when exposed to different space flight factors, then we find:

$$u_{50\phi} = \varrho(\tau_{50\phi} - \tau_{min}); \quad p_{n\phi} = \frac{u_{50\phi}}{u_{50}}. \tag{6.48}$$

We assume here that the characteristics of law of distribution $f(\tau)$ change only at the expense of parameter $p_{n\phi}$, i.e., parameters R, ρ and τ_{min} remain the same as when taking astromeasurements without considering space flight factors. This enables us to evaluate operator performance when there is a small volume of statistical data pertaining to the influence of different flight factors.

Thus, knowing the value of $p_{n\phi}$, we can calculate mathematical expectation $m(\tau^*)_\phi$ and dispersion $\sigma^2(\tau^*)_\phi$ of time spent by operator on astromeasurements when affected by different space flight factors on the basis of the following equations:

$$m(\tau^*)_\phi = \frac{R}{\varrho p_{n\phi}} + \tau_{min}; \quad \sigma^2(\tau^*)_\phi = \frac{R}{(\varrho p_{n\phi})^2}; \quad \tau_{99} = \tau_{min} + u_{99}. \tag{6.49}$$

The data obtained from several experimental studies were processed by the above-described method.

First series of experiments. In the course of the experiments the following time parameters were recorded: time spent by operator on astromeasurements in the operator-sextant system, which is the time from the moment the signal is given to start working to the moment bearing is determined (when the operator depresses button K); operator reaction time, which is the time between giving the signal to start working to the moment the operator starts to manipulate controls; time of making decision that sighting is completed, which is the interval between the moment the operator finishes handling the controls to the moment he depresses the button.

In the course of instruction, which occurred in 1 to 206 training cycles, it was demonstrated that the time spent by the operator on measurements in the last training cycles, 151-205, changed negligible and was characterized by the following parameters: v_{10} = 16.8 s; v_{25} = 17.5 s; v_{50} = 22.33 s; v_{75} = 27.5 s.

Using equation (6.41) we calculate:

$$s = \frac{v_{75} - v_{25}}{v_{25} - v_{10}} = \frac{27,5 - 17,5}{17,5 - 16,8} = 14,2.$$

The closest to $\bar{c} = 14.2$ will be a value of ε calculated with R = 2. For this reason, we shall take R = 2. Using formula (6.42) we make the following calculation:

$$\tau_{min} = v_{75} - \frac{u_{25}}{u_{75} - u_{25}}(v_{75} - v_{25}) =$$
$$= 27,5 - \frac{2,68}{2,68 - 0,98}(27,5 - 17,5) = 11,7 \text{ s}$$

Here u_{75} and u_{25} were taken from the tables with R = 2. Using (6.42) we calculate:

$$Q = \frac{u_{75} - u_{25}}{v_{75} - v_{25}} = \frac{2,68 - 0,98}{27,5 - 17,5} = 0,17 \text{ 1/s}$$

Hence, the asymptotic distribution of time spent on astromeasurements with sextant by the operator, without consideration of effects of space flight factors, will appear as:

$$f(\tau) = 0,17[0,17(\tau - 11,7)]e^{-0,17(\tau - 11,7)} \text{ with } \tau \geq 11,7 \text{ s}$$

Mathematical expectation and dispersion of time spent by trained operator on astromeasurements without consideration of space flight factors are:

$$m(\tau^*) = \tau_{min} + R/Q = 11,7 + 2/0,17 = 23,5 \text{ s};$$
$$D(\tau^*) = R/Q^2 = 2/(0,17)^2 = 69,3 \text{ s}^2$$

The time spent on astromeasurements by a trained operator with probability 0.99 is:

$$\tau = \tau_{min} + u_{\alpha}\sqrt{R}/Q = 11,7 + 2,6\sqrt{2}/0,17 = 30,5 \text{ s}$$

The distribution of time spent by the operator on astromeasurements at different stages of training can be written down as follows:

$$f(\tau) = [0,17 + 0,17\bar{p}_n(\tau - 11,7)]e^{-[0,17 + 0,17\bar{p}_n/2](\tau - 11,7)} \text{ with } \tau \geq 11,7 \text{ s}$$

where $\bar{p}_n = 1 - [0,7(n-1)/0,98]^{n-1}$

In order to estimate parameter α in (6.42), we separate training into training series (Table 6.5). In Table 6.5, j is the number of practice sessions per series. We calculate the value of $\bar{p}_n$ using the following equation:

$$\bar{p}_n = \frac{u_{50}(151 - 205) - \tau_{min}}{u_{50i} - \tau_{min}},$$

where u_{50} (151-205) is the median time spent by the operator on astromeasurements in the last training series, u_{50i} is the median time spent by the operator on astromeasurements in the ith training series.

From equation (6.45), substituting the values for n and p_1, we obtain:

$$159.99 = 205 - (1 - 0.234)\frac{1}{1-\alpha}$$

hence, $\alpha = 0.983$.

Table 6.5. Parameters of distribution of time spent on astromeasurements

Training series	u_{50}, s	$\overline{p}_n$	p_n^{xj}	p_n	τ_{99}, s
1 [illegible]	[illegible]	0,231	2,31	0,276	152,7
11 [illegible]	[illegible]	0,3	4,5	0,138	100,8
26 [illegible]	[illegible]	0,576	14,4	0,603	76,9
[illegible]	[illegible]	0,651	27,35	0,762	66,[illegible]
76 [illegible]	[illegible]	1,11	55,5	0,823	59,3
101 [illegible]	[illegible]	0,758	37,9	0,913	54,5
151 [illegible]	[illegible]	1	55	0,968	52,1

On the basis of the foregoing, we can calculate mathematical expectation and dispersion at different stages of training using formulas (6.46) and (6.47).

Table 6.6 lists the parameters of distribution of reaction time and operator's decision making time as to completion of astromeasurements with a sextant, without the influence of space flight factors.

Table 6.6. Parameters of distribution of reaction time and time of making decision that astromeasurements are terminated

Criterion	s	s	s	s		s	s	s	s	s	
Reaction time	[illegible]	0,566	1,057	1,735	10,6	2	0,06	1,47	1,42	0,925	1,55	[illegible],291	0,974
Decision-making time	[illegible]	[illegible],99	0,988	1,14	3,6	3	0,11	2,98	1,12	0,337	2,93	1,32	0,987

Table 6.7. Parameters of distribution of time of astromeasurements by operator under the influence of simulated space flight factors

Factor	$\mu_{n\Phi}$	$m(\tau_\Phi^*)$, s'	$\sigma(\tau_\Phi^*)$, s'	$\frac{\sigma^2}{m}$	$\frac{m(\tau_\Phi^*)\, m(\tau^*)}{m(\tau^*)} \cdot 100\%$	$\frac{\sigma^2(\tau_\Phi^*)}{\sigma^2(\tau^*)}$	$u_{50\Phi}$
Turning chair	0,984	93,69	71,5	56,5	0,8	1,03	22,50
Weightlessness	0,62	30,5	180,9	74,8	30,5	5,06	28,56
Irregular situation + weightlessness	0,553	33,44	226	92,3	42,3	3,28	30,91
Irregular situation	0,58	32,29	212,1	78,8	37	3,27	29,91

In these experiments, we examined the effects of different space flight factors on time spent by the operator on astromeasurements, as well as the effects of these factors on reaction time and decision-making time as to end of guidance process (Table 6.7). Analysis of Table 6.7 indicates that mathematical expectation $m(\tau^*)$ under the influence of space factors was 30-40% higher than the background value, whereas dispersion of astromeasurement time increased by more than 3 times. Table 6.8 lists the results of experimental studies of decision-making time referable to the the end of the astromeasurement process. Analysis of the figures in this table indicates that the time required to make this decision increases by 100-140% under the influence of the different space flight factors. Table 6.9 lists the results of experiments dealing with reaction time. Analysis of these data indicates that reaction time increased by 100-125% under the influence of the different space flight factors.

Table 6.8. Parameters of distribution of operator's decision-making time as to end of astromeasurement process

Factor	s						
Chair turning	[illegible]	[illegible]	1,00	[illegible]	2,73	Virtually no change	
Weightlessness	[illegible]	[illegible]	2,72	2,52	7,5	[illegible]	[illegible]
Irregular situation + weightlessn.	[illegible]	[illegible]	[illegible]	[illegible]	[illegible]	[illegible]	[illegible]
Irregular situation	[illegible]	[illegible]	2,00	[illegible]	5,33	78	[illegible]

Table 6.9. Parameters of distribution of operator's reaction time under the influence of simulated space flight factors

Factor	s		s^2	s^2	s		
Chair turning	[illegible]	[illegible]	1,15	[illegible]	4,70	No change	
Weightlessness	[illegible]	[illegible]	[illegible]	4,23	9,7	[illegible]	[illegible]
Weightlessn. + irregular situation	[illegible]	[illegible]	3,-	4,64	10,6	125	5,1
Irregular situation	[illegible]	[illegible]	[illegible]	1,12	5,64	15	[illegible]

Second series of experiments. Operators with professional skill participated in this series of experiments.

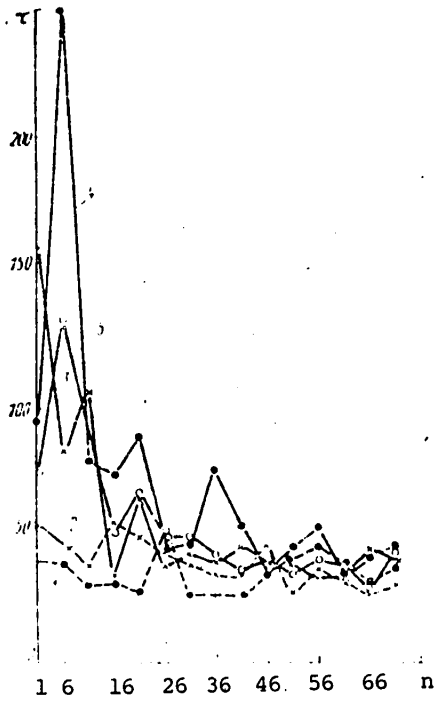

Figure 72.
Changes in astromeasurement time as a function of number of training sessions (τ is astromeasurement time)
1, 2) operators who participated previously in experiments
3, 4) operators who did not participate in experiments before
5) operator with professional skill

Unlike the first series of experiments, in this case astromeasurements were taken on the basis of other than point landmarks on the ground, and they were identified from navigation stars. The estimated time of performance of astromeasurements by the operators during training is listed in Table 6.10. Analysis of these results indicates that the changes in time parameters of astromeasurements by a professional operator in the course of instruction are close to the change in $m(\tau^*)$ for the entire group of trainees. However, there was considerably less scatter of values for time spent by professional operator on astromeasurements.

Third series of experiments. In this series we evaluated the time characteristics of astronavigational operations during simulation of a 3-day flight in space. In preparing for the 3-day experiment, operators were trained and each of them had 80 practice sessions.

Analysis of the training results shows that operators who had participated in experiments before (1 and 2 in Figure 72) showed an insignificant loss of skill after a 6-month break.

For the sake of comparison, the same figure illustrates changes in astromeasurement time as related to training unskilled operators (curves 3 and 4) and an operator with professional skill (curve 5), which show that the operator with professional skill "moves up" to the trained level with more stability (less scatter of results as to time spent on astromeasurements).

Table 6.10. Parameters of distribution of time spent by operator on astromeasurements during training

u_1 s	u_{min} s	v_{max} s	v_{min} s	R	σ_0 s	τ_{min} s	$m(\tau_0)$ s	$\sigma^2(\tau_0)$ s^2	τ_0 s	p_1	η
17,3	19,7	27,4	27,5	2	0,50	34,6	24,3	53,3	15,8	0,70	0,93

The time parameters of astromeasurements during the 3-day experiment were determined using the previously described method.

Figure 73 illustrates the curves for changes in estimating mathematical expectation of time spent by operator on astromeasurements for each operator during the 3-day experiment (astromeasurements were taken during 8-h shifts) and Figure 74 shows the analogous functions for reaction time.

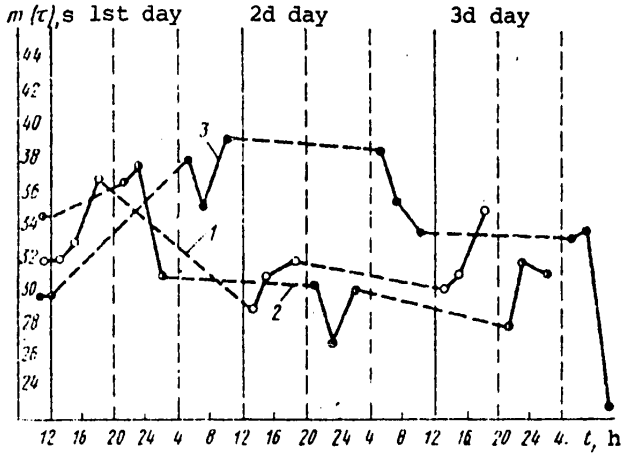

Figure 73. Changes in time spent on measurements during 3-day experiment (t time of day; $m(\tau^*)$ estimate of mathematical expectation of astromeasurement time); 1, 2, 3--operators

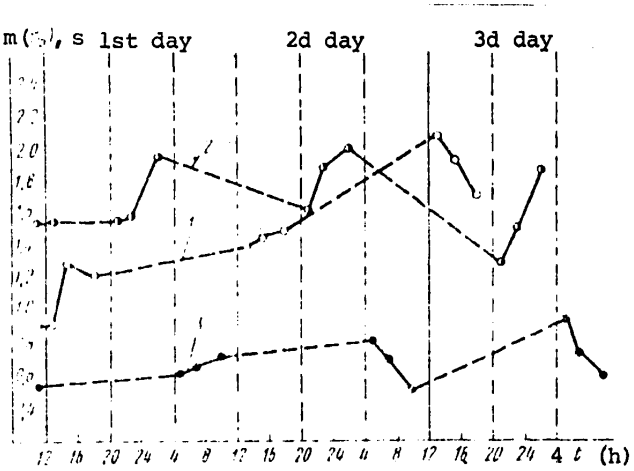

Figure 74. Changes in reaction time during 3-day experiment; 1, 2, 3--operators

Figure 75 illustrates the curves of change in estimation of mathematical expectation of astromeasurement time $m(\tau^*)$ (curve 1) and reaction time $m(\tau_r)$ (curve 2) in different training cycles n.

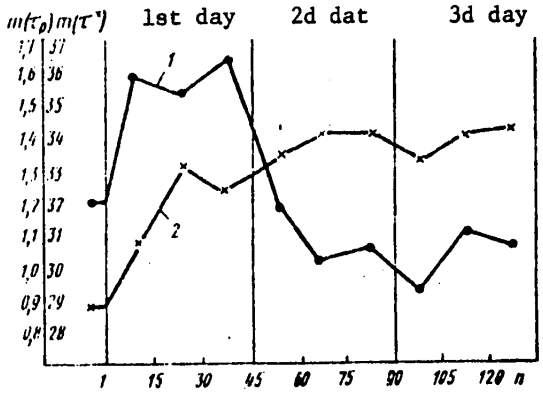

Figure 75. Functions of changes in estimates of mathematical expectation of astromeasurement time and reaction time during 3-day experiment

Analysis of the findings as to astromeasurement time shows that there was an increase on the first day to 20%, as compared to the background. On the second and third days, astromeasurement time diminished to the background level. Reaction time increased by 30% on the first day and then gradually increased.

6.4. Evaluation of Effects of Different Space Flight Factors on Accuracy of Astronomic Measurements

The accuracy of navigational readings made by an operator using a sextant is one of the main parameters determining the efficiency of the astronavigation system. For this reason, one must make a quantitative evaluation of this parameter of the astronavigation process.

It is known that when taking astroreadings with a sextant it is virtually impossible to obtain the true value of the measured angle. As a rule, various errors are contained in the readings, including instrument and operator errors. There can be systematic errors and random ones that are caused by numerous factors that cannot be taken into consideration.

The main cause of a systematic error is refraction of the atmosphere, astrodome and windows. In addition, noncoincidence with the initial position of the dial to the initial position of the mirror or prism (error in dial zero) could be the cause of systematic error.

Systematic errors can be detected and excluded from the measurement results. For example, when measuring from earth the angles between two stars (γ) or between a star and earth's horizon (h), the true values of these angles can be obtained by calculation, using the equations

$$\cos \gamma_0 = \sin \delta_1 \sin \delta_2 + \cos \delta_1 \cos \delta_2 \cos(\alpha_1 - \alpha_2)$$

where γ_0 is the true angle between stars, δ_1, δ_2 is inclination of stars, α_1, α_2 is right ascension of stars, and

$$\sin h_0 = \sin \phi \sin \delta + \cos \phi \cos \delta \cos (S_{Gr} - \alpha + \lambda)$$

where h_0 is the true angle between the star and earth's horizon, ϕ is the latitude of the point at which the reading was taken, δ is inclination of the stars, S_{Gr} is Greenwich sidereal time at the moment of reading, α is right ascension of the star and λ is longitude of the point at which the reading was taken.

At the same time, these angles could be measured several times by many operators, and then we would have N measured values of angle $\gamma_i(h_i)$, where i is the measurement number.

Knowing γ_i and γ_0 we can determine the absolute error of the ith reading:

$$\Delta\gamma_i = \gamma_0 - \gamma_i$$

When there is a large number of readings N, the following equation should apply:

$$\sum_{i=1}^{N} \Delta\gamma_i = 0.$$

This statement is based on the following thesis of error theory: when there is a large number of measurements, random errors of the same magnitude but different sign are encountered at the same frequency.

Random errors due to numerous factors that cause them to appear are distributed according to the normal law (this is also confirmed in many experiments). Consequently, dispersion D or standard deviation σ is the exhaustive estimate of accuracy of astromeasurements after exclusion of systematic error.

The standard deviation for N readings can be calculated using the following equation:

$$\sigma_\gamma = \sqrt{\frac{\sum_{i=1}^{N} (\gamma_0 - \gamma_i)^2}{N}}.$$

With a low N, one uses the following equation to obtain an unshifted estimate:

$$\sigma_\gamma = \sqrt{\frac{\sum_{i=1}^{N} (\gamma_0 - \gamma_i)^2}{N-1}}.$$

By using this quantitative estimate, one can demonstrate the influence of the following factors on accuracy of astromeasurements: professional training of the operator; weightlessness and confinement in a closed space; various factors (stress, emergency situation, etc.); type of astronomic measurement taken, etc.

In the results submitted below of testing the effect of the above factors on accuracy of the operator-sextant system, we used the relative standard deviation (RSD) as a criterion. This criterion was introduced to demonstrate the effect of a factor under study, not only with regard to a specific instrument or visualization model used, but to obtain generalized results.

Table 6.11 lists the results of studying the effect of professional training of an operator on accuracy of measurements in the operator-sextant system. This table shows that operators with stable professional skill (cosmonauts) take astronomic readings with 2-3 times more accuracy than operators who are not specialists, who had performed 100 to 140 such operations before the study.

Table 6.11. Relative standard deviation of errors in astromeasurements for different types of readings

Operator	Star-star	Star-landmark	Star-horizon	Landmark-landmark
Unskilled operators	2.52	3.0	3.45	5.07
Cosmonaut-operators	1.0	1.35	1.45	1.7

Table 6.12. Relative standard deviation of errors in astromeasurements for different types of readings under the influence of simulated space flight factors

Factor	Star-star	Star-landmark	Star-horizon	Landmark-landmark
None	1.0	1.19	1.67	2.53
Coriolis acceleration	1.37	1.46	2.04	2.81
Weightlessness	1.35	1.49	2.0	2.95
Weightlessness + irregular situation	1.76	1.89	2.27	3.35
Irregular situation	1.12	2.16	1.69	3.46

The results of testing the effects of various factors, using the method described in section 5.5, are listed in Table 6.12. As can be seen, an irregular situation simulated by the method of posthypnotic suggestion had the least effect on accuracy of readings. The scatter of results is apparently attributed to differences in mental stability of operators who participated in the experiments. It must be noted that there were cases when an operator was unable to take readings at all in a simulated irregular situation.

The type of astronomic measurement is one of the main factors determining the accuracy of readings (Tables 6.11 and 6.12).

The program of a 3-day space flight was simulated, with concurrent recording of physiological parameters and performance (including accuracy) to test the effect of time spent in a closed and confined area (mockup of manned spacecraft cabin) and hypnotically suggested partial weightlessness on efficiency of the astronavigation system. Table 6.13 lists the relative RSD of reading errors that were demonstrated in this experiment. Analysis of the data in this table shows that the accuracy of astromeasurements on the first day of simulated flight diminishes by a mean of 30%, after which there is adjustment to "flight" conditions.

Table 6.13. Relative standard deviations of astromeasurement errors in 3-day experiment

Operator	Background	First day	Second day	Third day
Operator A	1.0	1.42	1.08	1.18
Operator B	1.11	1.31	1.19	1.06
Operator C	0.89	1.07	1.24	1.04
Average operator	1.0	1.30	1.17	1.09

The results of these studies are indicative of the strong influence of specific space flight factors on accuracy of readings. Hence, it is mandatory to consider these factors in designing systems of the operator-sextant type and in screening operators. In view of the fact that these results were obtained under simulated conditions and, therefore, constitute essentially a qualitative description of the effects of the above-mentioned factors, one should call the attention of researchers to obtaining strictly validated quantitative evaluation of the degree of their influence under real conditions.

6.5. Algorithm for Evaluating the Accuracy of Solving Astronavigation Problems by the Recurrence Method

The main purpose of astronavigation is to define the navigational parameters of flight (coordinates of location, vectors of flight speed and direction angles). In a manned spacecraft, this task can be performed by means of an inertial navigation system and a space sextant, which is used to correct the latter (see Chapter 4).

In order to make corrections, one must first form an observation, i.e., obtain the difference between measured values of some navigation parameter and value of the same navigation parameter obtained with the INS [inertial navigation system].

Let us assume that the operator-cosmonaut uses the sextant to measure angle Θ_{meas} between the direction of the terrestrial landmark C (ϕ_{lm}, λ_{lm}) and navigational star S (δ, α) (Figure 76).* The same angle Θ_{calc} can be calculated using the onboard digital computer from the INS data using the equation:

(6.50)

where x, y, z are coordinates of location of the spacecraft in the inertial system of coordinates OXYZ, calculated from INS data, ϕ_{lm}, λ_{lm} are the geographic latitude and longitude of the specified landmark [lm], δ and α are inclination and right ascension of the specified navigation star, R_0 is the mean radius of earth

$$\cos \alpha_{lm} = \cos \phi_{lm} \cos \lambda_{lm}; \cos \beta_{lm} = \cos \phi_{lm} \sin \lambda_{lm};$$
$$\cos \gamma_{lm} = \sin \phi_{lm}; \cos \alpha^* = \cos \delta \cos \lambda;$$
$$\cos \gamma^* = \sin \delta; \cos \beta^* = \cos \delta \sin \lambda.$$

*A variant of this problem is submitted above in a somewhat different form (see Chapter 4).

On the basis of the information obtained from the INS (Θ_{calc}) and sextant (Θ_{meas}) observation z is formed as the difference between calculated and measured size of angles, i.e.,

$$z = \Theta_{calc} - \Theta_{meas} = \Delta\Theta_{calc} - \Delta\Theta_{meas} \qquad (6.51)$$

where $\Delta\Theta_{calc}$ is the error that appears due to error of defining coordinates in INS and $\Delta\Theta_{meas}$ is the error of measuring angle Θ with use of the sextant.

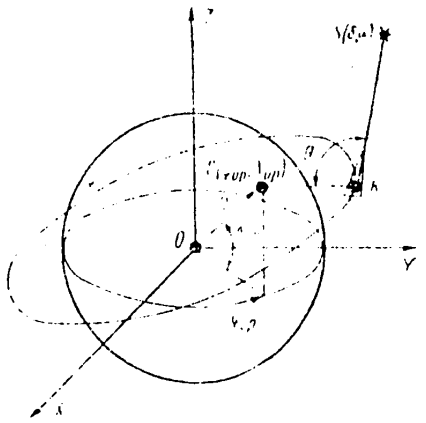

Figure 76.
Calculation of angle between direction of star and terrestrial landmark [op--landmark]

To change finding (6.51) to the general appearance of $z = H_x + v$, one must submit calculation error $\Delta\Theta_{calc}$ in the form of error of determination of coordinates of the location of the spacecraft. For this purpose, let us take the partial derivatives for coordinate elements x, y and z:

$$\Delta\Theta_{calc} = \frac{\partial\Theta}{\partial x}\Delta x + \frac{\partial\Theta}{\partial y}\Delta y + \frac{\partial\Theta}{\partial z}\Delta z \qquad (6.52)$$

where

$$\frac{\partial\theta}{\partial x} = \frac{\cos\alpha^* N + M(x - R_0\cos\alpha_{1m})}{N\sqrt{N}\sin\theta};$$

$$\frac{\partial\theta}{\partial y} = \frac{\cos\beta^* N + M(y - R_0\cos\beta_{1m})}{N\sqrt{N}\sin\theta};$$

$$\frac{\partial\theta}{\partial z} = \frac{\cos\gamma^* N + M(z - R_0\cos\gamma_{1m})}{N\sqrt{N}\sin\theta};$$

$$M = (R_0\cos\alpha_{1m} - x)\cos\alpha^* + (R_0\cos\beta_{1m} - y)\cos\beta^* + (R_0\cos\gamma_{1m} - z)\cos\gamma^*;$$

$$N = (R_0\cos\alpha_{op} - x)^2 + (R_0\cos\beta_{1m} - y)^2 + (R_0\cos\gamma_{1m} - z)^2.$$

In matrix form, equation (6.52) has the following appearance:

$$\Delta\Theta_{calc} = \left[\frac{\partial\theta}{\partial x}\ \frac{\partial\theta}{\partial y}\ \frac{\partial\theta}{\partial z}\right]\begin{vmatrix}\Delta x\\ \Delta y\\ \Delta z\end{vmatrix}. \qquad (6.53)$$

Substituting (6.53) in (6.51) and designating $\Delta\Theta_{meas} = \nu$, we shall obtain, with consideration of errors in determining flight speed:

$$z = \left[\frac{\partial\theta}{\partial x}\ \frac{\partial\theta}{\partial y}\ \frac{\partial\theta}{\partial z}\ 0\ 0\ 0\right]\begin{vmatrix}\Delta x\\ \Delta y\\ \Delta z\\ \Delta V_x\\ \Delta V_y\\ \Delta V_z\end{vmatrix} + \nu, \qquad (6.54)$$

or in the general form of:

$$z = Hx + v,$$

where $H = \left[\frac{\partial\theta}{\partial x}\ \frac{\partial\theta}{\partial y}\ \frac{\partial\theta}{\partial z}\ 0\ 0\ 0\right]$;

$$x = [\Delta x\ \Delta y\ \Delta z\ \Delta V_x\ \Delta V_y\ \Delta V_z]^T.$$

We assume that the statistical characteristics of errrors v of astromeasurements are known and governed by the conditions of:

$$M\{v\} = 0;\ M\{vv^T\} = R\delta(t-\tau)$$

where M{...} is the symbol of mathematical expectation, R is the correlation matrix of error vector v and $\delta(t-\tau)$ is delta function.

The obtained observation z can be used to calculate estimates of errors of determination by means of INS of navigational parameters $\hat{x}$ and covariation matrix of dispersion of these estimates of errors $P(t)$. Since there are measurement errors when using a sextant in the astronavigation system, there will, of course, also be estimation errors:

$$\delta\hat{x} = x - \hat{x}$$

where $\delta\hat{x}$ is absolute error of estimation of the vector of state of errors of determination of navigation flight parameters with the use of the INS.

Absolute error of estimating mistakes and standard deviations of these estimates of mistakes (square root of diagonal elements of matrix P) could be the quantitative indicators of accuracy of the astronavigation system.

On the basis of the foregoing, it can be stated that it is necessary to know the real values of mistakes in determining coordinates x and their estimates $\hat{x}$, as well as standard deviations of estimates $\sigma\hat{x}$, in order to examine the accuracy of solving astronavigation problems with the use of the INS and space sextant. These values can only be obtained by solving the entire navigation problem. Use of mathematical and half-scale models makes it possible to solve navigation problems on the ground. The astronavigation research-training unit (ARTU) described in Section 6.1 is a good basis for this purpose.

The algorithm for estimating accuracy of solving problems of autonomous navigation with the use of a space sextant is contained in the ARTU computer system. The distinctive feature of this navigation method is that the recurrence method is used to process the results of navigational readings with the use of the optimum Kalman linear filter. Chapter 4 has a mathematical description of this method.

In view of the limited storage provided in the ARTU computer system, a simplified mathematical model was developed to solve this problem. In particular, we simulated the flight of a manned spacecraft in a circular orbit in the equatorial plane, and measurements were taken at a constant rate.

Figure 77 illustrates the block diagram of the model produced in the ARTU. The contents of the different units of the mathematical model inputted in the computer system of the ARTU are as follows.

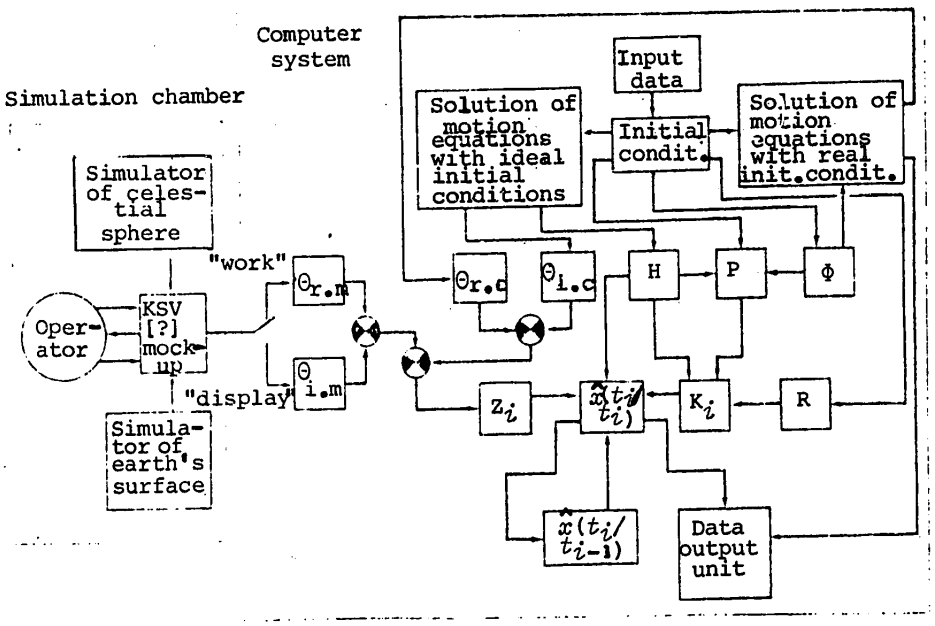

Figure 77. Block diagram of mathematical model for evaluating accuracy of solving astronavigation problems

$\Theta_{i.c}$, $\Theta_{r.c}$, $\Theta_{i.m}$, $\Theta_{r.m}$) ideal and real calculated and measured navigational angles in ith reading

H) linkage matrix

P) covariation error matrix

Φ) transitional error matrix

Z_i) ith observation

$\hat{x}(t_i/t_i)$) vector for estimating errors in determining coordinates and speed of spacecraft flight at time t_i according to readings made at time t_i, inclusively

$\hat{x}(t_i/t_{i-1})$) vector of estimates of mistakes in determining coordinates and flight speed at time t_i according to readings taken at preceding step (at time t_{i-1})

K_i) matrix of weighted coefficients at time t_i

R) covariation matrix of vector of mistakes in navigational readings

1. Input data unit:

R_0 = 6371.21 km--mean radius of earth;
H = 150 km--altitude of spacecraft flight;

$$\Omega = \frac{V_{Kp}}{R_0+H} = \frac{7.8}{6521.21} \frac{1}{s}$$ --angular velocity of manned spacecraft;

$\left.\begin{matrix}\varphi_{1m} = 60^\circ \\ \lambda_{1m} = 0^\circ\end{matrix}\right\}$--geographic latitude and longitude of location of terrestrial landmark;

$\left.\begin{matrix}\alpha = 0^\circ \\ \delta = 90^\circ\end{matrix}\right\}$--coordinates of navigational star;

$\left.\begin{matrix}\sigma_{LO} = \sigma_{RO} = \sigma_{SO} = 10 \text{ km} \\ \sigma_{VLO} = \sigma_{VRO} = \sigma_{VSO} = 10^{-2} \text{ km/s}\end{matrix}\right\}$--standard deviation of error of determining location and flight speed at the point of extraction in orbital system of coordinates;

$\sigma_\nu = 1^\circ$--standard deviation of measurement error

2. Unit of initial conditions:

$$x_{u0} = R_0 + H; \quad x_{p0} = x_{u0} + \Delta x_0; \quad \begin{bmatrix}\Delta x_0 \\ \Delta y_0 \\ \Delta z_0\end{bmatrix} = B \begin{bmatrix}\Delta L_0 \\ \Delta R_0 \\ \Delta S_0\end{bmatrix}; \quad \Delta L_0 = \xi\sigma_{L0};$$
$$y_{u0} = 0; \quad y_{p0} = y_{u0} + \Delta y_0; \quad \Delta R_0 = \xi\sigma_{R0};$$
$$z_{u0} = 0; \quad z_{p0} = z_{u0} + \Delta z_0; \quad \Delta S_0 = \xi\sigma_{S0};$$
$$V_{xu0} = 0; \quad V_{xp0} = V_{xu0} + \Delta V_{x0}; \quad \begin{bmatrix}\Delta V_{x0} \\ \Delta V_{y0} \\ \Delta V_{z0}\end{bmatrix} = B \begin{bmatrix}\Delta V_{L0} \\ \Delta V_{R0} \\ \Delta V_{S0}\end{bmatrix}; \quad \Delta V_{L0} = \xi\sigma_{VL0};$$
$$V_{yu0} = V_{kp} = V_{yp0} = V_{yu0} + \Delta V_{y0}; \quad \Delta V_{R0} = \xi\sigma_{VR0};$$
$$= 7{,}8 \text{ km/s}$$
$$V_{zu0} = 0; \quad V_{zp0} = V_{zu0} + \Delta V_{z0}; \quad \Delta V_{S0} = \xi\sigma_{VS0}$$

where OXYZ is the inertial system of coordinates (X and Y in the equatorial plane, Z over the axis of earth's rotation), O_1LRS is the accompanying trihedron of reference of the orbital system of coordinates (L along orbit, R along local vertical, S forms a right orthogonal trihedron with L and R), ξ are random numbers distributed according to the normal law with $M[\xi] = 0$ and $M[\xi^2] = 1$, B is the matrix of passage from orbital system of coordinates (O_1LRS) to inertial system (OXYZ):

$$B = \begin{bmatrix}\cos\Omega t & \sin\Omega t & 0 \\ -\sin\Omega t & \cos\Omega t & 0 \\ 0 & 0 & 1\end{bmatrix}.$$

Subscripts и and p refer to ideal and real coordinates, respectively.

The value of the covariation matrix of mistakes in setting initial conditions at the initial point in time has the following appearance:

$$P_0 = \begin{bmatrix}\sigma_L^2 & & & & & & 0 \\ & \sigma_R^2 & & & & & \\ & & \sigma_S^2 & & & & \\ & & & \sigma_{VL}^2 & & & \\ & & & & \sigma_{VR}^2 & & \\ 0 & & & & & & \sigma_{VS}^2\end{bmatrix}.$$

3. Unit for solving equations of motion with ideal initial conditions:

$$x_{Hi} = (R_0 + H) \cos \Omega t_i;$$
$$y_{Hi} = (R_0 + H) \sin \Omega t_i;$$
$$z_{Hi} = 0$$

where $t_i = t_{i-1} + h = ih$; h is the measurement (observation) frequency ["pitch"], h = 5 min; i is the number of measurements taken, i = 1, 2, 3, ..., n.

4. Unit for solving equations of motion with real initial conditions:

$$x_{pi} = x_{Hi} + \Delta x_i = (R_0 + H) \cos \Omega t_i + \Delta x_i;$$
$$y_{pi} = y_{Hi} + \Delta y_i = (R_0 + H) \sin \Omega t_i + \Delta y_i;$$
$$z_{pi} = z_{Hi} + \Delta z_i = \Delta z_i,$$

where $\begin{bmatrix} \Delta x \\ \Delta y \\ \Delta z \end{bmatrix}_i = B_i \begin{bmatrix} \Delta L \\ \Delta R \\ \Delta S \end{bmatrix}_i$ are elements of errors in determining coordinates in the OXYZ inertial system of coordinates;

$\begin{bmatrix} \Delta L \\ \Delta R \\ \Delta S \\ \Delta V_L \\ \Delta V_R \\ \Delta V_S \end{bmatrix}_i = \Phi \begin{bmatrix} \Delta L \\ \Delta R \\ \Delta S \\ \Delta V_L \\ \Delta V_R \\ \Delta V_S \end{bmatrix}_{i-1}$ are elements of errors in coordinates and flight speed in the orbital system of coordinates.

The transition matrix of errrors of determining coordinates and flight speed in the orbital system of coordinates in the case of constant frequency of observations can be written down as follows:

$$\Phi = \begin{bmatrix} 2c-1 & 2s-3\Omega h & 0 & (4s-3\Omega h)\Omega & 2(c-1)\Omega & 0 \\ s & 2-s & 0 & 2(1-c)\Omega & s/\Omega & 0 \\ 0 & 0 & c & 0 & 0 & s/\Omega \\ -\Omega s & \Omega(c-1) & 0 & 2c-1 & s & 0 \\ \Omega(1-s) & \Omega(3\Omega h-s) & 0 & 3\Omega h-2s & 2-c & 0 \\ 0 & 0 & \Omega s & 0 & 0 & c \end{bmatrix},$$

where c = cos Ωh; s = sin Ωh.

5. Unit for calculating angle between direction of terrestrial landmark and navigational star.

As we have shown above, one can calculate angle Θ between the directions of specified terrestrial landmark and navigational star by using equation (6.50).

In order to obtain the value of the ideal calculated angle $\Theta_{i.c}$ in the equation for M and N one must insert the values of coordinates x_H, y_H and z_H, and to calculate real angle $\Theta_{r.c}$ one must introduce x_p, y_p and z_p.

6. Unit for calculating linkage [connection] matrix.

The matrix for linkage of astronomic measurements H can be written in the following form:

$$H_i = \left[\frac{\partial \theta_{i.c}}{\partial x} \quad \frac{\partial \theta_{i.c}}{\partial y} \quad \frac{\partial \theta_{i.c}}{\partial z} \quad 000 \right],$$

where

$$\frac{\partial \theta_{i.c}}{\partial x} = \frac{\cos \alpha^* N_i - M_i (R_0 \cos \alpha_{lm} - x_{ni})}{N_i \sin \theta_{i.c}};$$

$$\frac{\partial \theta_{i.c}}{\partial y} = \frac{\cos \beta^* N_i - M_i (R_0 \cos \beta_{lm} - y_{ni})}{N_i \sin \theta_{i.c}};$$

$$\frac{\partial \theta_{i.c}}{\partial z} = \frac{\cos \gamma^* N_i - M_i (R_0 \cos \gamma_{lm} - z_{ni})}{N_i \sin \theta_{i.c}}.$$

7. Unit of optimum filter.

Calculation of optimum estimates of errors made in determining coordinates of location and spacecraft flight speed is made in the computer system of the ARTU, on the basis of solving the following matrix equations of the optimum linear filter of Kalman:

$$\hat{X}(t_i/t_i) = \hat{X}(t_i/t_{i-1}) + K(t_i)[z_i - H_i \hat{X}(t_i/t_{i-1})];$$

$$K(t_i) = P(t_i/t_{i-1}) H_i^T [H_i P(t_i/t_{i-1}) H_i^T + R]^{-1};$$

$$P(t_i/t_i) = P(t_i/t_{i-1}) - K(t_i) H_i P(t_i/t_{i-1});$$

$$P(t_i/t_{i-1}) = \Phi P(t_{i-1}/t_{i-1}) \Phi^T;$$

$$\hat{X}(t_i/t_{i-1}) = \Phi \hat{X}(t_{i-1}/t_{i-1}).$$

where $\hat{X}(t_i/t_{i-1}) = \begin{vmatrix} \Delta\varphi \\ \Delta R \\ \Delta S \\ \Delta V_x \\ \Delta V_y \\ \Delta V_z \end{vmatrix}$ is vector of estimates of errors in determining coordinates and spacecraft flying speed in orbital system of coordinates O_1LRS at time t_1 (ith reading) taken with space sextant through time t_{i-1} inclusively;

$P(t_i/t_{i-1})$ is the covariance matrix of errors in estimates of vector of system status at time ti calculated from information as of time t_{i-1} inclusively; $P(t_i/t_i)$ is the same with consideration of observation at time t_i; $K(t_i)$ is the matrix of weighted coefficients at time t_i; R is the covariance matrix of the vector of errors in navigational readings v. For a one-dimensional measurement of "star--terrestrial landmark" the covariance matrix of errors in measurement of R equals dispersion of errors of measurement $[R] = \sigma_v^2$; z_i is the ith observation formed on the basis of information obtained from the INS ($\Theta_{r.c} - \Theta_{i.c}$) and space sextant ($\Theta_{r.m} - \Theta_{i.m}$), and it is the actual difference between calculated and measured angle Θ at time t_i:

$$z_i = \Theta_{r.c} - \Theta_{i.c} + \Theta_{r.m} - \Theta_{i.m} = \Delta\Theta_1 + \Delta\Theta_2$$

where $\Delta\Theta_1$ is error of determining angle Θ due to difference between real and ideal vectors of spacecraft state and $\Delta\Theta_2$ is overall error, including operator error, instrument error, error of converters, etc.

8. Printer unit.

The results of running the program for estimating the accuracy of solving navigation problems by the recurrence method with use of the space sextant, the algorithm of which was described above, the following are printed out:

$\Theta_{r.m}$--real measured angle, to check proper choice by operator of specified navigational stars and landmarks;
$\Delta\Theta_{2i}$--overall error of ith measurement, including operator error as one of its elements;
ΔL_i, ΔR_i, ΔS_i, ΔV_{Li}, ΔV_{Ri}, ΔV_{Si}--errors in determining coordinates and spacecraft flying speed in the O_1LRS system of coordinates;
$\hat{\delta}L_i$, $\hat{\delta}R_i$, $\hat{\delta}S_i$, $\hat{\delta}V_{Li}$, $\hat{\delta}V_{Ri}$, $\hat{\delta}V_{Si}$--absolute errors in estimates of mistakes made in determining coordinates and flying speed in O_1LRS system of coordinates, where:

$$\hat{\delta}L = \Delta L - \hat{\Delta L}; \quad \hat{\delta}V_L = \Delta V_L - \hat{\Delta V}_L;$$
$$\hat{\delta}R = \Delta R - \hat{\Delta R}; \quad \hat{\delta}V_R = \Delta V_R - \hat{\Delta V}_R;$$
$$\hat{\delta}S = \Delta S - \hat{\Delta S}; \quad \hat{\delta}V_S = \Delta V_S - \hat{\Delta V}_S;$$

$\hat{\Delta L}$, $\hat{\Delta R}$, $\hat{\Delta S}$, $\hat{\Delta V}_L$, $\hat{\Delta V}_R$, $\hat{\Delta V}_S$ are estimates of mistakes in determining coordinates and flying speed in the O_1LRS system of coordinates; $\hat{\delta}_L$, $\hat{\delta}_R$, $\hat{\delta}_S$, $\hat{\delta}_{VL}$, $\hat{\delta}_{VR}$, $\hat{\delta}_{VS}$ are standard deviations of estimates of errors in coordinates and flying speed in O_1LRS system of coordinates.

The above algorithm is used for experimental evaluation of accuracy of solution by cosmonaut-operator of navigation problems by the recurrence method with the use of the space sextant.

The results obtained in the experimental studies with regard to estimates of accuracy of determining the coordinates of spacecraft location $\hat{\delta}L$ made by three operators are illustrated in Figures 78, 79 and 80. Figure 78 illustrates the estimates of error δL obtained when subject A worked on the first (*1*, *2*, *3*) and third (*7*, *8*, *9*) days of flight.

Figures 79 and 80 illustrate estimates of error $\hat{\delta}L$ obtained during work by subjects B and C during the 3 days of flight (curves *1-9*). Analysis of these results shows that there is some scatter between estimates of accuracy of determination of coordinates obtained during work by the same operator during different sessions of solving astronavigation problems. Thus, this scatter constituted $\hat{\delta L}_{min}$ = 2 km and $\hat{\delta L}_{max}$ = 8 km for subject A in the 75th min of "flight." Figure 81 illustrates errors averaged for each day in estimates of mistakes in determining coordinates $\hat{\delta}L$ obtained for the work of subject A on the first (*1*) and third (*2*) days.

Figures 82 and 83 illustrate analogous results obtained for the performance of subjects B and C in the 3 days (curves *1*, *2*, *3*). These data indicate that there is no overt correlation between accuracy of evaluation of determination of coordinates and time of day in the 3-day period. For all three subjects, the scatter of mean daily estimates constituted 1.5-6 km.

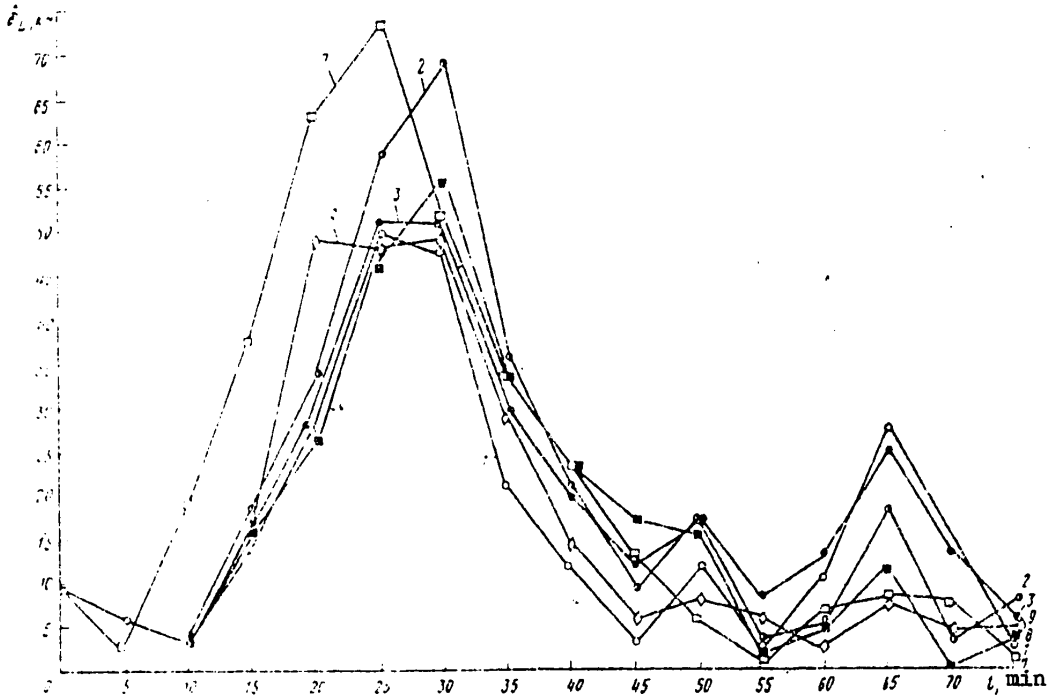

Figure 78. Error in estimate of mistake in determining spacecraft coordinate as a function of navigation system operating time with 5-min intervals between readings, subject A

Figure 84 illustrates the estimates averaged for the entire 3-day experiment for each operator (curve *1* for subject A, curve *2* for subject B and curve *3* for subject C). From these curves we can see that the individual distinctions of trained operators had little effect on accuracy of evaluations of determination of coordinates of the spacecraft's location. The scatter of average values of $\hat{\delta L}$ in the 75th min of flight for the 3 days constituted 3-5 km.

On the whole, these experimental studies dealing with accuracy of determination of coordinates of the spacecraft's position indicate that it is possible for a cosmonaut-operator to solve astronavigation problems using a sextant within the available time after adequate training, the absolute error being $\hat{\delta L}$ - 3 ... 5 km. Other coordinates of the vector of evaluating errors have considerably lower absolute error factors. In order to improve the accuracy of solving astronavigation problems it is necessary to upgrade the instrumental precision of the sextant and increase the number of sessions of making astronavigational readings.

6.6. Standard Evaluation of Operator Performance in Taking Astromeasurements With a Sextant

For standard evaluation of the performance of different operators during training on an ARTU for astronavigational measurements, it is expedient to select a proportion

of excellent, good, satisfactory and unsatisfactory ratings that would yield an encouraging average grade. The initial parameters for standard evaluation could be the time and accuracy of operator's astronavigational measurements.

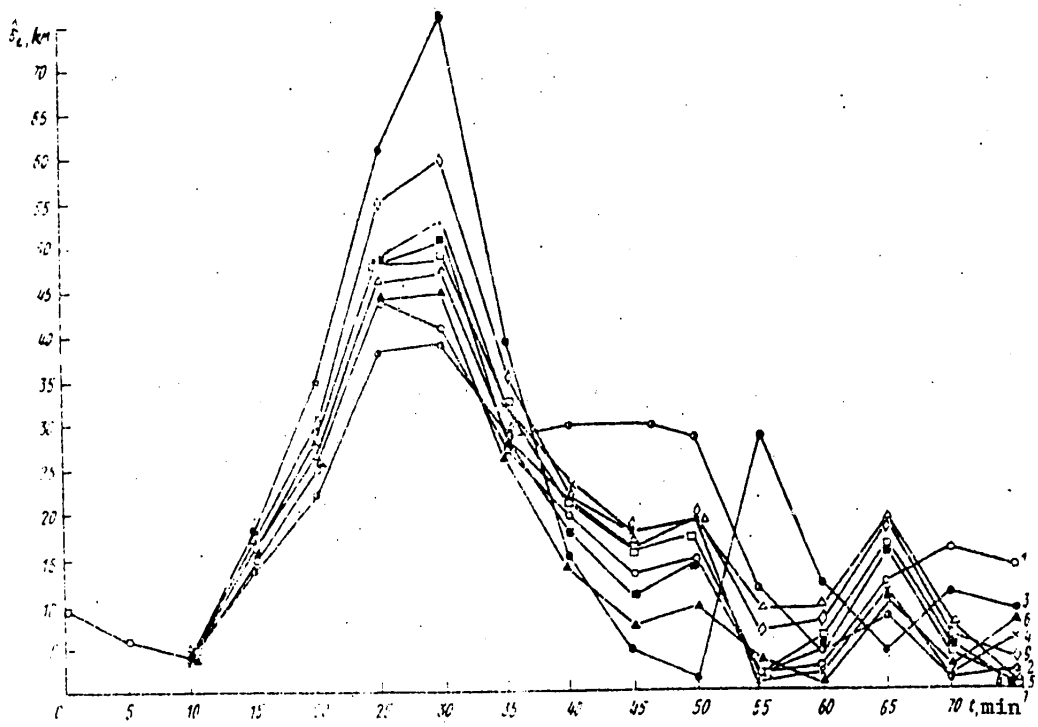

Figure 79. Error in estimate of mistake in determining spacecraft coordinate as a function of navigation system operating time with 5-min intervals between readings, subject B

Let us discuss determination of the time-related standard evaluation of operator training. According to the space flight conditions, available time τ_{av} for operator to take astromeasurements using a sextant and terrestrial landmarks can be calculated on the basis of the following equation

$$\tau_{av} = \frac{H(R_0 + H)}{RV} \tan \gamma \qquad (6.56)$$

where R_0 is mean radius of earth, H is altitude of orbital flight, V is orbital velocity of flight and γ is the angle of sighting terrestrial landmark along flight course.

Table 6.14 lists the available sighting time for the terrestrial landmark, in seconds, at different flight altitudes and sighting angles.

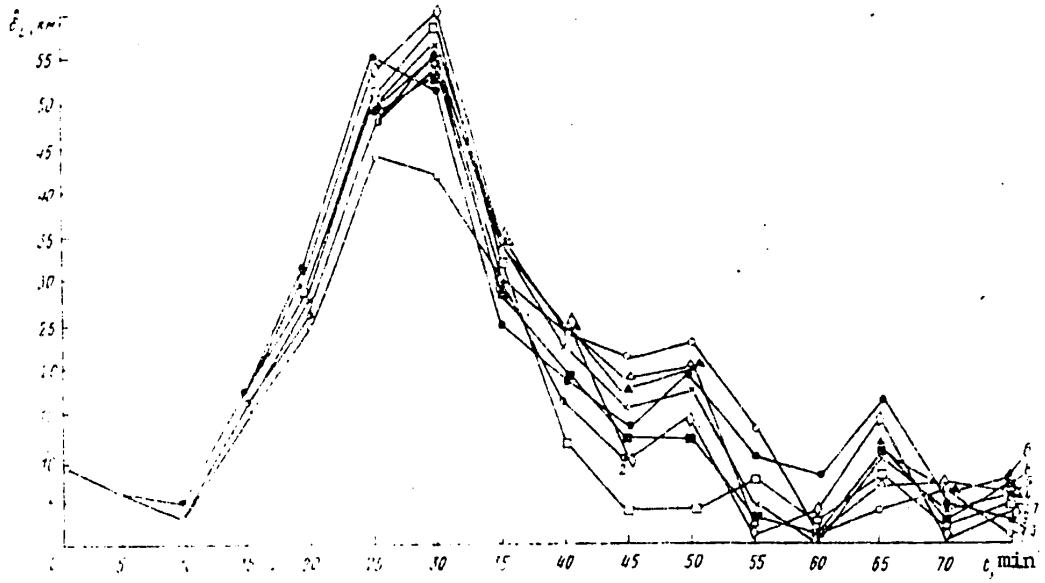

Figure 80. Error in estimate of mistake in determining spacecraft coordinate as a function of navigation system operating time with 5-min interval between readings, subject C

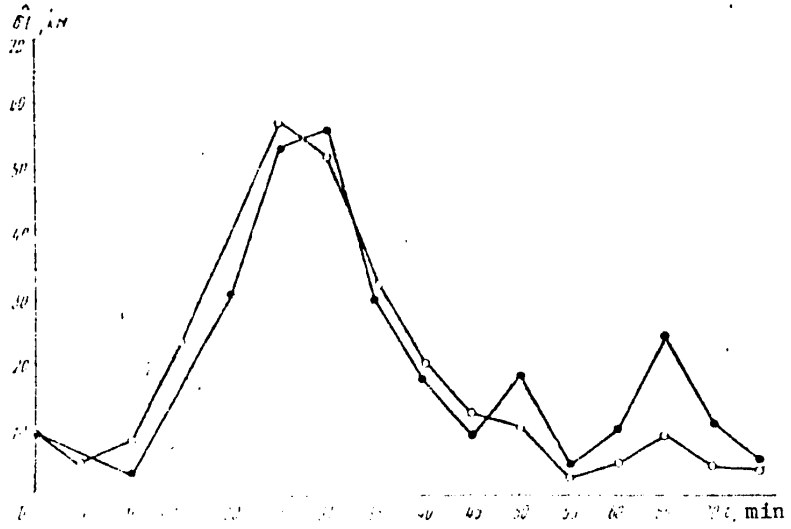

Figure 81. Daily averages of errors in estimating mistake in determining spacecraft coordinate as a function of navigation system operating time, subject A

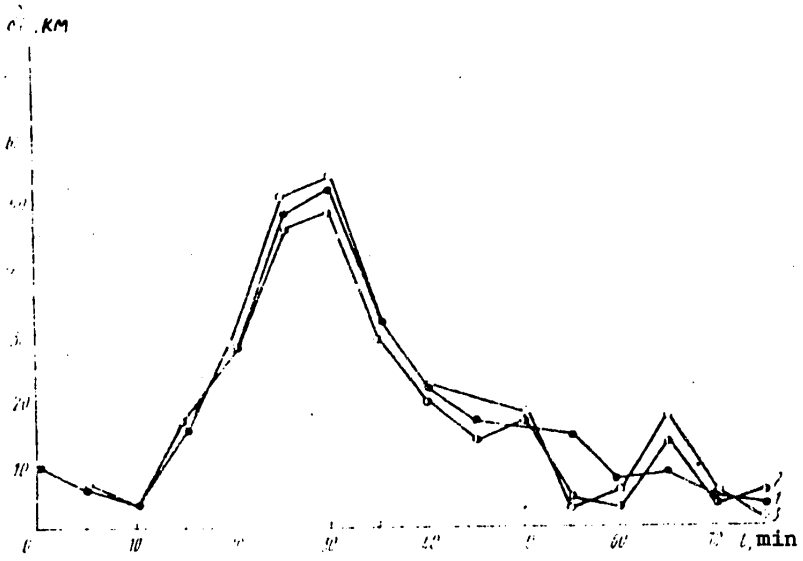

Figure 82. Daily averages of errors in estimating mistake in determining spacecraft coordinate as a function of navigation system operating time, subject B

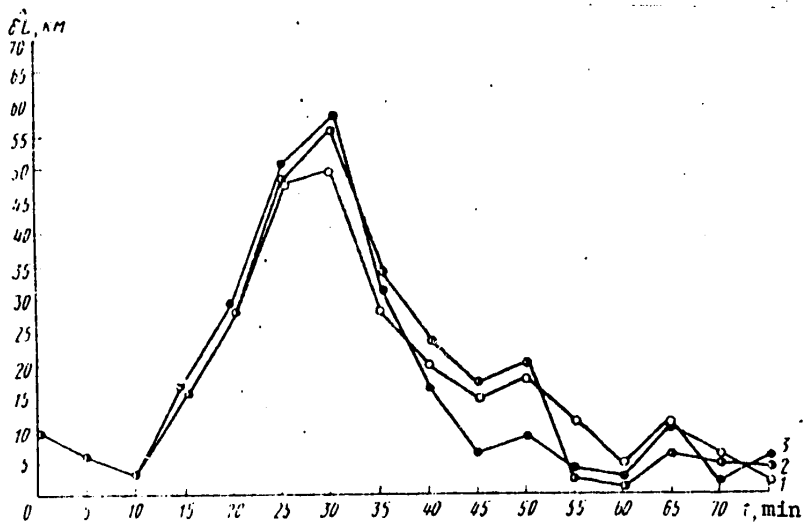

Figure 83. Daily averages of errors in estimating mistake in determining spacecraft coordinate as a function of navigation system operating time, subject C

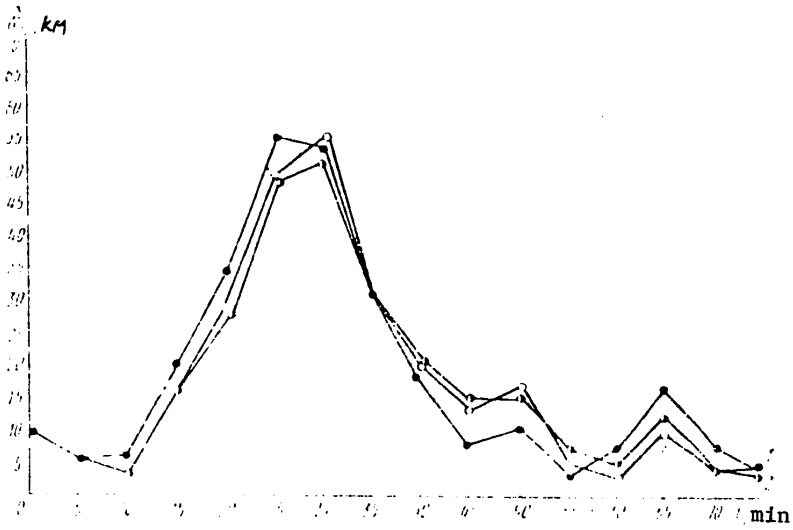

Figure 84. Errors in estimating mistakes of determining spacecraft coordinates as a function of navigation system operating time, averaged for 3 days of work

1) subject A 2) subject B 3) subject C

Table 6.14. Estimated time (seconds) of viewing terrestrial landmark at different flying altitudes and sighting angles

Sighting angle, degrees	Flying altitude, km		
	100	200	300
45	13	26.5	40.5
60	22.5	45.5	70

Considering the specifications of the space sextant, the time spent by the operator on astromeasurements in orbital flight should not exceed 45 s. Operator productivity diminishes when space flight factors (weightlessness, vestibular stimulation, negative emotions, etc.) are present.

As shown by the experimental studies of operator performance using a sextant with simulation of space flight factors (see Chapter 2), actual time for taking astronavigational measurements could be increased by 30-40%, as compared to training on the ground. Consequently, the time available to the operator for astromeasurements in orbital flight should be reduced, for example, from 45 to 27 s. This standardized evaluation of time is considered satisfactory.

As we have mentioned above (see 6.36), the experimental studies established that the time spent by the operator on astromeasurements using a sextant can be described by a gamma distribution:

$$f(\tau) = \begin{cases} \dfrac{\rho p_n}{(R-1)!}\,[\rho p_n(\tau - \tau_{min})]^{R-1}\, e^{\rho p_n(\tau-\tau_{min})} & \text{with } \tau > \tau_{min} \\ 0 & \text{with } \tau \leqslant \tau_{min} \end{cases} \tag{6.57}$$

where τ_{min} = 11.7 s, R = 2, ρ = 0.17 1/s and p_n depends on operator proficiency (for a well-trained operator p_n = 1).

On the basis of (6.57), the probability that the operator will perform the astro-measurements in specified time τ_{sp} can be determined from the formula:

$$p(\tau - \tau_{sp}) = \int_{\tau_{min}}^{\tau_{sp}} f(\tau)\, d\tau \tag{6.58}$$

Integral (6.58) is linked with a partial gamma function and tabulated. Setting τ_{sp} = 27 s, let us calculate the value of $u = \rho(\tau_{sp} - \tau_{min}) = 0.17(27 - 11.7) = 2.6$, which corresponds to probability 0.72-0.73.

In order to determine the standard time corresponding to the "excellent" rating, let us establish in the table a value of p_n corresponding to probability of 0.5. Time τ_{50} = 22.7 corresponds to such a value of p_n.

In order to determine the standard time corresponding to a "good" rating, let us establish a quantile corresponding to probability:

$$\frac{0.72 + 0.5}{2} = 0.6$$

Then the standard time will be $\tau_{60} = u_{60}/\rho + \tau_{min} = 1.84/0.17 + 11.7 = 23.5$ s.

Thus, the time spent on astronavigational measurements by a well-trained operator using a sextant can be rated as follows: "excellent"--up to 18 s, "good"--up to 22.5 s, "satisfactory"--up to 27 s, "unsatisfactory"--27 s or more.

In order to determine the expected average grade, let us mention that the total number of "satisfactory," "good" and "excellent" ratings constitutes 72%, "excellent" constituting 50%, i.e., "satisfactory" and "good" make up 22%. On the other hand, the total number of "good" and "excellent" ratings constitutes 60%, then there will be 10% "good" ratings. Consequently, there will be 12% satisfactory and 28% unsatisfactory ones.

Ultimately, the expected score will be: 0.5•5+0.1•4+0.12•3+0.28•2 = 3.82. This is a low expected average score.

To raise the average grade, let us select a quantile corresponding to probability 0.7 to establish the time rated as "excellent." Then the quantile corresponding to probability of good scores is:

$$\frac{0.73 + 0.7}{2} = 0.71$$

Hence, there will be 70% excellent ratings, 1% good, 2% satisfactory and 27% unsatisfactory. The expected mean score will be 0.7+0.01•4+0.02•3+0.27•2 = 4.14. This is a rather high expected mean grade and it will be a stimulus for reducing measurement time.

Thus, the following standard ratings are established:

"excellent"--to $\tau_{ex} = u_{70}/\rho + \tau_{min} = 2.4/0.17 + 11.7 = 25.8$ s;
"good"--to $\tau_{gd} = u_{71}/\rho + \tau_{min} = 2.5/0.17 + 11.7 = 26.4$ s;
"satisfactory"--to $\tau_{sa} = u_{73}/\rho + \tau_{min} = 2.6/0.17 + 11.7 = 27$ s;
"unsatisfactory"--over $\tau_{sa} = 27$ s.

Standard ratings of astromeasurement time during training can also be established for untrained operators. The time spent by an operator on astromeasurements with the established standards can be submitted as follows at different stages of training:

"excellent"--to $\tau_{ex} = u_{70}/\rho p_n + \tau_{min}$;
"good"--to $\tau_{gd} = u_{71}/\rho p_n + \tau_{min}$;
"satisfactory"--to $\tau_{sa} = u_{72}/\rho p_n + \tau_{min}$;
"unsatisfactory"--over τ_{sa}. $P_n = 1 - \alpha^n(1 - P_0)$.

We can determine the values of α and P_0 experimentally. As we have shown previously (see Section 6.3), $P_n = 1 - (0.974)^n \times (1-0.291) = 1 - (0.974)^n \cdot 0.709$; consequently, by setting the number of practice sessions one can calculate P_n and determine the standard time for the different ratings.

As an example, let us state that $n = 10$; then $P_{10} = 1 - (0.974)^{10} \times 0.709$, while standard time will be:

$$\tau_{ex} = \frac{2,4}{0,17 \cdot 0,78} + 11,7 = 29,8 \text{ s};$$

$$\tau_{gd} = \frac{2,5}{0,17 \cdot 0,78} + 11,7 = 30,6 \text{ s};$$

$$\tau_{sa} = \frac{2,6}{0,17 \cdot 0,78} + 11,7 = 31,3 \text{ s};$$

$$\tau_{uns} = 31,3 \text{ s}.$$

Hence, there will be 70% excellent ratings, 1% each for good and satisfactory, 28% for unsatisfactory. The expected mean score will be:

$$0.7 \cdot 5 + 0.01 \cdot 4 + 0.01 \cdot 3 + 0.28 \cdot 2 = 4.13$$

This is a high enough expected average grade and it would serve as a stimulus for reducing astromeasurement time.

Standard rating of accuracy of astromeasurements taken by operators is based on the following considerations. Experimental studies using the analog-digital unit of the autonomic navigation system revealed that the accuracy of superposing navigation stars and terrestrial landmarks in the center of the visual field of the sextant depends little on the number of training sessions. The errors of measurements are governed by the normal law with mathematical expectation $m(\Delta^*) = 0$ and standard deviation $\sigma(\Delta^*) = 3.45'$.

Since mean square error $\sigma(\Delta^*)$ is a gauge of accuracy of astromeasurements, by selecting the correlation between ratings, we can write down the standards for accuracy in the following general form:

standard for "excellent" rating: $\Delta\gamma_{ex} = K_1\sigma(\Delta^*)$;
standard for "good" rating: $\Delta\gamma_{gd} = K_2\sigma(\Delta^*)$;
standard for "satisfactory" rating: $\Delta\gamma_{sa} = K_3\sigma(\Delta^*)$;
standard for "unsatisfactory" rating: $\Delta\gamma_{uns} = K_4\sigma(\Delta^*)$,

where $\Delta\gamma_{ex}$, $\Delta\gamma_{gd}$ and $\Delta\gamma_{sa}$ are maximum mean errors of astromeasurement defined by the corresponding rating; K_1, K_2, K_3 and K_4 are coefficients characterizing the selected proportions of standard ratings; $\sigma(\Delta^*)$ is the mean square error of astronavigation measurements using a sextant.

Errors $\Delta\gamma$ are governed by the normal law, and for this reason we can determine the probability that error ($|\Delta\gamma|$) does not exceed the standards for "excellent," "good," "satisfactory" and "unsatisfactory" on the basis of the following:

$$P_1(|\Delta\gamma| < \Delta\gamma_{ex}) = \hat{\Phi}\left(\frac{K_1\Delta\gamma_{ex}}{0{,}67\sigma(\Delta^*)}\right);$$

$$P_2(|\Delta\gamma| < \Delta\gamma_{gd}) = \hat{\Phi}\left(\frac{K_2\Delta\gamma_{gd}}{0{,}67\sigma(\Delta^*)}\right);$$

$$P_3(|\Delta\gamma| < \Delta\gamma_{sa}) = \hat{\Phi}\left(\frac{K_3\Delta\gamma_{sa}}{0{,}67\sigma(\Delta^*)}\right);$$

$$P_4(|\Delta\gamma| < \Delta\gamma_{uns}) = 1 - P_3,$$

where P_1, P_2 and P_3 are probabilities that absolute measurement errors will not exceed the standards for "excellent," "good" and "satisfactory," respectively, or the probability that the error will fall into the specified interval; P_4 is the probability that the measurement error will exceed standard $\Delta\gamma_{sa}$; $\hat{\Phi}$ is reduced Laplace function.

One can select coefficients K_1, K_2 and K_3 by making calculations and comparisons of different variants of standard ratings. Let us determine for $\sigma(\Delta^*) = 3.45'$ the probability that measurement errors with use of sextant will fall into each of the confidence intervals, on the assumption that $K_1 = 0.8$, $K_2 = 1.2$ and $K_3 = 1.8$.

We can then obtain:

$$P_1(|\Delta\gamma| < \Delta\gamma_{ex}) = \hat{\Phi}\left(\frac{0{,}8\sigma(\Delta^*)}{0{,}67\sigma(\Delta^*)}\right) = \hat{\Phi}(1{,}19) = 0{,}58;$$

$$P_2(|\Delta\gamma| < \Delta\gamma_{gd}) = \hat{\Phi}\left(\frac{1{,}2\sigma(\Delta^*)}{0{,}67\sigma(\Delta^*)}\right) = \hat{\Phi}(1{,}81) = 0{,}78;$$

$$P_3(|\Delta\gamma| < \Delta\gamma_{sa}) = \hat{\Phi}\left(\frac{1{,}8\sigma(\Delta^*)}{0{,}67\sigma(\Delta^*)}\right) = \hat{\Phi}(2{,}69) = 0{,}93;$$

$$P_4(|\Delta\gamma| < \Delta\gamma_{uns}) = 1 - P_3 = 0{,}07.$$

Hence, 58% of the ratings are excellent and 7% unsatisfactory.

In order to determine the percentage of good and satisfactory ratings it must be borne in mind that 77% is referable to the sum of "good" and "excellent" ratings, while 93% is referable to "satisfactory," "good" and "excellent." Hence, there will be (77-58)% = 19% good and (93-58-19)% = 16% satisfactory ratings.

On the basis of the foregoing, the error made by the operator when taking astromeasurements with a sextant can be rated as follows: "excellent"--up to 2.7'; "good"--up to 4.2'; "satisfactory"--up to 7.21' and "unsatisfactory"--over 7.21'.

With this variant of selected standards, the expected average grade of operator ratings will be: 0.58•5+0.19•4+0.16•3+0.07•2 = 4.28. This is a rather good average score and it will be an incentive for the operator to improve measurement performance.

For space sextants with $\sigma(\Delta^*) = 1'$, standard ratings with an average score of 4.28 will be: "excellent"--0.8'; "good"--1.2'; "satisfactory"--1.8'; "unsatisfactory"--over 1.8'.

To rate an operator's performance as a whole for the duration of a navigation session, we need a generalized criterion that takes into consideration both the accuracy of readings and time spent on taking them. The generalized average expected score for accuracy and time of performing astromeasurements with a sextant, which would constitute 4.21 with average score of 4.28 for accuracy and 4.13 for measurement time, could serve as such a criterion of operator proficiency.

A criterion selected in the form of polynomial $K = A\sigma(\Delta) + B\sigma(\tau^*) + C$, which includes error $\sigma(\Delta)$ in the operator-sextant system and time $\sigma(\tau^*)$ spent by operator to take astromeasurements using a sextant, could be one of the possible variants of this criterion. Coefficients A, B and C are selected on the basis of the results of statistical processing of astronavigational measurements by the least squares method.

However, use of this criterion alone to evaluate the professional performance of cosmonaut-operators in a system of autonomous astronavigation cannot presume to be entirely objective. This is attributable to the fact that identical errors in astromeasurements could yield substantially different results with regard to errors in determining the piloting and navigational parameters of flight as a function of time of the navigation session and type of orbit (normal or irregular).

6.7. Evaluation of Operator Training According to Quality of Performance of Astronavigation Tasks

Optimization of modern systems of autnomous astronavigation is very closely related to refinement of operator training, as the chief element in this system. At the same time, a high level of operator training, as is the case for specialists in any other occupation, is directly related to refinement of methods of evaluating their proficiency and constant monitoring of training results.

However, development of criteria and methods for rating cosmonaut performance or, more precisely, training level, is among the most difficult problems, and to solve it one must make combined use of modern advances in various scientific disciplines. Mathematical methods should play a prominent role here.

The known ratings and characteristics, which have been well-developed for technical equipment and closed automatic control systems are not suitable for quantitative evaluation of a cosmonaut's work capacity. The reason is that an operator and, in particular, a cosmonaut is notable for an immeasurable wider variation of all his qualities, traits and characteristics. They can change rapidly and over considerable ranges, depending on external working conditions of the cosmonaut, on

his internal, psychological set, physical condition, activities and many other factors. For this reason, the first and main distinction of quantitative ratings of a cosmonaut's work capacity is their stochastic nature, since the experimental data obtained each time characterize only a certain specific condition of the cosmonaut or system at a given point in time, under given conditions, set, etc., but are not suitable for yielding any generalized evaluations. This problem is the most important and, at the same time, the most difficult as it applies to a research object such as a cosmonaut-operator.

Many authors have tried to describe the performance (training level [proficiency]) of human operators [15, 31]. We shall describe elsewhere (see Section 7.1) one of them, which has been developed and used extensively. At the present time, researchers (methodologists) must content themselves with the dynamics of critical parameters of a given type of special work. To assess operator proficiency, it is methodologically expedient to single out two ratings: immediate [operational] evaluation of quality of operator performance referable to a specific activity and, on the other hand, comparative evaluation of operator training for performing a task with consideration of a series of training [practice] sessions within a specific period of time. The later rating should characterize the degree of stability of operator work in accordance with the required standards.

The methods of quantitative analysis of every such complex systems as the astronavigation systems of a spacecraft are aimed at obtaining special [partial] criteria of efficiency of performing different operations, which is characterized by such parameters as accuracy (errors), time and energy spent to perform a specified task. In more complicated cases, one uses criteria such as probability of solving a given problem within a specific time under specified conditions, degree of completion of the solution, etc.

Some researchers use, if it can be thus put, unilateral generalized ratings of performance to describe ergatic systems. Thus, A. A. Bulat et al. use, as a generalized criterion of level of operator training, an integral evaluation, which is based essentially on technical parameters, such as control time, energy expenditure, accuracy of control, etc. [15].

Another approach to the problem of evaluating the quality of operator training involves the recording of various physiological parameters. Authors assess, on the basis of dynamics thereof, the psychophysiological tension of the operator and, from these parameters, stability of skill [14, 56, 57, 64, 75].

In some cases, one can assess the quality of cosmonaut training in astronavigation operations by comparing current characteristics of special [partial] performance parameters to the maximum values thereof, with which the entire problem can still be solved. Thus, in one of the series of experiments conducted in the pressurized cabin of a spacecraft, the subjects used an algorithm for solving a navigation problem. The first part of the problem consisted of mathematical operations using a Vega keyboard computer and tables. The second part consisted of determining input data for subsequent calculations by means of graphs. Work time and accuracy of solution were recorded at each stage of calculation.

Figure 85 illustrates the values of time spent on running the algorithm by two subjects, as well as mean values before and during the experiment. This figure shows the maximum time, exceeding which could cause failure in solving the problem.

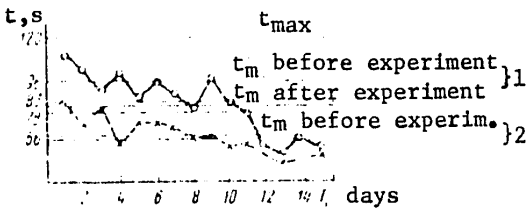

Figure 85.
Time characteristics of subjects 1 and 2 in the problem solving process as a function of number of training sessions n [t_m--mean time]

As can be seen from the submitted data, performance of both the first and second subject did not exceed this range, even during the most difficult, adaptational stage of the experiment. Consequently, with regard to this special criterion it can be noted that the operators were adequately trained to solve navigational problems and were able to perform the task under certain "stressful" experimental conditions.

At one time we noted that development of skill in controlling systems based on the tracking operation depends largely on the operator's professional training for work with other systems [38]. Thus, the characteristics of tracking reaction of A. G. Nikolayev were somewhat higher than those of the copilot of the Soyuz-9 spacecraft. Apparently, this is attributable to the fact that the commander, A. G. Nikolayev, is a pilot; his training, prior professional work were related to control movements of the order of visual and motor coordination, i.e., his controlling (tracking) skill was labile and rapidly "adjusted" to other types of similar work. On the other hand, control of tracking creates a stable conceptual model, which is used actively when switching to other control systems.

We submitted this thesis to experimental verification. A large group of subjects, consisting of students from an engineering school who were unfamiliar with the astronavigation system, achieved the results (time of taking measurements) in the course of training that are illustrated in Figures 86 and 87. Another group of subjects, also with no prior knowledge about this astronavigation system, consisted of USSR pilot-cosmonauts. Their achievement is also illustrated in the figures (solid lines). As can be seen from these data, the latter group is superior to the student group in all parameters. The instruction period for cosmonauts consisted of about 40-50 training sessions (70-80 for the first group). At all stages of training, their parameters for performance time were 50-60% better than for the first group. A comparative analysis of mistakes in astronavigational operations also revealed that the pilot-cosmonauts performed the work with considerably less scatter of obtained data, and accuracy was 2-3 times higher than that of ordinary subjects. It should be noted that there was manifestation of previously established skills in the work of the professional operators. They used small economical movements for control, holding the controls lightly, often with two fingers, rather than grasping with the palm of the hand. Small wrist muscle movements were used for control. In addition, the training process was not associated with psychophysiological tension.

Thus, professional skill in controlling an astronavigational measurement instrument has a beneficial effect on speed and quality of training in the specialty of astronavigator.

This fact is linked the most closely to the extremely important problem of relearning and "transfer" of skill. It is also encountered under the name of the problem of skill interaction in the psychological literature. Many experimental works deal with it. However, the problem of transfer and interaction of skills

has not been sufficiently investigated, although the success of training qualified operators for various control systems depends on its scientific solution.

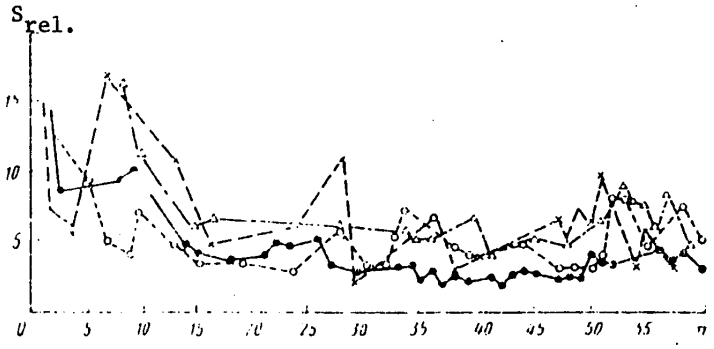

Figure 86. Integral-quadratic criterion for rating operator performance quality as a function of number of training sessions n

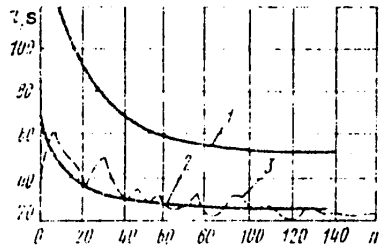

Figure 87.
Astromeasurement time as a function of number of training sessions n

1) operator group τ_{99}
2) operator group $m(\tau^*)$
3) operator with professional skills

We have tried to demonstrate that it is sufficient to analyze the dynamics of operator performance quality in the course of training to assess his proficiency in working with astronavigation systems. This can be done. But using special criteria does not yield the optimum evaluation. It is necessary to work out generalized criteria that would be based on both the reliability features of machine work and functional parameters of a man included in the system as a separate unit.

6.8. Operator's Psychophysiological Characteristics in the Manual Mode of Navigation

Automation of control processes implies optimum distribution of functions between the machine and man. Man is usually charged with the duty of "insuring" the equipment, in the event of partial failure. For this reason, we studied here the operations that a man must perform in the event of failure of the onboard computer. Concrete astronavigation problems made up by a special algorithm served as information models.

Operator work consisted of performing successive arithmetic operations. The next stage of work was with graph-nomograms. The time of beginning and ending each operation was entered in a special log.

Concurrently with running the specified work algorithms, we examined such psychophysiological functions as logical thinking, immediate memory, motor coordination activity, etc.

The obtained results were used as base data to work out forms of presenting logical and arithmetic material, logical algorithm systems that would provide for high efficiency of operators in this type of work.

Psychophysiological Characteristics of Operator Performance in Solving Autonomous Astronavigation Problems Using an Alphanumeric Computer

It is possible to obtain and process information in a system of autonomous astronavigation if there is a high-speed computer with memory units aboard the manned spacecraft. Of course, the ANC [alphanumeric computer] must be small in size and operate reliably. If the ANC has a failure, man takes on its functions. In this case, he has to perform many arithmetic and logic operations, and under certain working conditions this could lower the overall reliability of the system. Moreover, participation of man as an element in the autonomic navigation system could prolong significantly the time required to solve astronavigation problems. Apparently, a search must be made of the optimum combination of human and machine capabilities to assure reliability of the process of control and navigation of space flight. This problem can be resolved if the psychophysiological capabilities of man are taken into consideration when designing manned spacecraft.

Numerous experimental studies and manned space flights have demonstrated convincingly that it is expedient to have semiautomatic control and navigation systems, in which the principle of optimum use of both man and machine is applied.

Thus, American researchers compared the reliability of operation of onboard automated systems with numerous back-ups and systems including an operator. It was established that, at first, the work capacity of all systems was the same, but already on the 4th day of simulated flight the work capacity of the automatic system began to decline. However, by the 14th day, the work capacity of systems with 4-fold back-up was rated as satisfactory, whereas the reliability of the system that included man was found to be much greater than that of automated ones.

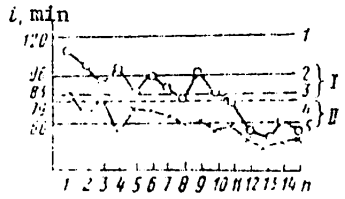

Figure 88.
Running time for algorithm of autonomous astronavigation using an ANC by subjects I and II as a function of training sessions n
1) presentations
2, 4) average before experiment
3, 5) average after experiment

Of course, including man in any chosen spacecraft navigation system is preceded by comprehensive determination of his role in this system, his capabilities with regard to performance of concrete operations. In the case in question of solving autonomous astronavigation problems using an ANC, the operators worked with a set of test tables which listed the results of the preceding stage, i.e., astronomic parameters measured with the sextant. In these experiments, data about primary astromeasurements were given to operators in sealed envelopes, which contained a set of charts for calculating intermediate results, as well as a log with the algorithm for calculations. In these experiments, we used the Vega general purpose computer that is small in size.

The offered algorithm for solving the astronavigation problem consisted of two parts that differed in structure of work. The first consisted of mathematical operations (7-digit numbers). The second part involved mainly determination of base information by means of charts for subsequent calculations. Work starting and finishing time was entered in the appropriate columns of the flight log.

The problem was considered solved when the operator made no mistakes in the course of the calculations that would alter the digits in the 5th or higher positions. Performance of arithmetic operations according to a specific algorithm with specified accuracy, provided all operations were performed in the time reserved for them, was the decisive factor in this methodological procedure. Two operators participated in these tests, and they were trained to work with the Vega ANC 2 h a day for 6 days.

Figure 88 illustrates the time spent on running the algorithm for autonomous navigation by both operators under normal experimental conditions. As can be seen in this figure, both curves present a tendency toward rising throughout virtually the entire experiment. This is probably attributable not only to the influence of the adaptation process but, to some degree, to the level of operator training.

However, it can be noticed that the operators spent the least time on the problem using the specified algorithms on the 12th-13th day, which virtually coincided with the end of the experiment. For this reason, the improvement of performance in this case can also be interpreted as being the result of diminished tension of psychophysiological processes.

The fact that average time spent on solving the algorithm decreased by 15% for both subjects at the end of the experiment confirms that, even in such a complicated activity as arithmetic operations, one observes continuation of the training process, refinement of skill in performing the different elements of the overall experiment. In another instance, when there is a rather long interval between performance of operations for autonomous astronavigation, one may observe some decrease in work skill. The presence of a training unit aboard manned spacecraft would make it possible to maintain a stable skill throughout the period of the space flight.

The distribution of functions between the operator and computer implies, of course, not only separation of parts of the overall algorithm in order to program them for the ANC. Since human characteristics are different when performing various mathematical operations, as well as when working with charts and nomograms, one must determine the question of form in which the algorithm data should be submitted to obtain optimum characteristics for the entire system. The choice of one of the forms of graphic presentation of specific parts of the algorithm is made in order to improve reliability of work and reduce solving time.

Thus, one can obtain the quantitative characteristics of operator performance in such studies, with regard to solving logic and arithmetic problems inherent in autonomous navigation of a manned spacecraft and, consequently, one can determine whether it is possible to perform a large amount of arithmetic work, including work under extreme conditions.

Evaluation of quality of solving the algorithm was made by means of determining the mistakes made by the operator when solving problems with simulation of a flight

program. Table 6.15 lists the number of errors made by operators in parts of the algorithm that are different in type of work.

Table 6.15. Distribution of errors in different types of work

Operators	Errors, %	
	work with tables	work with charts and nomograms
No 1	82	18
No 2	73	27

As can be seen from the data listed in Table 6.15, both operators made most mistakes when working with the tables in the first part of the algorithm. In the course of the experiment, this part of the algorithm offered the least opportunity to improve work skill. However, the part that was predominantly logical and required much concentration was, strange as it seems, characterized by a tendency toward improving.

In this case, the dynamics of operator performance quality throughout the experiment were of great interest. There was negligible increase in mistakes made in the first part of the algorithm for the first few days. Most mistakes were made by the operators on the 11th experimental day, when the research program called for 15% oxygen in the room air.

An opposite tendency was noted in running the logical part of the algorithm. This can apparently be explained as follows. Logic operations are less impervious to interference when performed under normal conditions. In this case, normal conditions refer to the absence of emotional tension, exposure to deleterious environmental factors, etc.

However, when we could have expected the greatest number of mistakes in running the algorithm according to the experimental conditions for the first few days of the adaptation period, we demonstrated, on the contrary, improved work with it, i.e., performance of logic operations under extreme conditions may be sufficiently efficient and resistant to interference.

We stress the fact that the experiment was complicated and tests limited to only two operators and, in spite of the fact that similar results were obtained for both subjects, they cannot be deemed statistically reliable. For this reason, the findings of this experiment should be interpreted as illustrative, but we shall still try to find an explanation for the demonstrated distinctions.

The first, automated part of the algorithm is rather time-consuming, but still it is the preliminary stage of work, which yields primary data for the second part of the algorithm. The second part of the algorithm yields the result, which should be considered the finite [final] one in reaching the goal. Thus, the second stage, being the final one, gains the significance of psychological stimulation, which mobilizes adaptive mechanisms in the body, its psychophysiological reserves, and thereby increases reliability of the operator's work. For this reason, concentration of attention on this phase of work leads to inhibition of other parts of the cerebral cortex, and this could be the precondition for worsening of the other activity, which is simpler in its algorithmic structure.

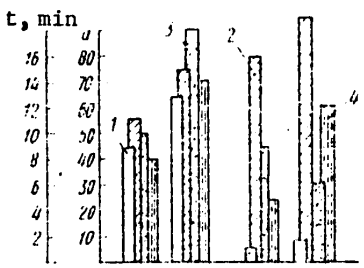

Figure 89.
Characteristics of operator performance in manual solution of algorithm of autonomous astronavigation (a--number of errors)
1) base data 3) 6th day
2) 1st day 4) 11th day

There is another possible approach to interpretation of this phenomenon, based on the hypothesis expounded by B. M. Teplov in 1955 [69]. According to this hypothesis, the assumption was advanced that low work capacity can be interpreted as the result of high reactivity. If we consider the theoretical theses of I. P. Pavlov concerning the types of nervous system, this hypothesis is valid for a weak nervous system. For this reason, it would hardly be correct to interpret the obtained data from this point of view.

The closest step in this direction was the work of V. D. Nebylitsin [80], in which he demonstrated an inverse correlation between the functional state of the nervous system and reliability of function of the visual analyzer. Thus, the question remains open and it must be answered in specially conducted experiments.

In the same experiment, we also tested the possibility of solving the algorithm of autonomous astronavigation without using a computer. The same parts of the algorithm, but in a somewhat abbreviated variant, were used for analysis. Three experiments were conducted with each operator. Analysis of the results revealed that they presented the same direction of changes and, consequently, it was possible to submit them in the form of averaged data for one crew (Figure 89).

In this case, of interest is the relationship between mistakes and working time at the extreme (according to gas composition of respiratory air mixture) stage of the experiment, namely the 11th day. Analysis of the time required to solve this algorithm revealed that it was the shortest, closest to the initial, background data on the 11th day. However, the number of mistakes increased by 27% at this period. This tendency of change in performance characteristics (time and accuracy of work) under extreme conditions is not unexpected, and it is present in a number of other instances. But, for the time being, we are not able to offer a comprehensive psychophysiological analysis of such a trend in changes in work quality, to demonstrate the specific mechanisms causing such differences in the dynamics of the parameters studied referable, it would seem, to homogeneous activity. Evidently, the cause should be sought in the distinctive features of the structure of a given activity and evaluation of its significance to performance.

CHAPTER 7. METHOD FOR OVERALL EVALUATION AND FORECASTING QUALITY OF OPERATOR PERFORMANCE IN SOLVING ASTRONAVIGATION PROBLEMS (ACCORDING TO CHARACTERISTICS OF HIS PSYCHOPHYSIOLOGICAL STATE)

7.1. The Question of Generalized Evaluations in Psychophysiology of Space-Related Work

The problem of improving the quality of performance of an operator in complex control systems is one of the most important and pressing problems of engineering psychology.

In designing modern man-machine systems, it is imperative to take into consideration the fact that the operator will be solving his problems under the influence of many factors. A change in psychophysiological state of the operator is one of the main factors.

We do not yet have a general classification of objective psychophysiological states of an operator, and on the whole this problem can be viewed as formalization of qualitative features of his performance on the basis of recreating their statistical dependence on a certain base system of psychophysiological and technical parameters. This is also an important question in solving astronavigation problems by a cosmonaut.

The question of optimizing the cosmonaut instruction and training process requires immediate work on solving problems of objective generalized evaluation of cosmonaut proficience, which could be used to formulate the principles of construction of feedback with the training system, operator-simulator-instructor system and to create the necessary conditions for effective control of training.

The problem is important, theoretically warranted and necessary in practice, but it must be noted that many authors are skeptical about the possibility of a universal approach to the solution of this range of problems. We shall not dwell on a description of the efforts made by different authors of generalized evaluation of performance, but shall cite one example that characterizes the thinking of researchers in this direction as it applies to cosmonaut work. Let a given form of cosmonaut work be described by parameters α_1, α_2, α_3, ..., α_n. Let the conditions be such that these parameters must have maximum values for optimum work quality. Let us designate the same parameters obtained in ground-based experiments as α_1', α_2', α_3', ..., α_n', and values obtained in space as α_1'', α_2'', α_3'', ..., α_n''. Then the generalized evaluation of operator work quality referable to this form of cosmonaut work A_{gen} can be expressed in the following form:

$$A_{gen} = \frac{1}{n}\left(\frac{\alpha_1''}{\alpha_1'} + \frac{\alpha_2''}{\alpha_2'} + \frac{\alpha_3''}{\alpha_3'} + \ldots + \frac{\alpha_n''}{\alpha_n'}\right),$$

or

$$A_{gen} = \frac{1}{n}\sum_{i=1}^{n}\frac{\alpha_i''}{\alpha_i'}.$$

Parameter A is measured in the range of 0 to 1. Indeed, if the value of parameters of quality of work in space would be the same as under the calm conditions of a laboratory, this type of work would not be subjected to the influence of space stress factors, and the level of cosmonaut work capacity in flight could be evaluated on the basis of the results of ground-based experimental studies. Otherwise, as is usually the case, the values of the parameters studied (α_1", α_2" ...) are found to be lower than on earth (α_1', α_2', ...) and then A_{gen} is less than 1, characterizing the relative decline in quality of cosmonaut work referable to this form of activity in flight, as compared to ground-based conditions. Sometimes, it is more convenient to use percentages instead of fractions of 1, and for this the value of A_{gen} is multiplied by 100. It should be borne in mind that in making a choice of parameters one must take only those that are functionally independent of one another.

It is logical to assume that the significance of all parameters selected for the generalized evaluation in the general case will not be the same. Some may be important to evaluation of a given type of work and others, less important. For example, when a cosmonaut is engaged in docking spacecraft in orbit, it is more important not to use too much fuel and the time spent on this operation is less important; at another time, the reverse may be true, etc. For this reason, it is expedient to introduce into the expression for generalized evaluation the value of the "weight" of each parameter, which would take into consideration the importance of each of them in the overall performance by the cosmonaut. If we consider that the sum of "weights" is:

$$\sum_{i=1}^{n} w_i = 1$$

the expression for the generalized evaluation will have the following appearance:

$$A_{gen} = w_1\frac{\alpha_1''}{\alpha_1'} + w_2\frac{\alpha_2''}{\alpha_2'} + w_3\frac{\alpha_3''}{\alpha_3'} + \ldots + w_n\frac{\alpha n''}{\alpha_n'}$$

or

$$A_{gen} = \sum_{i=1}^{n} w_i\frac{\alpha_i''}{\alpha_i'}.$$

There are some debatable questions about this solution, for example, how to define the mathematical expression of the significance of the "weight" of each parameter; there are elements that are difficult to execute, for example, to obtain a set of values of parameters for space conditions, but expressly this model is the first attempt at solving the formulated problem.

7.2. Evaluation of Psychophysiological State of an Operator and Forecasting the Quality of His Performance

As we have already stated, maximum reliability of spacecraft control can be obtained only if there is a wise combination of operation of automatic systems and actions of the operator.

Studies have shown that total automation of control of a dynamic system is not economically justified. Thus, with complete automation of control, automation of 10-15% of the work of an operator usually costs just as much as 60-70% partial automation [40]. Moreover, it is virtually impossible to take into consideration in advance, in the design of an automatic control unit, all the diversity of situations, in which it is imperative to make the correct decision about a change in the control program. The job of making important decisions in critical situations will always belong to man.

On the other hand, one must consider the fact that the specific conditions of space flight, particularly a long one, affect man's work capacity. For example, cosmonaut B. B. Yegorov spent 1.5-2 times more time on operations with equipment aboard the Voskhod spacecraft than on earth. V. M. Komarov spent twice as much time on movements related to guidance of the craft than in a training spacecraft.

During long-term flights, the cosmonaut's work capacity diminishes significantly under the influence of the regular and prolonged effects of deleterious space flight factors [75].

Thus, engineering psychological design of the cosmonaut's work should be considered the most effective means of improving the reliability of the cosmonaut-spacecraft system.

One of the most important routes for designing cosmonaut work is to develop special systems that evaluate, on the basis of current psychophysiological parameters, the state of the operator, his ability to control the system and, finally, systems that can forecast in good time possible changes in the state of the operator that could lead to inadmissible worsening of the quality of his work pertaining to the control of the dynamic characteristics of the system.

A number of difficulties arise in assessing the state of an operator according to his psychophysiological parameters.

Thus, it is imperative to have not only a qualitative, but quantitative description of man's work capacity states in terms of parameters of his psychophysiological state in order to make such an assessment.

At the present time, efforts to define the work capacity of an operator inevitably lead to qualitative descriptions.

It is obvious that such definitions, which are essentially correct and reflect the essential features of the working state, but are too general, make it difficult to use precise quantitative methods of evaluating states.

Many authors follow the route of determining the psychophysiological characteristics of specific states of man, without offering a general definition of state or

relating the state of an operator to some quantitative indicator of the quality of his performance. Thus, A. N. Luk'yanov and M. V. Frolov [55] are concerned with identification of two states: state of emotional tension and state of attention (defining, for example, the state of attention as selective readiness to react in a specific way to a specific signal).

The distinctive feature of the proposed approach to evaluation and prediction of the quality of operator performance according to psychophysiological characteristics is that, from the very outset, the concept of man's work capacity is defined for each type of activity in terms of a criterion of quality of performance thereof.

The activity of an operator aboard a spacecraft is a special form of human labor, and it is characterized by the following distinctions: need to perform a complex set of diverse forms of work operations, the successful performance of which is possible only if the appropriate complex skills are present and maintained on a high professional level; uniqueness of external conditions, under which the cosmonaut works (weightlessness, hypokinesia, limited space, etc.); severe manifestation of such psychophysiological states of a cosmonaut as fatigue, vestibular disorders, emotional stress, etc.

These space flight factors affect the cosmonaut as an integral unit, and the systems approach must be used to examine their effects on performance efficiency.

In our opinion, construction of an integral rating of quality of performance, which takes into consideration the influence of conditions under which the work is done, as well as parameters of the cosmonaut's psychophysiological state, is the most consistent and promising implementation of the systems approach to analysis of the complex operator work of a cosmonaut.

7.3. Methods of Devising Quantitative Criteria of Effectiveness of Operator Work

The first stage in development of methods of evaluating and predicting the quality of operator performance according to the characteristics of his psychophysiological state is the stage of construction of quantitative criteria of achievement resulting from the operator's performance of the type of work under study.

The performance of an operator related to control of a system, for example, the work of a cosmonaut in the operation of spacecraft docking, etc., is a purposeful precision-type of work. The operations performed by an operator when manipulating the controls must be done in the required order and so precisely as to assure the required accuracy in solving the problem put to the operator, for example, accuracy of finding coordinates in astronavigation, precise docking, etc.

Thus, the precision with which an operator solves a problem put to him is determined by the specifications for the system, and it is always specified in terms that describe the actions performed by the operator. The concrete activity of an operator in solving this type of problem is in the nature of precision movements under visual monitoring of execution thereof.

As a rule, the requirements for precision movements of an operator are integral, i.e., generally speaking, they can be reduced to the requirement that a certain functional of the error in operator work at a fixed period of time be low enough.

The integral of square error, for a given fixed segment of time or the entire time of performing the operation is an example of a widely used elementary functional of this type.

For high-speed analysis of the quality of operator performance in solving pursuit tracking problems, a monitoring [control] method was developed that permits evaluation of the dynamics of the integral evaluation of tracking accuracy on the basis of two numerical characteristics. The task of pursuit tracking is a good experimental model of virtually any type of operator work pertaining to the control of dynamic characteristics of a technical system, since it is a problem of visual and motor coordination. Moreover, each such type of tracking (compensatory or pursuit) is usually an element of an operator's real work.

The pursuit tracking problem consists of the following. There are a target and operator mark on an oscillograph screen. The target moves over the oscillograph screen as specified by the experimenter, and it is usually corrected by an analog computer. The operator mark can move when the operator manipulates the control (handle), and movement is related to movement of the mark in accordance to some specific law. The most elementary type of such relationship is the proportional dependence of deflection of the mark on the screen on deflection of the handle away from the zero position (zero order system).

The operator's task consists of continuously superposing the mark and the target. In our experiments, we used the integral of square of error (deviation of mark from target on the oscillograph screen) for fixed, consecutive and identical periods of time as the quantitative gauge of quality of operator performance of the specified task.

The proposed method of monitoring [checking] the quality of operator performance referable to tracking makes it possible to develop a method of ongoing preventive monitoring of quality of operator performance, which is based on the use of the stochastic [probability] distribution of values of the integral of tracking error square in successive and equal intervals of time.

It is logical to assume that tracking errors, i.e., the difference between the signal and operator's response, are distributed approximately in accordance to the normal law with mathematical expectation of zero and some dispersion. Indeed, tracking errors originate from a large number of factors that hinder tracking, each of which individually has minimal adverse effect on tracking accuracy. Consequently, according to the limit theorem of probability theory, tracking error resulting from the aggregate effect of these factors should be distributed according to the normal law. True, some distortion of normal probability distribution of error magnitude arises because of the constant corrections made in tracking, but we can disregard this distortion here. It should be noted that positive and negative errors of the same magnitude are encountered equally often in tracking problems, which is tantamount to the assumption that the mean error equals zero. Finally, analysis of experimental data usually confirms the validity of this assumption.

Tracking accuracy was evaluated on the basis of counting the values of the integral of the square (or some of squares with a discrete signal) of errors in consecutive and equal time periods. It is known that the sum of squares m of equal normally distributed values with zero mathematical expectation and single [or unit] standard deviation has a χ^2 distribution with m degrees of freedom, the density of which

we shall designate as $k_m(\kappa)$. Let us recall that the mathematical expectation of this distribution equals m and dispersion $2m$.

In the case under discussion, the values of the integral of squared error z in fixed and equal periods of time are obtained by summation (according to the expounded hypothesis) of equally distributed normal summands with zero mean and a certain dispersion σ^2. The sum of such summands will have a distribution density $\frac{1}{\sigma^2} k_m\left(\frac{\kappa}{\sigma^2}\right)$, mathematical expectation $M_z = m\sigma^2$ and dispersion $D_z = 2m\sigma^4$. Indeed,

$$M_z = \int \frac{x}{\sigma^2} k_m\left(\frac{x}{\sigma^2}\right) dx = \sigma^2 \int k_m(z)\, dz = m\sigma^2;$$

$$D_z = \frac{1}{\sigma^2} \int (x - m\sigma^2)^2 k_m\left(\frac{x}{\sigma^2}\right) dx = 2m\sigma^4.$$

Thus, by recording the values of the integral of squared error z and adding the values of M_z and D_z, we can restore the number of degrees of freedom m that equals the number of normally distributed addends and dispersion of these summands σ^2 using the formulas:

$$\sigma^2 = D_z/2M_z;\ m = 2M_z^2/D_z$$

Knowing m and σ^2, we can construct distribution with density $\frac{1}{\sigma^2} k_m\left(\frac{\kappa}{\sigma^2}\right)$ of values of squared error integral z, which enables us to construct the criterion of tracking quality. Let $\chi_P^2(m)$ be the value found in the tables for P--percentile value of χ^2 distribution with m degrees of freedom, i.e., $P\{z > \chi_P^2(m)\} = P$, %. Then values of squared error integral z greater than $\chi_P^{\sigma 2}(m) = \sigma^2\chi_P^2(m)$ will appear only in P% of the cases. Experiments involving operator tracking of a point moving uniformly over a circumference or back-and-forth over a segment of a line at a constant speed made it possible to check the validity of the proposed method.

Figure 90 illustrates a histogram of values of squared error integral for successive 1-s periods of time, which was obtained with the operator tracking a mark moving back and forth at a constant speed. The histogram presents the typical appearance of a χ^2 distribution.

Figure 91 illustrates an example of using this criterion for on-going preventive monitoring of quality of operator performance during continuous and prolonged (about 1 h) tracking of a signal moving over the circumference at a constant speed. The boldface bottom curve indicates in arbitrary units the averaged values of squared error integrals z, each of which is counted for a 1-s period of time. The dash line represents the 95% boundary of values of squared error integrals; values of squared error integrals for 1-s tracking exceeding the 95% boundary can appear only in 5% of the cases, which is unlikely in practice. The numbers of the consecutive 1-min intervals during which data are inputted in the computer are noted on the x-axis. There were 30-s intervals between input periods, and the operator continued to track in these intervals, although data about tracking accuracy were not fed into the computer. The curve illustrating the behavior of 95% boundary of tracking accuracy shows drastic worsening of accuracy when moving from the 8th to the 9th time interval, which corresponds to the 12th-13th min of tracking. We also see that there is abrupt appearance of instability of tracking accuracy. Let us mention that, during this time, the mean integral of squared error (solid bottom

curve) increases insignificantly in the transition from the 8th to the 9th interval. This could have been expected, since the 95% boundary of accuracy takes into consideration not only the mean value, but dispersion of values of the squared error integral.

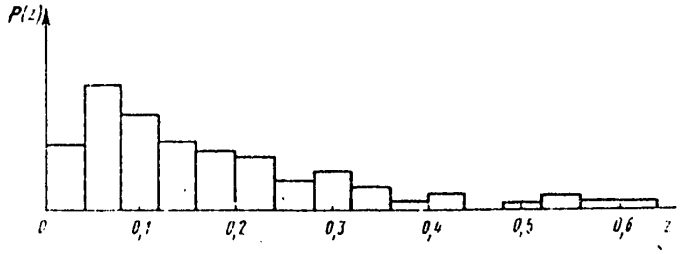

Figure 90. Histogram of distribution of values of integral of squared error of tracking in consecutive, equal periods of time

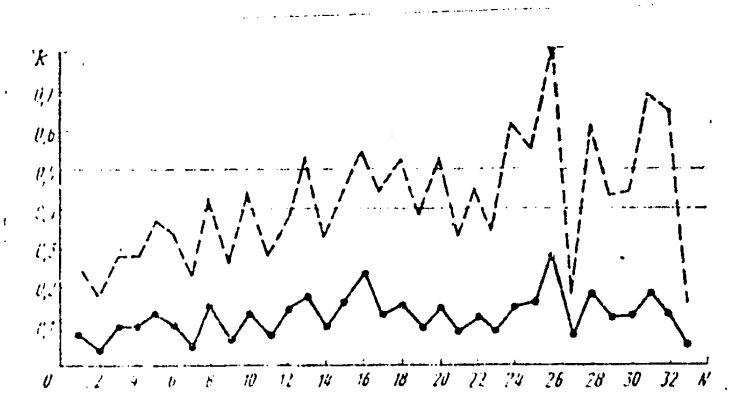

Figure 91. Dynamics of change in quality of tracking during a long-term experiment

The described criterion makes it possible to construct the procedure for ongoing preventive monitoring of quality of operator performance. Let the requirements for operator tracking accuracy, dictated by the precision of the system controlled by the operator, be such that an emergency situation is considered to be one where the operator makes tracking errors z exceeding 0.5 in the arbitrary units we are using. Then, by drawing a preventive boundary corresponding to the maximum permissible level of operator errors z (in Figure 91, this boundary is traced by the dash line for $z = 0.40$), at the end of the 7th time interval we shall obtain a signal that is a warning that operator performance quality is worsening. Figure 91 shows that an irregular situation occurs at the end of the 13th interval (dash-line curve).

7.4. Algorithm for Evaluating and Forecasting the Quality of Operator Performance With Consideration of Characteristics of His Psychophysiological State

Analysis of different types of operator work enabled us to distinguish the main psychophysiological systems that essentially determine the quality of performance of a given type of work. Analysis of conditions, under which the operator will work, must take into consideration the possibility of occurrence of stress situations, the need to work in a state of fatigue or severe emotional excitement, etc.

On the basis of preliminary analysis of psychophysiological content and conditions of operator work, we can define a certain set of psychophysiological features of the functional state of an operator.

Analysis of studies dealing with the choice of characteristics of the state of an operator indicates that they were investigated by different authors for different conditions of many such characteristics.

Thus, such features as alpha rhythm of the background EEG, succession of intervals of the cardiac cycle and inspiration phases were used to assess states of heightened attention [55]. Several EEG parameters, heart rate and several parameters of the verbal signal were also used to asses the operator's states of emotional tension [55]. The method of determination of differential threshold of visual contrast sensibility is commonly used to assess the functional state of the visual channel, and for the acoustic channel determination is made of the differential threshold for volume and frequency of sound.

Tests of attention, immediate [operative] memory, simple motor reaction and reaction of choice, tests of operative thinking, visual and motor coordination (pursuit and compensatory tracking) and others are often used.

In many works, the question of correlation with a given human state is studied for each of the parameters discussed. However, there are virtually no works that tried to make a complex evaluation of performance quality according to an entire set of characteristics of the state of an operator with determination of the characteristics that are the most informative for assessment of the quality of a given form of work. Such attempts were made in [90], which considered the possibility of forming an integral evaluation of work capacity of spacecraft crew members.

Let us mention another work [8], which briefly describes an approach to evaluation and prediction of operator performance quality according to the characteristics of his state.

At the first stage, one must develop a quantitative criterion of operator work quality for each of the tested types of work, in accordance with the relevant requirements or specific technical elements of the control systems.

At the second stage, it is necessary to make an experimental study of the quantitative values of the selected criterion of operator performance quality as a function of the characteristics of his state for each of the studied types of work. And, as we have already stated before, it is desirable to simulate as fully and accurately as possible the operator states that could appear under the influence of different factors involved in a real activity. At this stage, it is desirable

to take into consideration the maximum possible number of parameters, which could be characteristics of the state.

Finally, at the third stage, one must select for each of the tested types of work the set of the most informative parameters characterizing the quality of this type of work out of the number of recorded parameters, and forecast the quality of performance using expressly these parameters, which have the most prognostic value.

At the second stage, one constructs the generalized evaluation of operator performance quality η according to the preselected parameters of his state $\xi_1, \ldots, \xi_k$, using η in the form of polynomial $\eta = P_q(\xi_1, \ldots, \xi_k)$ of a certain fixed rank [power] of the corresponding values of parameters $\xi_1, \ldots, \xi_k$. Expression of quality criterion η in the form of polynomial of state parameters $\xi_1, \ldots, \xi_k$ is justified because any rather smooth function can be approximated with any degree of accuracy with a polynomial of a high enough rank.

Let us note that, in the simplest linear case ($q = 1$), the polynomial has the appearance of $q = \Theta_1\xi_1 + \ldots + \Theta_k\xi_k + \Theta_0$, so that coefficients $\Theta_1, \ldots, \Theta_k$ can be interpreted (after appropriate standardization of parameters) as the "weights" of state parameters during a given type of work. A variant of the generalized least squares method, in which the standard approximation error is minimized, was used to find coefficients $\Theta_1, \ldots, \Theta_k$ of polynomial $\eta = P_q(\xi_1, \ldots, \xi_k)$.

On the additional assumption that the errors present multidimensional normal distribution, the generalized sample evaluations obtained by this method coincide with the sample estimates by the maximum-likelihood method [90].

Use of this method leads, by calculating the values of estimates of parameters $\Theta_1 \ldots, \Theta_k$, to a system of k linear equations with k unknowns. The coefficients of the system's matrix are coefficients of covariance of state parameters $\xi_1, \ldots, \xi_k$ with one another, while the right parts are coefficients between state parameters $\xi_1, \ldots, \xi_k$ and performance quality η.

Let us describe in greater detail the algorithm for evaluating and predicting the quality of operator performance η according to the characteristics of his psychophysiological state.

The program gives a certain value for the criterion of performance quality $\eta = \{\eta_1, \ldots, \eta_l\}$.

It is mandatory to introudce the vector criterion, since the quality of a rather complex activity can be characterized only by a set of parameters that cannot, generally speaking, be reduced to one scalar criterion of quality. Thus, accuracy of appropriate control movements and time spent by the operator on solving control problems are the most frequently encountered features of operator actions in controlling dynamic systems. To describe the quality of such work, it is expedient to use a two-dimensional criterion, $\eta = \{\eta_1, \eta_2\}$, where η_1 is the accuracy characteristic and η_2 is problem solving time. There may be a difference in relationship of criterion elements η_1 and η_2 to operator state, so that it is expedient to evaluate each element of the quality criterion as a function of different values of parameters that characterize the state.

In view of the foregoing, the algorithm includes vector values of the criterion; however, to avoid redundancy we shal describe the algorithm for the scalar instance, which really corresponds to the algorithm of evaluation and prediction of each element of the vector criterion.

Let the state be characterized by a set of parameters $\xi_1, \ldots, \xi_k$. As we have already explained above, we first search for η as a function of $\xi_1, \ldots, \xi_k$ in the form of polynomial $\eta = P_q(\xi_1, \ldots, \xi_k)$ of rank [power] q. The program is designed to calculate (more precisely, estimate) the coefficients of the polynomial the order of magnitude of which does not exceed 10^2. The linear part of the polynomial takes into consideration quality criterion η as a function of each parameter of state $\xi_i (i = 1, \ldots, k)$ separately. The quadratic part considers the combined effect on criterion η of all sorts of paired combinations of parameters such as $\xi_i \xi_j (i, j = 1, \ldots, k)$. In the case of a quadratic polynomial, we shall have:

$$\eta = P_2(\xi_1, \ldots, \xi_k) = \Theta_0 + \Theta_1 \xi_1 + \ldots + \Theta_k \xi_k + \sum \Theta_{ij} \xi_i \xi_j$$

After adding for all derivatives $\xi_i \xi_j (1 \leqslant i < j \leqslant k)$ the designations $\xi_{k+1}, \ldots, \xi_{\frac{k(k+3)}{2}}$ and for coefficients $\Theta_{ij} (1 \leqslant i < j \leqslant k)$ the designations $\Theta_{k+1}, \ldots, \Theta_{\frac{k(k+3)}{2}}$, the problem of calculating the coefficients of the quadratic polynomial $\eta = P_2^2(\xi_1, \ldots, \xi_k)$ apparently amounts to the problem of calculating the coefficients of a first-degree polynomial:

$$\eta = \Theta_0 + \Theta_1 \xi_1 + \ldots + \Theta_k \xi_k + \Theta_{k+1} \xi_{k+1} + \ldots + \Theta_{\frac{k(k+3)}{2}} \xi_{\frac{k(k+3)}{2}}$$

which depends on a greater (than k) number of variables $\frac{k(k+3)}{2}$.

We can continue with the description, without loss of generality for a first-degree polynomial, which is related to a certain number (let us again designate it as k) of variables that equals the number of parameters of state, if the calculations are made for a first-degree polynomial, and an equal number $\frac{k(k+3)}{2}$, where k is the number of state parameters, if the calculations are made for a second-degree [quadratic] polynomial.

Let us recall that, at the first stage of the experiments, for a certain set of points in time $t = t_1, \ldots, t_N$ calculation is made of the quality criterion $\eta(t)$ and parameters characterizing the state $\xi_1(t), \ldots, \xi_k(t)$.

Let us use $y_1^*, \ldots, y_N^*$ to designate the observed values of $\eta(t)$ for $t = t_1, \ldots, t_N$ and $x_{ij}, \ldots, x_{Nj}$ to designate the values of $\xi_i(t)$ (for all $i = 1, \ldots, k$) for $t = t_1, \ldots, t_N$. First we center and standardize in the program all of the base data obtained from the experiment, i.e., we calculate:

$$x_{ij} = \frac{x_{ij}^* - M_{\xi j}}{\sqrt{D_{\xi j}}} \quad (i = 1, \ldots, N;\ j = 1, \ldots, k),$$

where $$M_{\xi j} = \frac{1}{N} \sum_{i=1}^{N} x_{ij}^*; \quad D_{\xi j} = \frac{1}{N-1} \sum_{i=1}^{N} (x_{ij}^* - M_{\xi j})^2,$$

we also calculate $y_i = \frac{y_i^* - M_{y_i}}{\sqrt{D_{y_i}}} (i = 1, \ldots, N)$,

where $M_{y_i} = \frac{1}{N} \sum_{i=1}^{N} y_i^*$; $D_{y_i} = \frac{1}{N-1} \sum_{i=1}^{N} (y_i^* - M_{y_i})^2$.

Then, using the least squares method, we search for estimates $\hat{\theta}_1, \ldots, \hat{\theta}_k$ of coefficients $\theta_1, \ldots, \theta_k$ of polynomial $\eta = P(\xi_1, \ldots, \xi_k)$ for standardized and centered values of $\eta, \xi_1, \ldots, \xi_k$. As we know, estimates $\hat{\theta}_1, \ldots, \theta_k$ are found in a system of K linear equations with K unknowns of the $X'X\hat{\theta} = X'\vec{y}$ type, where X is a rectangular matrix with elements $x_{ij} (i = 1, \ldots, N; j = 1, \ldots, k)$; X' is the transposed matrix; $\hat{\theta} = \{\hat{\theta}_1, \ldots, \hat{\theta}_k\}$ is the vector of estimates of matrix coefficients; $\vec{y} = \{y_1, \ldots, y_N\}$ is the vector of criterion η values calculated at times $t = t_1, \ldots, t_N$.

Thus, the coefficients of the system matrix are covariances of state characteristics, while the first parts of the system are covariances between state characteristics and performance quality criterion.

The accuracy of approximation of η as a function of $\xi_1, \ldots, \xi_k$ is characterized by:

$$S^2 = \frac{1}{N-k} \left[\sum_{i=1}^{N} y_i^2 - \theta_1 \sum_{i=1}^{N} y_i x_{1i} - \ldots - \theta_k \sum_{i=1}^{N} y_i x_{ki} \right].$$

The forecast (or more precisely, the static forecast) of performance quality $\hat{y}$, calculated from state characteristics $\hat{x}_1, \ldots, \hat{x}_k$, is calculated with the formula:

$$\hat{y} = M_y + \sqrt{D_y} \left[\theta_1 \frac{\hat{x}_1 - M_{x1}}{\sqrt{D_{x1}}} + \ldots + \theta_k \frac{\hat{x}_k - M_{xk}}{\sqrt{D_{xk}}} \right]$$

for each vector $\{\hat{x}_1, \ldots, \hat{x}_k\}$. The accuracy of forecasting with a specified level of significance is also calculated using the following equations:

$$\hat{y} - tS\sqrt{D_y}\sqrt{1+a} < \hat{y} < \hat{y} + tS\sqrt{D_y}\sqrt{1+a},$$

where $$a = \sum_{j,l=1}^{k} p_{jl} \hat{x}_j \hat{x}_l.$$

Here p_{ij} are elements of the matrix that is the reciprocal of the matrix in the system of calculating evaluations $\hat{\theta}_1, \ldots, \hat{\theta}_k$ of polynomial coefficients. Numerical parameter t depends on the level of significance of sample size N that is taken.

For N>50, parameter $t = 1.96$ for a significance level of 0.95 and $t = 1.2$ for a significance level of 0.90. The values of parameter t increase in the case of small

samples. Thus with significance level of 0.95 for N = 20, parameter t = 2.10; for N = 15, parameter t = 2.15; for N = 10, parameter t = 2.20 and for N = 5, parameter t = 2.6.

Thus, the described method permits forecasting the quality of operator performance according to the characteristics of his psychophysiological state, which are recorded just prior to work on the assumption that there will not be appreciable change in his state during the period of time required to perform that work.

7.5. Simplified Block Diagram for Forecasting Operator Performance Quality Aboard Spacecraft

Evaluation of accuracy of forecasting the quality of operator performance makes it possible to solve the problem of screening a relatively small number of the most informative parameters without appreciably impairing the accuracy of the forecast. Such selection must be made in order to be able to forecast the quality of cosmonaut performance aboard a spacecraft.

Experiments revealed that the parameters of test performance on special simulators are the most informative. The design of the simulators should provide for utmost approximation of parameters of performance on the simulator to the parameters of real work. In this case, forecasting the quality of real performance according to quality of simulator performance is the most accurate. Moreover, it is found possible to limit oneself in forecasting of this type ("forecasting performance according to performance") to a very small number of parameters characterizing the changes in the state of the operator that are important to proper execution of real work.

Thus, at the first stage, let us assume that the most informative parameters of state from the standpoint of evaluating and forecasting performance quality have been selected. These parameters are recorded aboard the spacecraft, and evaluation of coefficients of polynomial $\eta = P_q(\xi_1, \ldots, \xi_k)$ has already been made in preliminary experiments. Then calculation of performance quality according to state parameters amounts to calculation of the values of polynomial $\eta = P_q(\xi_1, \ldots, \xi_k)$ with already known coefficients, as well as calculation of accuracy of forecast $\Gamma_\pm$ using the formulas given above.

Analysis of the experimental data revealed that the accuracy of forecast $\Gamma_\pm$ depends little on the concrete values of the vector of state $\hat{x}_1, \ldots, \hat{x}_k$, from which the forecast is made. For this reason, one can calculate approximately the accuracy of the forecast using the formulas $\Gamma_\pm = \hat{y} \pm \gamma$, where

$$\gamma = tS\sqrt{D_y}\sqrt{1+\tilde{a}};\quad \tilde{a} = \sum_{j,l=1}^{k} p_{jl}\tilde{x}_j\tilde{x}_l.$$

Here, $\hat{x}_1, \ldots, \hat{x}_k$ are averaged values of the observed parameters of operator state.

In the simplest case of a first-degree polynomial (q = 1), the quality of performance is approximated by the expression $\eta = \Theta_1\xi_1 + \ldots + \Theta_k\xi_k + \Theta_0$.

Consequently, calculation of forecast $\hat{y}$ of performance quality η amounts, in this simplest case, to summation with set weights $\hat{\theta}_1, \ldots, \hat{\theta}_k$ of the obtained values for $\hat{x}_1, \ldots, \hat{x}_k$ of parameters $\xi_1, \ldots, \xi_k$. It must be borne in mind that one can rely on the forecast of performance quality η only to the extent of the accuracy determined by γ, which is calculated in advance, at the first stage.

7.6. Examples of Forecasting Operator's Professional Performance

As we have described above, the problem of developing a generalized criterion for evaluating and forecasting the quality of man's performance according to current psychophysiological parameters implies that there is a good enough relationship between values of the criterion characterizing performance and current values of recorded parameters. In order to find this function and then be able to use it to assess performance quality from the psychophysiological parameters, at the first stage of laboratory studies one must simulate precisely as full a set as possible of the different conditions, under which real work will be performed. In constructing the generalized criterion, it is assumed that the performance quality as a function of psychophysiological parameters is the same for the entire range of change in conditions. The change in performance quality is attributable only to a change in man's state, reflecting a change in values of psychophysiological parameters rather than change in nature of this function.

There was a special experiment in which operators were able to work under drastically different conditions (initial conditions (background) and effects on man of space flight factors). Under such conditions, the operators had to perform complex operator work: visual and motor problems of tracking, radio communication, dynamic tests, etc.

The physiological parameters of the operator's state (pulse, respiration, temperature) were recorded during this work and at rest, with estimation of arrhythmia, change in pulse and exertion in dynamic test.

Operator performance in transmitting radiograms (standard text, 100 symbols) was rated by a special criterion, which took into consideration the speed and reliability of transmission, as well as specifications for proper timing of elements of transmitted symbols. Operator performance in the test for superposition of moving marks was also rated with a special criterion, which took into consideration technical requirements, accuracy of work and work time. Operator work in the mode of radiotelegraphy, as well as work on superposition of moving marks, were considered alternately as the main regular work.

Mathematical analysis of all information obtained, both with the initial data and under the influence of factors simulating real space flight factors, enabled us to obtain a generalized evaluation of operator readiness for the main control tests, i.e., his current [operative] work capacity. We used the following as the parameters: pulse rate, arrhythmia, skin resistance, changes in pulse rate and exertion of the operator in the dynamic test. Parameters of visual acuity, as well as characteristics of operator performance in superposition of moving marks and in the radiotelegraphy mode, were included in the generalized evaluation, in order to describe the operator's communication channels.

The above-described software ["mathematical apparatus"], based on a modification of the least squares method, which permits determination of the numerical values of

polynomial $P_q(\xi_1, \ldots, \xi_k)$, as well as evaluation of accuracy of function $\eta = P_q(\xi_1, \ldots, \xi_k)$, was used to find the concrete form of function $\eta = P_q(\xi_1, \ldots, \xi_k)$. Evaluation of accuracy of function $\eta = P_q(\xi_1, \ldots, \xi_k)$ makes it possible to select for each type of work the sets of parameters that provide maximum accuracy of function $\eta = P_q(\xi_1, \ldots, \xi_k)$ for a given type of work. Thus, the proposed method enables us to evaluate the significance of different sets of psychophysiological parameters to describe each type of work studied.

This method of evaluating the quality of operator performance according to his current psychophysiological parameters was tested in an analysis of experimental data. The algorithm for finding the generalized criterion was solved in the form of a computer program. Table 7.1 lists the values of coefficients Θ_i of parameters of function $\eta = P_q(\xi_1, \ldots, \xi_k)$ with $q = 1$, for which the coefficients have the meaning of each parameter in the description of the chosen form of work.

Table 7.1. Values of parameters for two types of operator work

Work	Pulse rate	Pulse rate dispers.	Skin resistance	Difference in		Visual acuity	Quality of	
				pulse in dynamic test	exertion in dynamic test		superp. of moving marks	radiogram transmission
In radiotelegraphy mode	0.211	0.204	0.072	-0.166	-0.290	0.251	0.340	--
Superpostion of moving marks	0.068	0.378	0.037	-0.287	0.227	-0.133	--	0.536

The values of criteria characterizing performance quality and values of psychophysiological parameters were submitted to centering and standardizing operations; for this reason, the values of the "weights" in this table for a given form of work have the meaning of a rating of relative importance of each parameter. Analysis of the data listed in the table shows that, for each of the two selected forms of work (working in radiotelegraphy mode and work to superpose moving marks), the other work is the most significant indicator (superposition of marks for work in radiotelegraphy mode and vice versa), which always participated in the evaluation as a psychophysiological parameter (the "weights" constitute 0.340 and 0.536, respectively, and they are each the maximum in their own set). Coefficient Θ_i of dispersion of pulse rate was rather significant in both forms of work, which shows that there is a link between increase in arrhythmia and worsening of performance quality. The actual pulse rate was found to be significant (0.211) for work in the radiotelegraphy mode, which involves considerable physical tension, and much less significant (0.068) for the calmer work of superposing moving marks. Interestingly enough, a relatively higher (0.290) and negative coefficient, with which increment of exertion in the dynamic test is contained in the formula, was obtained for the same reasons. Thus, the data in this table indicate that the more significant parameters were those whose psychophysiological basis was referable to complex processes of higher nervous activity (superposition of moving marks, as well as indicators of variability of parameters of some autonomic processes).

Figure 92 illustrates the quality of approximation of real performance quality (solid line) determined with concrete function $\eta = P_q(\xi, \ldots, \xi_k)$ (dash line). Data for

the background experiment are shown on the left and those for the experiment with the use of different factors are on the right. We see that our criterion permits quite good differentiation between these two states. The developed method of obtaining a generalized evaluation of performance quality makes it possible to forecast the quality of a selected work according to values of psychophysiological indicators. We excluded seven sets of data for points in time selected at random to test the possibility of forecasting performance quality by the procedure of finding the coefficients. After a specific form of function $\eta = P(\xi_1, \ldots, \xi_k)$ was found from the rest of the data, we made a forecast of performance quality using the seven omitted points in time and corresponding values of only psychophysiological parameters.

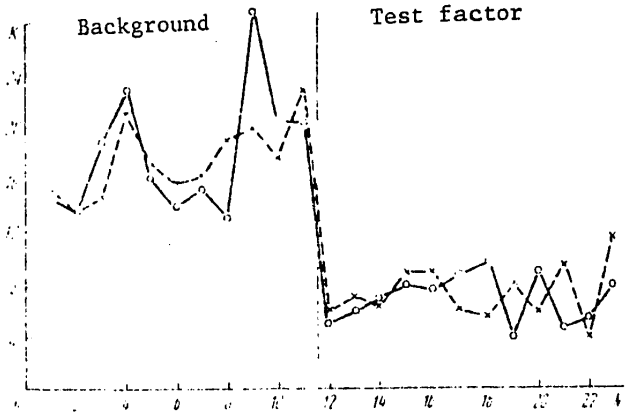

Figure 92. Quality of approximation of real performance by functions of parameters

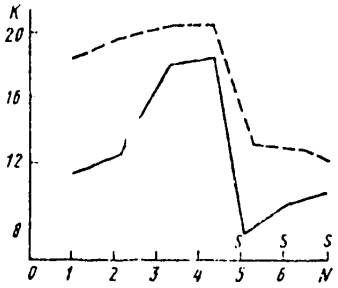

Figure 93. Forecasting cosmonaut performance according to psychophysiological parameters (K--performance quality criterion; N--test number; S--stress factor)

In Figure 93, the dash line illustrates the obtained forecast values η. In the same figure, the solid line shows the real performance quality in the radiotelegraphy mode. Let us mention that the first four time segments are referable to the main experiment and the last three to the experiment with use of stimuli ["factors"]. The data illustrated in Figure 93 indicate that the proposed method has a good potential for predicting performance quality according to psychophysiological parameters.

This method was tested on the astronavigation research-training unit (ARTU). In the course of the experiments, we recorded the time spent by an operator on astronavigation measurements using a space sextant. The same parameter was predicted by the method of generalized evaluation. We used the above-described

parameters, decision making time, reaction time, integral of squared error, pulse rate and dispersion of pulse rate. Calculation of coefficients of polynomial η was made on the basis of 14 astromeasurements in each experiment. The parameters recorded automatically with each reading and time of performance of astromeasurements were stored in the ARTU computer system. The time spent on astromeasurements was predicted on the basis of the readings obtained from 15 measurements, and we recorded the real time. The method of generalized evaluation can also be used to solve astronavigation problems (for example, to determine whether it is possible to take astromeasurements when time is short).

CONTENTS

10,657
CSO: 8144/1145

END